CGER-REPORT

ISSN 1341-4356

CGER-I103-2012

CGER'S SUPERCOMPUTER MONOGRAPH REPORT Vol. 18

Development of Process-based NICE Model and Simulation of Ecosystem Dynamics in the Catchment of East Asia (Part III)

Tadanobu Nakayama

Center for Global Environmental Research

National Institute for Environmental Studies, Japan

CGER-REPORT

ISSN 1341-4356

CGER-I103-2012

CGER'S SUPERCOMPUTER MONOGRAPH REPORT Vol. 18

Development of Process-based NICE Model and Simulation of Ecosystem Dynamics in the Catchment of East Asia (Part III)

Tadanobu Nakayama

Center for Global Environmental Research

National Institute for Environmental Studies, Japan

CGER'S SUPERCOMPUTER MONOGRAPH REPORT Vol.18

Development of Process-based NICE Model and Simulation of Ecosystem Dynamics in the Catchment of East Asia (Part III)

Tadanobu Nakayama

Edited by:
Center for Global Environmental Research (CGER)
National Institute for Environmental Studies (NIES)

Coordination for Resource Allocation of the Supercomputer:
Center for Global Environmental Research (CGER)
National Institute for Environmental Studies (NIES)

Maintenance of the Supercomputer System:
Environmental Information Department (EID)
National Institute for Environmental Studies (NIES)

Operation of the Supercomputer System:
NEC Corporation

Copies of this report can be obtained by contacting:
Center for Global Environmental Research (CGER)
National Institute for Environmental Studies (NIES)
16-2 Onogawa, Tsukuba, Ibaraki , 305-8506 Japan
Fax: +81-29-858-2645
E-mail: www-cger@nies.go.jp

The report is also available as a PDF file.
See: http://www.cger.nies.go.jp/ja/activities/supporting/publications/report/index.html

ISSN 1341- 4356, CGER-I103-2012

Foreword

The Center for Global Environmental Research (CGER) at the National Institute for Environmental Studies (NIES) was established in October 1990. CGER's main objectives are to contribute to the scientific understanding of global change and to identify solutions for pressing environmental problems. CGER conducts environmental research from interdisciplinary, multi-agency, and international perspectives, provides an intellectual infrastructure for research activities in the form of databases and a supercomputer system, and makes the data from its long-term monitoring of the global environment available to the public.

CGER installed its first supercomputer system (NEC SX-3, Model 14) in March 1992. That system was subsequently upgraded to an NEC Model SX-4/32 in 1997, and an NEC Model SX-6 in 2002. In March 2007, we replaced that system with an NEC Model SX-8R/128M16 in order to provide an increased capacity for speed and storage. We expect our research to benefit directly from this upgrade.

The supercomputer system is available for use by researchers from NIES and other research organizations and universities in Japan. The Supercomputer Steering Committee evaluates proposals of research requiring the use of the system. The committee consists of leading Japanese scientists in climate modeling, atmospheric chemistry, ocean environment, computer science, and other areas of concern in global environmental research. In the 2007 fiscal year (April 2007 to March 2008), sixteen proposals were approved.

To promote the dissemination of the results, we publish both an Annual Report and occasional Monograph Reports. Annual Reports give the results for all research projects that have used the supercomputer system in a given year, while Monograph Report presents the integrated results of a particular research program.

This Monograph Report presents the results following the 11th publication (Part I) and the 14th publication (Part II) which were published previously. The new process-based catchment model, called the National Integrated Catchment-based Eco-hydrology (NICE) model, was applied to various catchments in East Asia. The results obtained in this research will allow us to clarify the various kinds of interactions among human activities and water–heat–mass cycles and their impacts on environmental degradation for sustainable development of human society in catchments.

In the years to come, we will continue to support environmental research with our supercomputer resources and disseminate practical information on our results.

January 2012

Yasuhiro Sasano
Director
Center for Global Environmental Research
National Institute for Environmental Studies

Preface

This volume of CGER'S SUPERCOMPUTER MONOGRAPH REPORT series is the 18th publication of research outcomes achieved by users of the supercomputer facilities at the Center for Global Environmental Research (CGER), National Institute for Environmental Studies (NIES). The author has so far developed the new process-based catchment model, called the National Integrated Catchment-based Eco-hydrology (NICE) model, to evaluate ecosystem dynamics in the catchments of East Asia.

Though water resources are vital for human activity, its overuse causes the serious hydrologic change such as drying out river, groundwater fall, and seawater intrusion, et al. It also causes various ecosystem degradations and serious burden on the environment. However, effective management of water resource is also powerful for decision-making and adaptation strategy for sustainable development.

This monograph (Part III) succeeds the 11th publication (Part I) and the 14th publication (Part II) published previously. This volume reviews the NICE processes newly developed since Part I was published and describes how these models have been applied to various catchments in East Asia. The result indicates effective management of water resource is powerful for achieving win-win solution about hydrothermal pollutions in eco-conscious society. The NICE model is now being expanded to include another process including regional atmospheric and ocean models, *et al*. for evaluating various ecosystems and their relation to the surrounding regions. This subsequent research will be reported in the next monograph (Part IV) in the near future. The author hopes that the publication we present here will facilitate further research on the sustainable development of human society in catchments. In particular, the author hopes that it will help to clarify the various kinds of interactions among human activities and water–heat–mass cycles and their effects on environmental degradation.

January 2012

Tadanobu Nakayama

Tadanobu Nakayama
Senior Researcher
Center for Global Environmental Research
National Institute for Environmental Studies

Contents

List of Figures

Chapter 1

Chapter 2

Chapter 3

Chapter 4

Chapter 5

List of Tables

Chapter 1

General Introduction

1.1 Background

Human activity has dramatically changed ecosystem dynamics in East Asia. In particular, adaptation from rural settings or the wilderness to urban or agricultural settings has greatly affected the surrounding ecosystems in catchments. Environmental pollution has recently come to be synonymous with degradation of water and thermal environments and the contamination of urban areas (Fig. 1.1). To facilitate sustainable development, it is necessary to quantify the mechanisms of ecosystem change and execute adaptation strategies to develop sustainability for the active recovery of local natural environments that have been damaged. In this context, numerical models are powerful tools used in river- and basin-wide initiatives.

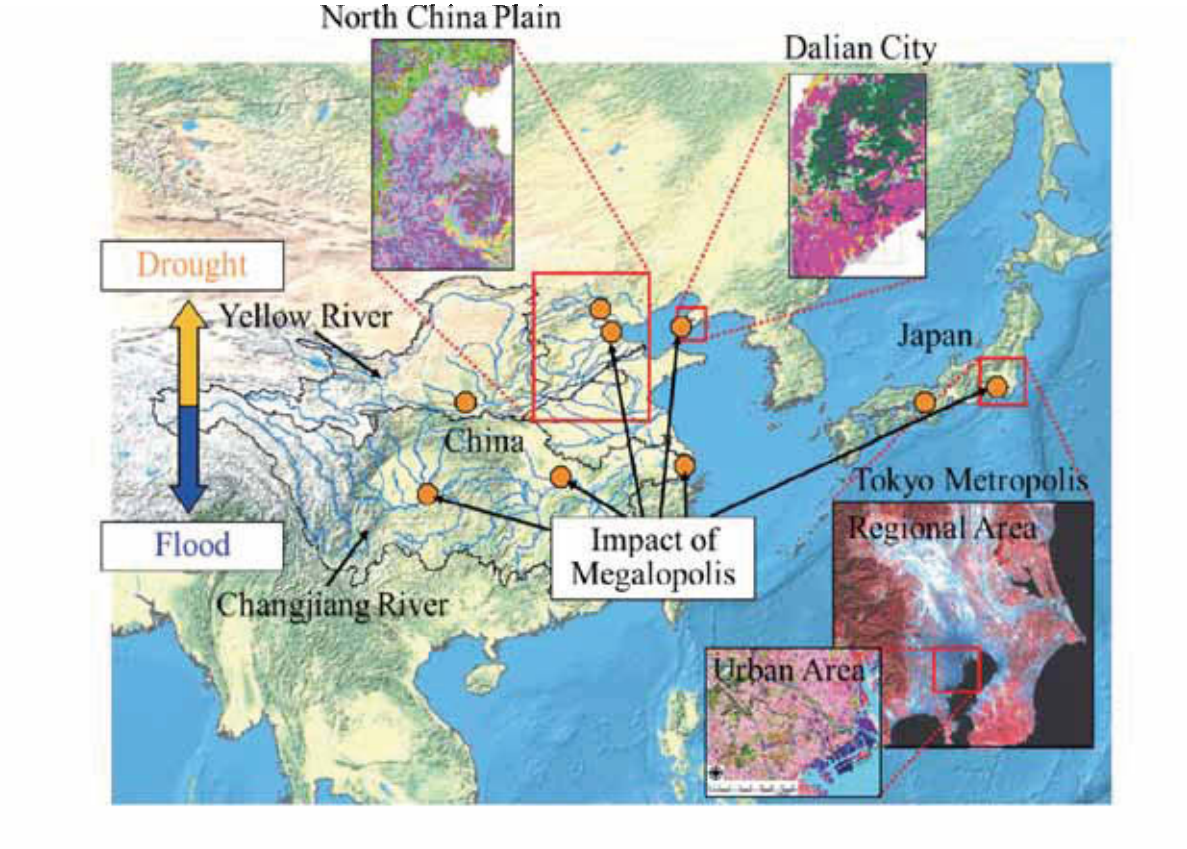

Fig. 1.1 Evaluation of ecosystem degradation by cyclic changes in water, heat, and mass described in this study.

The hydroclimate between the northern and southern regions of China is diverse (Fig. 1.1) (Nakayama, 2011a, 2011b; Nakayama and Watanabe, 2008b). The North China Plain (NCP) is located downstream of the Yellow River and has a semi-arid climate. Because it is one of the country's most important agricultural regions, this area experiences critical water shortages (Brown and Halweil, 1998; Shimada, 2000; Chen *et al*., 2003; Nakayama *et al*., 2006). In addition, this region includes vast metropolitan areas such as Beijing and Tianjin. The demand for water here has intensified usage conflicts between the upstream and downstream areas in addition to similar conflicts between agricultural and municipal–industrial sectors. This region, once water-rich in the 1950s, has become water

deficient because of various ecosystem degradations including the drying of the Yellow River, the near closure of the Hai River, and groundwater degradation in the NCP (Liu and Xia, 2004; Nakayama, 2011a, 2011b; Nakayama *et al*., 2006). These conditions have created large depression cones and land subsidence in urban areas. In addition, saline–alkaline areas have expanded on land due to seawater intrusion in the coastal zone (Brown and Halweil, 1998; Shimada, 2000; Chen *et al*., 2003; Nakayama, 2011a). Several researchers have stated that China's demand for natural resources already exceeds the environment's capacity to sustain this densely populated land (Varis and Vakkilainen, 2001). Because Dalian is located at the southern tip of the Liaodong Peninsula, the region has limited access to fresh water. Most of the city's water, necessary for its rapid economic growth, is drawn from the remote Biliu Reservoir located at the middle of the river. Since the completion of this reservoir in 1984, most of the water has been piped to Dalian, resulting in a shift from water-rich to water-poor catchment areas, as evidenced by the drying of the downstream river, reduction in groundwater levels, and seawater intrusion, all of which have been observed in other regions in northern China (Ren *et al*., 2002; Nakayama *et al*., 2006, 2010).

Moreover, urban heat islands, created by the expansion of cities and industrial areas, have become a significant environmental problem, worldwide (Oke, 1987). The Japanese government has taken various measures to mitigate this problem in the Tokyo metropolitan area (Fig. 1.1) by rearranging surface layers, reconstructing older buildings and urban geometry, applying green infrastructure systems, increasing energy efficiency, and managing traffic–transportation systems. Another effective strategy for heat island mitigation is the promotion of vaporization through the use of water-holding pavements in conjunction with light-colored and vegetated surfaces (Chang *et al*., 2007; Nakayama and Fujita, 2010). Because the heat relaxation properties in the newly symbiotic pavements are closely related to the heat capacity of water and the conductivity of the pavement, it is estimated that groundwater use in almost constant temperature as a heat sink would be an effective method for heat island compensation (Ministry of Environment, 2004). However, the metropolitan area has also undergone severe damage through hydrologic cycle imbalances; for example, flooding and buoyant forces have compromised underground infrastructures that were installed to regulate groundwater usage (Endo, 1992; Nakayama *et al*., 2007). The severity of water and thermal pollution in marine areas has increased over time. Water resources such as rivers, lakes, seas, and groundwater are important for the mitigation of urban heat islands. Watersides, open parks, and green areas have become valuable urban cool islands (Ministry of Environment, 2004). A policy to promote infiltration into the aquifer is also important to prevent ground degradation (Nakayama and Hashimoto, 2011; Nakayama *et al*., 2007, in press).

The current monograph (Part III) succeeds our 11th publication (Part I) in 2006 (Nakayama and Watanabe, 2006b) and our 14th publication (Part II) in 2008 (Nakayama, 2008c). The catchments described in this monograph are representative of areas in East Asia, in which human activity has greatly affected the environment. Although water resources are vital for human activity, overuse causes significant hydrologic changes including drying rivers, receding groundwater levels, and seawater intrusion in addition to ecosystem degradation and severe environmental burden. However, the effective management of water resources is also important in the planning and execution of sustainable development strategies. This monograph illustrates the possibility for sound recovery of the hydrologic cycle with simultaneous creation of thermally stable environments. The results indicate that effective management of water resources is critical for achieving favorable solutions to hydrothermal pollution in an eco-conscious society.

1.2 Model Description of Process-based Model Applicable to Urban Areas

In a previous study, the author developed the National Integrated Catchment-based Eco-hydrology (NICE) model, which includes surface-unsaturated–saturated water processes and assimilates land-surface processes, describing phenology variations on the basis of satellite data (Nakayama, 2008a, 2008b, 2008c, 2009, 2010, 2011a, 2011b; Nakayama and Fujita, 2010; Nakayama and Hashimoto, 2011; Nakayama and Watanabe, 2004, 2006a, 2006b, 2008a, 2008b, 2008c; Nakayama *et al*., 2006, 2007, 2010, in press) (Fig. 1.2). NICE is a 3-D, grid-based eco-hydrology model. This model has been coupled with complex subsystems in irrigation, urban water usage, stream junctions, and dams and canals to develop integrated human and natural systems and to analyze the impact of anthropogenic activity on eco-hydrologic change. In the Simple Biosphere model 2 (SiB2), the unsaturated layer vertically divides the canopy into two layers and the soil into three layers (Sellers *et al*., 1996). In the saturated layer, NICE solves 3-D groundwater flow for both unconfined and confined aquifers. The hillslope hydrology including freezing–thawing processes can be expressed by the two-layer surface runoff model. NICE links each submodel by considering water–heat fluxes, including the gradient of hydraulic potential between the deepest unsaturated layer and the groundwater, effective precipitation, and seepage between the river and groundwater.

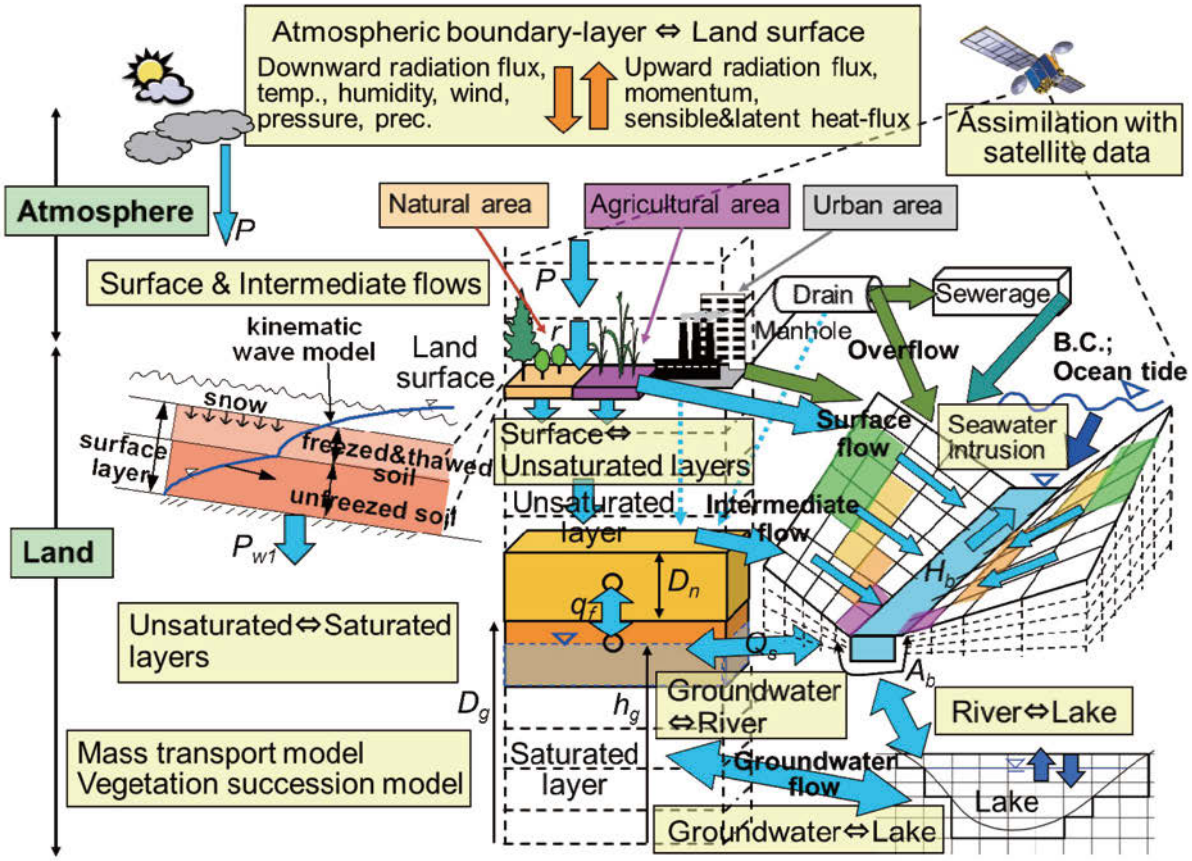

Fig. 1.2 Process-based National Integrated Catchment-based Eco-hydrology model.

For agricultural applications, NICE is coupled with Decision Support Systems for Agro-technology Transfer (DSSAT) (Ritchie *et al*., 1998), in which an automatic irrigation mode supplies crop water requirements for field cultivation (Nakayama *et al.*, 2006; Nakayama, 2011a, 2011b) and cultivation of paddy fields (Nakayama and Watanabe, 2008b). This model includes the various functions of representative crops such as wheat, maize, soybean, and rice and automatically simulates their dynamic growth processes. Plant growth is based on biomass formulation, which is limited by various reduction factors such as light, temperature, water, and nutrients (Nakayama, 2011a; 2011b; Nakayama and Watanabe, 2008b; Nakayama *et al*., 2006). Most of the water supplied to major cities and cultivated fields in the NCP and Dalian is transported through a network of reservoirs and canals (Nakayama, 2011a; Nakayama *et al*., 2006, 2010) (Fig. 1.1). Because limited data are available on discharge control at most of the dams adjacent to these reservoirs, a constant ratio of inflow to outflow—instead of the more complicated storage–runoff function model—was used for the major dams for which no data were available (Nakayama, 2011a). NICE was also coupled with the urban canopy model (UCM) to include the effects of the hydrothermal cycle on various pavements, and with the Regional Atmospheric Modeling System (RAMS) (Pielke *et al*., 1992) to include hydrothermal interaction in urban areas (Nakayama and Fujita, 2010; Nakayama and Hashimoto, 2011; Nakayama *et al*., in press). Downward short- and long-wave radiation, precipitation, atmospheric pressure, air temperature, air humidity, and wind speed simulated by the atmospheric model were input into the UCM, whereas momentum, sensible, latent, and long-wave flux simulated by the UCM were input into the atmospheric model at each time step. This procedure ensures that the feedback process of water and heat transfers between the atmospheric region and the land surface are implicitly included in the simulation process.

The NICE series has expanded to include additional processes, including regional atmospheric and ocean models, for evaluating various ecosystems and their relation to surrounding regions. The details of the existing NICE series are presented in the following references.

1.3 Objective and Method

To study the ecosystem dynamics in the catchments of East Asia, the author has previously developed a method to combine a grid-based numerical model, ground-truth observation data, and satellite data (Fig. 1.3). In this monograph (Part III), the author reviews the new processes of NICE developed after Parts I (Nakayama and Watanabe, 2006b) and II (Nakayama, 2008c) and describes how these models were applied to the catchments wherein water resources, economic growth, and ecosystem degradation relations with the environment require urgent evaluation. The main study areas are northern China, including the NCP (2011a, 2011b; Nakayama *et al*., 2006, 2010), and the Tokyo metropolitan area (Nakayama and Hashimoto, 2011; Nakayama *et al*., 2007, in press) (Fig. 1.1). The final objective of the current monograph is to present a method by which to combine numerical models, satellite imagery, and statistical analysis to clarify the relationship between water resources and economic growth, which adversely affects the ecological balance. The process-based model uses complex subsystems to simulate hydrological changes such as the drying of rivers and groundwater degradation resulting from human intervention in order to evaluate the relationship between urban development and sustainable water resource management in the catchments. In addition, the model simulates the effects of urban geometry and anthropogenic exhaustion on changes in water and heat cycles in the megalopolis. Moreover, the author

presents a procedure to visualize related environmental pollution such as the missing role of hydrothermal interactions in atmospheric, land, and marine areas. This procedure offers an integrated assessment system for effective strategies that could reveal methods of solving the complex nature of water challenges and support plans for sustainable development.

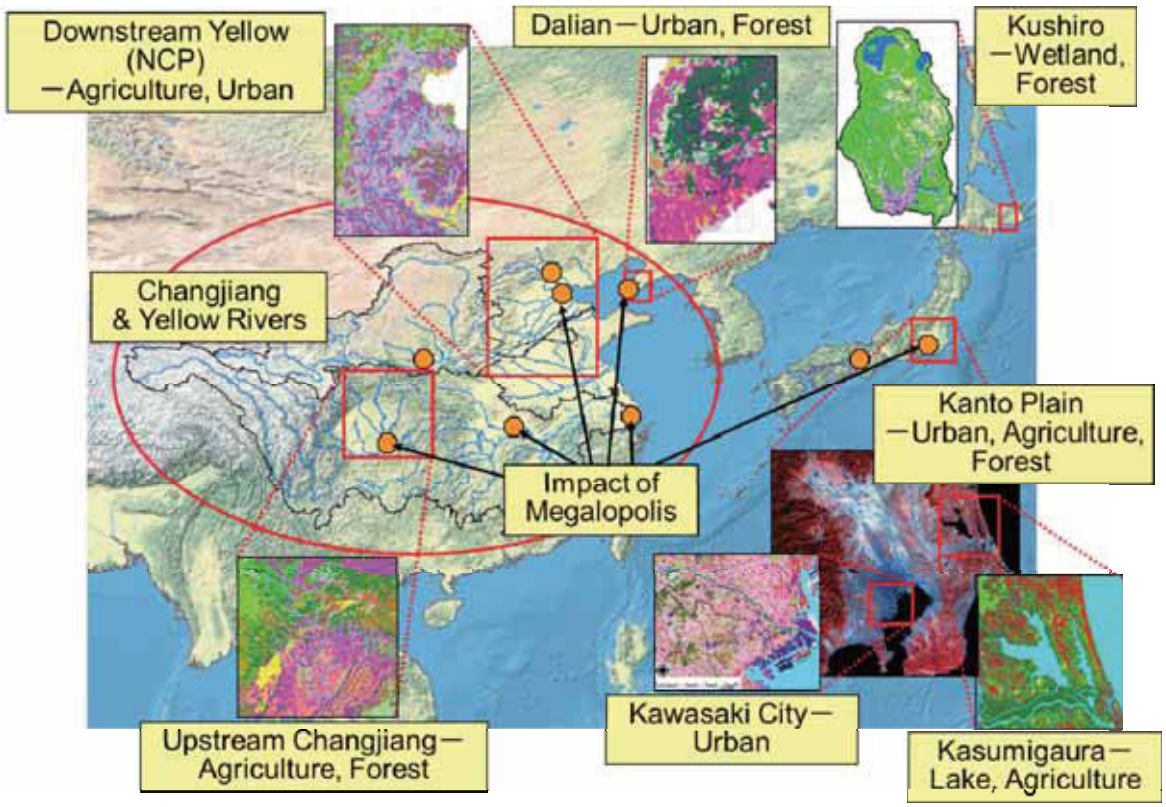

Fig. 1.3 Ecosystem highlighting various regions in East Asia.

References

Brown L.R., Halweil B. (1998) China's water shortage could shake world food security. World Watch, 11(4), 10-18.

Chang C.R., Li M.H., Chang S.D. (2007) A preliminary study on the local cool-island intensity of Taipei city parks. Landscape and Urban Planning, 80, 386-395.

Chen J.Y., Tang C.Y., Shen Y.J., Sakura Y., Kondoh A., Shimada J. (2003) Use of water balance calculation and tritium to examine the dropdown of groundwater table in the piedmont of the North China Plain (NCP). Environmental Geology, 44, 564-571.

Endo T. (1992) Confined groundwater system in Tokyo. Environmental Geology and Water Sciences, 20, 21-34.

Liu C., Xia J. (2004) Water problems and hydrological research in the Yellow River and the Huai and Hai River basins of China. Hydrological Processes, 18, 2197-2210, doi:10.1002/hyp.5524.

Ministry of Environment (2004) Report on heat-island measures by controlling anthropogenic exhaustion heat in the urban area. http://www.env.go.jp/air/report/h16-05/ (in Japanese).

Nakayama T. (2008a) Factors controlling vegetation succession in Kushiro Mire. Ecological Modelling, 215, 225-236, doi:10.1016/j.ecolmodel.2008.02.017.

Nakayama T. (2008b) Shrinkage of shrub forest and recovery of mire ecosystem by river restoration in northern Japan. Forest Ecology and Management, 256, 1927-1938, doi:10.1016/j.foreco.2008.07.017.

Nakayama T. (2008c) Development of process-based NICE model and simulation of ecosystem dynamics in the catchment of East Asia (Part II), CGER's Supercomputer Monograph Report, 14, NIES, 91p., http://www-cger.nies.go.jp/publication/I083/i083.html.
Nakayama T. (2009) Simulation of ecosystem degradation and its application for effective policy-making in regional scale. In River pollution research progress, Mattia N. Gallo, Marco H. Ferrari (eds), 1-89 (Chapter 1), Nova Science Pub., Inc., New York.
Nakayama T. (2010) Simulation of hydrologic and geomorphic changes affecting a shrinking mire. River Research and Applications, 26(3), 305-321, doi:10.1002/rra.1253.
Nakayama T. (2011a) Simulation of complicated and diverse water system accompanied by human intervention in the North China Plain. Hydrological Processes, 25, 2679-2693, doi:10.1002/hyp.8009.
Nakayama T. (2011b) Simulation of the effect of irrigation on the hydrologic cycle in the highly cultivated Yellow River Basin. Agricultural and Forest Meteorology, 151, 314-327, doi:10.1016/j.agrformet.2010.11.006.
Nakayama T., Fujita T. (2010) Cooling effect of water-holding pavements made of new materials on water and heat budgets in urban areas. Landscape and Urban Planning, 96, 57-67, doi:10.1016/j.landurbplan.2010.02.003.
Nakayama T., Hashimoto S. (2011) Analysis of the ability of water resources to reduce the urban heat island in the Tokyo megalopolis. Environmental Pollution, 159, 2164-2173, doi:10.1016/j.envpol.2010.11.016.
Nakayama T., Watanabe M. (2004) Simulation of drying phenomena associated with vegetation change caused by invasion of alder (Alnus japonica) in Kushiro Mire. Water Resources Research, 40, W08402, doi:10.1029/2004WR003174.
Nakayama T., Watanabe M. (2006a) Simulation of spring snowmelt runoff by considering micro-topography and phase changes in soil layer. Hydrology and Earth System Sciences Discussions, 3, 2101-2144.
Nakayama T., Watanabe M. (2006b) Development of process-based NICE model and simulation of ecosystem dynamics in the catchment of East Asia (Part I), CGER's Supercomputer Monograph Report, 11, NIES, 100p., http://www-cger.nies.go.jp/publication/I063/I063.html.
Nakayama T., Watanabe M. (2008a) Missing role of groundwater in water and nutrient cycles in the shallow eutrophic Lake Kasumigaura, Japan. Hydrological Processes, 22, 1150-1172, doi:10.1002/hyp.6684.
Nakayama T., Watanabe M. (2008b) Role of flood storage ability of lakes in the Changjiang River catchment. Global and Planetary Change, 63, 9-22, doi:10.1016/j.gloplacha.2008.04.002.
Nakayama T., Watanabe M. (2008c) Modelling the hydrologic cycle in a shallow eutrophic lake. Verh International Verein Limnology, 30.
Nakayama T., Yang Y., Watanabe M., Zhang X. (2006) Simulation of groundwater dynamics in North China Plain by coupled hydrology and agricultural models. Hydrological Processes, 20(16), 3441-3466, doi:10.1002/hyp.6142.
Nakayama T., Watanabe M., Tanji K., Morioka T. (2007) Effect of underground urban structures on eutrophic coastal environment. Science of the Total Environment, 373(1), 270-288, doi:10.1016/j.scitotenv.2006.11.033.
Nakayama T., Sun Y., Geng Y. (2010) Simulation of water resource and its relation to urban activity in Dalian City, Northern China. Global and Planetary Change, 73, 172-185, doi:10.1016/j.gloplacha.2010.06.001.
Nakayama T., Hashimoto S., Hamano H. (in press) Multi-scaled analysis of hydrothermal dynamics in Japanese megalopolis by using integrated approach. Hydrological Processes.
Oke T.R. (1987) Boundary layer climates, Methuen Press, London.
Pielke R.A., Cotton W.R., Walko R.L., Tremback C.J., Lyons W.A., Grasso L.D., Nicholls M.E., Moran M.D., Wesley D.A., Lee T.J., Copeland J.H. (1992) A comprehensive meteorological modeling system-RAMS. Meteorology and Atmospheric Physics, 49, 69-91.
Ren L., Wang M., Li C., Zhang W. (2002) Impacts of human activity on river runoff in the northern area of China. Journal of Hydrology, 261, 204-217.
Ritchie J.T., Singh U., Godwin D.C., Bowen W.T. (1998) Cereal growth, development and yield. Understanding Options for Agricultural Production, eds. Tsuji G.Y., Hoogenboom G. & Thornton P.K., Kluwer: Great Britain, 79–98.
Sellers P.J., Randall D.A., Collatz G.J., Berry J.A., Field C.B., Dazlich D.A., Zhang C., Collelo G.D., Bounoua L. (1996) A revised land surface prameterization (SiB2) for atomospheric GCMs. Part I : Model formulation. Journal of Climate, 9, 676-705.
Shimada J. (2000) Proposals for the groundwater preservation toward 21st century through the view point of hydrological cycle. Journal of Japan Association of Hydrological Sciences, 30, 63-72 (in Japanese).
Varis O., Vakkilainen P. (2001) China's 8 challenges to water resources management in the first quarter of the 21st Century. Geomorphology, 41, 93-104.

Chapter 2

Diverse Water System Accompanied by Human Intervention in the North China Plain

Abstract

The author has coupled the National Integrated Catchment-based Eco-hydrology (NICE) model series with dam–canal systems (NICE-CNL) in agricultural and urban areas. This combined model was applied to the North China Plain (NCP) and the lower reaches of the Yellow River in China, where water shortages and the resultant environmental degradation have become increasingly critical over time. This model provided a good reproduction of the hydrologic cycle, including river discharge, soil moisture, evapotranspiration, groundwater level, and crop production of summer maize and winter wheat, through accurate estimations of crop water usage in the absence of detailed statistical data. The simulation showed that overexploitation of groundwater for irrigation and industrial usage has a marked effect on the water dynamics in the NCP because, in addition to industrial and domestic water usage, the river water volume is smaller than that necessary for irrigation. The model reasonably reproduced the trend in groundwater degradation observed during the previous half century and included cone depression formations near major cities, which the author was unable to reproduce in previous research. Moreover, the simulation clarified the relationship of this water shortage and the low discharge rate of the Hai River into the Bohai Sea. Further, the simulated result of the density current and solute transport processes clarified that these water cycle changes have caused a considerable amount of seawater intrusion and a decrease in crop productivity in coastal areas, as shown by the Normalized Difference Vegetation Index (NDVI) gradient estimated from satellite imagery. In this chapter, we show a significant improvement in the process-based model, which enables clarification of the diverse water system and contains important implications for the evaluation of degraded ecosystems and environments located on the fluctuating boundary between freshwater and marine areas.

Keywords: diverse water system, integrated catchment-based eco-hydrology model, water shortage, seawater intrusion, NDVI, ecosystem degradation

2.1 Introduction

The North China Plain (NCP) is located in the eastern part of China, between 35°00′N and 40°30′N and between 113°00′E and 119°30′E. It includes all the plains of the Hebei Province, metropolitan Beijing and Tianjin, and the northern parts of the plains in the Shandong and Henan provinces (Fig. 2.1). The region surrounded by the Taihang Mountains to the West, the Yanshan Mountains to the North, the Bohai Sea to the East, and the Yellow River to the south is a giant alluvial plain formed by the deposition of the Yellow, Hai, and Luan rivers and their tributaries (Chen, 1996). Located in a semi-arid climatic zone, this large region—encompassing an approximate area of 1.36×10^5 km^2 and about 112 million people (Brown and Halweil, 1998; Shimada, 2000; Chen *et al*., 2003; Nakayama *et al*., 2006)—has suffered severe water shortages attributed to its function as one of the most important grain producing areas in China. This water demand has intensified usage conflicts between the upstream and downstream areas in addition to that between the agriculture and municipal–industrial sectors. As a result, this region, water-rich in the 1950s, has undergone various ecosystem changes resulting in the drying of the Yellow River, the near closure of the Hai River, groundwater degradation, and seawater intrusion in the NCP.

In addition, increasing development and use of water resources has led to the complete drainage of the Yellow River along the main course of its lower reaches and along its major tributaries. The most serious situation occurred in 1997, when the main river close to the sea dried up for 226 days and the no-flow region extended upstream to Liuyuankou in Kaifeng City, Henan Province, 704 km from the river mouth, which constituted 90% of the river length in the lower reaches (Chen *et al*., 2003; Liu *et al*., 2003; Xia *et al*., 2004; Yang *et al*., 2004). This event caused considerable damage to communities and the surrounding eco-environment. The Hai River catchment is located in the center of the NCP, occupying an area of approximately 3.20×10^5 km^2 and water resources of 372×10^8 m^3. Increased population and the developing economy in this region have resulted in severe water shortages in the 21st century. Baiyangdian Lake in Hebei Province, the largest natural lake in northern China, is also facing major water shortages due to severe drought and diversion for irrigation and drinking water (Yin and Lan, 1995; Liu *et al.*, 2006). In this situation, the concept of flood resources development and utilization, known as flood resourcification, is important for increasing the water supply; through this process, most of the water on land is retained as far away as possible, (Wang *et al*., 2004). A previous survey of surface runoff and discharge into the sea during the last five decades has shown that an increasing number of dams and reservoirs have been constructed to increase the flood resourcification ability in three obvious phases (Guo and Cai, 2000). The stages characteristic of flood resourcification in this catchment are closely related to the history of water resource development. Because the rapid development of industry and urbanization and an increase in farmland irrigation have doubled water demand, the groundwater table has rapidly receded in the floodplains of the river's downstream areas over the previous half-century due to excessive irrigation water withdrawal (Liu and Xia, 2004; Liu and Zheng, 2004). This result has led to the creation of large depression cones and land subsidence in urban areas in addition to the expansion of saline–alkaline regions on land due to seawater intrusion in coastal zones (Brown and Halweil, 1998; Shimada, 2000; Liu *et al*., 2001; Chen *et al*., 2003; Nakayama *et al*., 2006). Because few studies have used numerical models to report the impact of human intervention on hydrologic changes in the NCP (Nakayama *et al*., 2006), it is important to evaluate these complex phenomena resulting from agricultural–industrial water usage and water transfer via dams, reservoirs, and canal systems.

The objective of this chapter is to evaluate these water–heat dynamics through a process-based model that combines the National Integrated Catchment-based Eco-hydrology (NICE) model series (Nakayama, 2008a, 2008b, 2008c, 2009, 2010, 2011a, 2011b; Nakayama and Fujita, 2010; Nakayama and Hashimoto, 2011; Nakayama and Watanabe, 2004, 2006a, 2006b, 2008a, 2008b, 2008c; Nakayama *et al*., 2006, 2007, 2010, in press) (Fig. 1.2) with dam–canal systems (NICE-CNL) and includes the density current and solute transport processes to simulate the relationship between hydrological change resulting from human intervention and seawater intrusion. In addition, the model clarifies the relationship between the drying of rivers and groundwater degradation. This model is expected to reveal methods of solving the complex nature of the water problems in the NCP, leading to more rational water usage and sustainability of the catchment ecosystem (Nakayama, 2011a, 2011b; Nakayama *et al*., 2006).

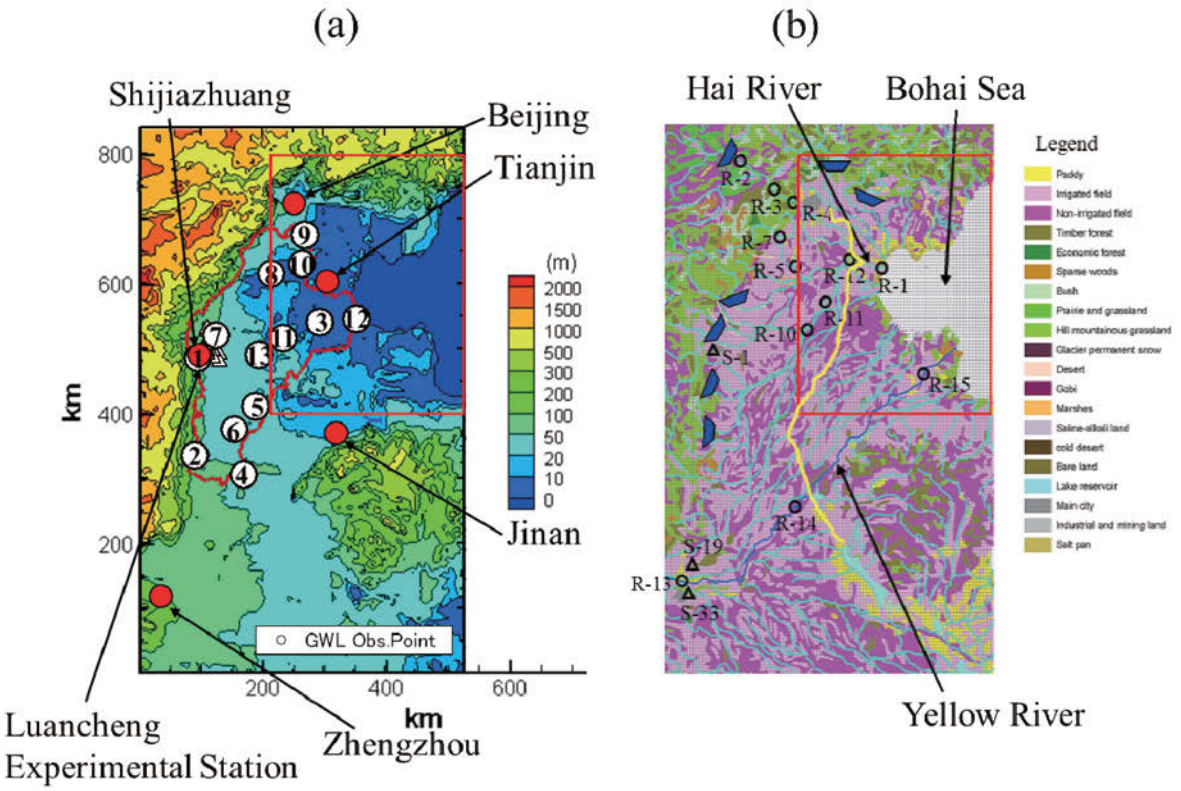

Fig. 2.1 Study area in the NCP showing (a) mean elevation and (b) land cover. In (a), the red line indicates the border of the NCP. The number shows the groundwater observation stations listed in Table 2.3. In (b), circles indicate the observation of river discharge, triangles indicate that of soil moisture recorded in Table 2.3, and blue trapezoids indicate the main reservoir. The yellow line represents the Grand Canal (South and North canals) where water is transferred from the southern to northern area in the South-to-North Water Transfer Project. The red square represents the simulation area of seawater intrusion, as shown in Fig. 2.5.

2.2 Methods

2.2.1 NICE Model Series in Natural and Agricultural Regions

The author has developed the NICE series of process-based catchment models applicable to natural, agricultural, and urban regions in catchment areas (Nakayama, 2008a, 2008b, 2008c, 2009, 2010, 2011a, 2011b; Nakayama and Fujita, 2010; Nakayama and Hashimoto, 2011; Nakayama and Watanabe, 2004, 2006a, 2006b, 2008a, 2008b, 2008c; Nakayama *et al*., 2006, 2007, 2010, in press). These NICE models link surface-unsaturated–saturated water and land-surface processes and describe variations in phenology on the basis of Moderate Resolution Imaging Spectroradiometer (MODIS) satellite data (Fig. 1.2). The submodels consider water and heat fluxes from the ground to the surface, including the gradient of hydraulic potential between the deepest layer of unsaturated flow and the groundwater level; the effective precipitation calculated from actual precipitation, infiltration into the upper soil moisture store, and evapotranspiration; and the seepage between river water and groundwater. In the agricultural field, NICE is coupled with Decision Support Systems for Agro-technology Transfer (DSSAT) (Ritchie *et al*., 1998), in which an automatic irrigation mode supplies crop water requirements for the cultivation of fields (Nakayama *et al.*, 2006; Nakayama, 2011a, 2011b) and paddy fields (Nakayama and Watanabe, 2008b). The model includes various functions of representative crops such as wheat, maize, soybean, and rice and automatically simulates their dynamic growth processes. The details are described in Chapter 1 and previous related papers (Nakayama, 2008a, 2008b, 2008c, 2009, 2010, 2011a, 2011b; Nakayama and Fujita, 2010; Nakayama and Hashimoto, 2011; Nakayama and Watanabe, 2004, 2006a, 2006b, 2008a, 2008b, 2008c; Nakayama *et al*., 2006, 2007, 2010, in press).

2.2.2 Water Transfer in Dam and Canal Systems

Numerous dams and canals populate the NCP because of the high agricultural, industrial, and domestic demand for water (Fig. 2.1b). Thousands of dams constructed beside the Taihang Mountains have prevented the water supply from reaching the plain area. Most of this stored water is transferred to major cities and to cultivated fields (Fig. 2.1b). Because limited data are available on discharge control at most of these dams, a constant ratio of inflow to outflow was used as the first approximation at the major dams, rather than the more complex storage–runoff function model used in a previous research (Sato *et al*., 2008). The water generally flows from the higher southwestern to the lower northeastern region in the Grand Canal (South and North canals) (Fig. 2.1b). When higher precipitation occurs at the Hai River catchment on the northern side of the NCP, water occasionally flows backward against the elevation. NICE-CNL simulates the discharge in the canal, assuming that this phenomenon is decided as the difference in hydraulic potential between both natural rivers; this indicates that the discharge that becomes backwater flow at the junction is dependent on the hydraulic potential difference in the same manner as that observed in the stream junction model (Nakayama and Watanabe, 2008b).

2.2.3 Satellite Analysis using NOAA/AVHRR Data

The NDVI is the difference in surface reflectivity between two wavelengths in the red (*RED*) and near-infrared (*NIR*) bands, normalized by their sum. The differential reflectance in these bands correlates strongly with the photosynthetic activity of the vegetation canopy

because of large spectral shifts in leaf optical properties. In the visible band, green leaves strongly absorb solar radiation in proportion to the chlorophyll content, absorbing more than 80% of the incoming red energy (Bacour *et al*., 2006), whereas the reflectance of bare soil is only slightly greater in the *NIR* than in the visible band.

The NDVI was calculated from NOAA/AVHRR satellite data with a resolution of 1.1 km; these data were collected across East Asia during 1982–1999. The original data were downloaded from WebPaNDA (2008) and re-sampled to change the resolution to 6.0 km by the nearest neighboring method. The data area was selected to match the simulation area (Fig. 2.1). To minimize the effects of clouds and atmospheric contaminants, we used composite data within a 10-day or monthly period that had the fewest clouds, as identified by the highest NDVI value. The NDVI was calculated as

$$NDVI = (NIR - RED)/(NIR + RED), \tag{2.1}$$

where *RED* is band 1 (visible, 0.58–0.68 μm), and *NIR* is band 2 (near-infrared, 0.725–1.10 μm). Theoretically, the NDVI varies between −1.0 and 1.0. The NDVI values range between −0.2 and 0.05 for snow, inland water bodies, deserts, and exposed soils, and increase from about 0.05 to above 0.7 with an increase in density and greenness of vegetation (Myneni *et al*., 1997). The NDVI can be used as an indicator of vegetation stress, particularly that caused by water shortage (Kogan, 1990; Singh *et al*., 2003). To reduce the impact of bare soil, clouds, and water bodies on the NDVI trends, we excluded from the analysis grid cells with NDVI <0.1 (Zhou *et al*., 2001, 2003; Piao *et al*., 2006). Crop production, defined as dry biomass by unit of surface, is also linearly related to time-integrated NDVI (TINDVI) (Yang *et al*., 1998) by using the Light Use Efficiency (LUE) model (Gower *et al*., 1999). A linear function existing between NDVI and absorbed photosynthetically active radiation (APAR) (Sellers *et al*., 1997) indicates that NDVI can be related to crop growth rate (CGR) as discussed on the basis of experimental field data (Calera *et al*. 2004).

2.3 Input Data and Boundary Conditions for Simulation

2.3.1 Meteorological Forcing Data

Six-hour reanalysis data of downward short- and long-wave radiation, precipitation, atmospheric pressure, air temperature, air humidity, wind speed at a reference level, fraction of photosynthetically active radiation (*FPAR*) and leaf area index (*LAI*), interpolated from International Satellite Land Surface Climatology Project (ISLSCP) data with a resolution of 1° × 1°, were input into each grid cell (Sellers *et al*., 1996). The precipitation, maximum and minimum temperature, and radiation of ISLSCP were compared with the observation data and were shown to be correct in a previous study (Nakayama *et al*., 2006). These corrected sites cover the entire study area in which groundwater fluctuation is influenced by agricultural water use. Because of the scarcity of recharge rate data in natural regions, except for research using the chloride mass balance method (Lee, 1996), these values were simulated by the SiB2 submodel of NICE-CNL at each time step and were inputted into the groundwater submodel. Details are given in Nakayama and Watanabe (2004).

2.3.2 Vegetation and Geological Properties

The mean elevation of each 5-km grid cell was calculated by using the spatial average of a global digital elevation model (DEM; GTOPO30) with a horizontal grid spacing of 30 arc-seconds (approximately 1-km mesh) (U.S. Geological Survey, 1996) throughout the NCP, including the Hai River and the lower reaches of the Yellow River (Fig. 2.1). Approximately 50 vegetation and soil parameters were calculated in each cell on the basis of vegetation class and soil texture obtained from the Vegetation and Soil Maps of China (1:4,000,000) (Chinese Academy of Sciences, 1988). The major parameters included vegetation cover, green fraction, albedo, surface roughness length and zero displacement height, soil conductivity, and soil water potential at saturation; in addition, several parameters of stomatal resistance were also included as these are associated with environmental factors. From the input soil texture and soil organic matter, the model calculated the hydrological parameters of the soil layers, such as water saturation content, the lowest water content required for crop growth, and the upper water content after free drainage and saturated water conductivity.

Around these catchments, the geology consists mainly of diluvium in the mountain areas (Taihang and Yanshan mountains and piedmont plains) and alluvium in the lowland and coastal areas (flood and coastal plains and fan). After calibrating the fit for the simulated hydraulic heads to the observed heads by scanning and digitizing the geological material (Geological Atlas of China, 2002), the author was able to divide the geological structure into four types, with a resolution of 5 km in the horizontal direction and 20 layers in the vertical direction, K_h and K_v, respectively, on the basis of hydraulic conductivity of specific stored porous material (S_s) and specific yield (S_y). These values were kept within the initial estimated known range previously reported (Shimada, 2000; Chen *et al*., 2002; Chen *et al*., 2003) (Table 2.1). A deep quaternary formation observed in the NCP generally reaching 400–600 m in depth was divided into four aquifers with unconfined groundwater in the first layer and confined groundwater in the second, third, and fourth layers at 38°N (Fig. 2.2). The thickness of the respective aquifers was 20–40 m, 60–130 m, 80–220 m, and 50–350 m; all aquifers consist of sand, gravel, fine sand, and silt. These geological structures are very similar to those reported previously (Zhu, 1992; Shimada, 2000; Chen *et al*., 2002), which indicates that the geological structures categorized by the author are sufficient for this simulation (Nakayama *et al*., 2006).

Table 2.1. Geological parameters used in numerical simulation.

Type	Soil Type	Horizontal Hydraulic Conductivity K_h (m/h)	Vertical Hydraulic Conductivity K_v (m/h)	Specific Storage S_s (1/m)	Specific Yield S_y
1	Gravel	5.0E+01	1.0E+01	1.0E-05	1.5E-01
2	Fine-to-medium sand	5.0E+00	1.0E+00	1.0E-04	1.5E-01
3	Finer than silt	5.0E-01	1.0E-01	1.0E-03	8.0E-02
4	Basement rock	5.0E-01	1.0E-01	1.0E-03	4.0E-02

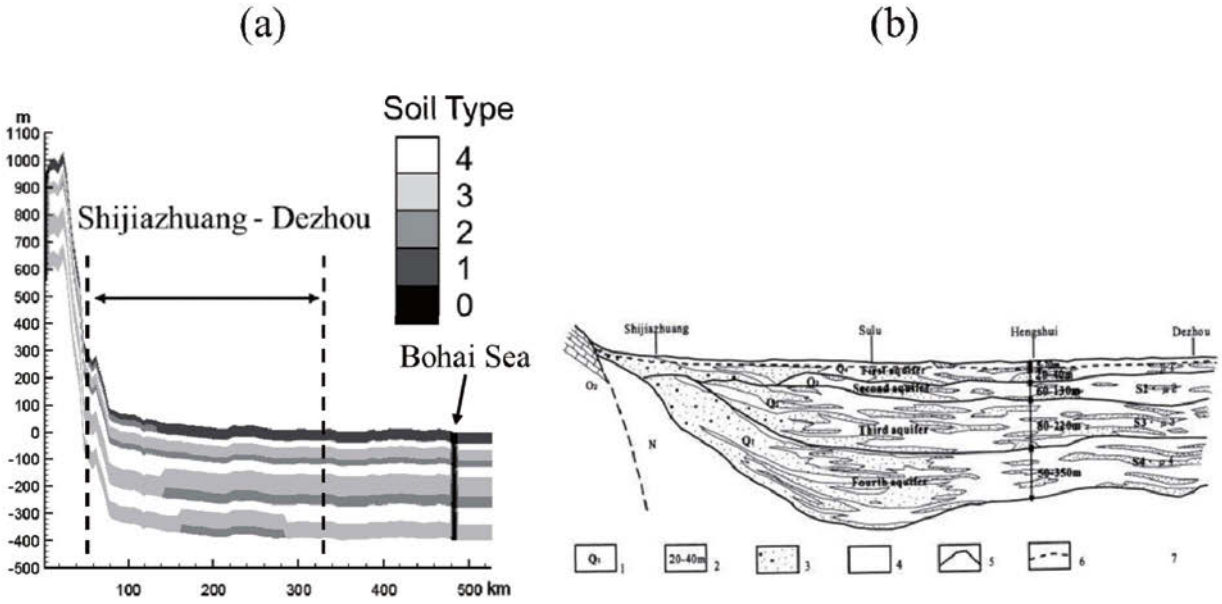

Fig. 2.2 Vertical geological structure at latitude 38°N in the NCP, obtained by (a) simulation and (b) previous research. In (a), the soil type shows the same value as that specified in Table 2.1. Soil type = 0 indicates the interface between sea and land. In (b), the cross-sectional profile of the NCP between Shijiazhuang (38.07°N, 114.55°E) and Dezhou (37.50°N, 116.30°E) is illustrated: 1: stratum age; 2: stratum thickness; 3: gravel and boulders; 4: clay and sandy clay; 5: aquifer boundary; and 6: water table.

2.3.3 Water Demand and Transfer Data in Urban Areas

Although previous research was able to reproduce the general trend of groundwater degradation in the NCP during the previous half-century, NICE-AGR was unable to reproduce cone depressions that occurred near major cities (Nakayama *et al*., 2006). Moreover, the water demands of the municipal and industrial sectors have dramatically increased, year-on-year, with the development of the social economy in the Hai River catchment area (Guo *et al*., 2000). These findings show that water usage in urban areas greatly affects the hydrological cycle in these regions. Table 2.2 shows the average water usage in 1987–1988 for the main cities in the NCP (Hebei Department of Water Conservancy, 1987, 1988). The amount of water used in the larger cities such as Beijing, Tianjin, Tangshan, and Qinhuangdao increased yearly. In particular, Beijing and Tianjin used substantial amounts of water for industrial and domestic applications. Therefore, because water usage in the major cities in the NCP was not negligible relative to their hydrological cycle, it is necessary to input them in the simulation (Nakayama, 2011a).

Table 2.2. Average water usage in 1987–1988 by major cities in the NCP (× 10000 m^3).

No.	City	Lat. (°)	Lon. (°)	Total	Irrigation	Processing	Industry	Domestic
C-1	Handan	36.60	114.47	69176.5	29604.0	290.5	27360.0	11922.0
C-2	Xingtai	37.06	114.49	26232.5	16310.0	0.0	6599.5	3323.0
C-3	Shijiazhuang	35.24	112.55	88011.0	77756.0	728.5	7484.0	2042.5
C-4	Baoding	38.85	115.49	64515.0	41414.0	1025.0	9780.0	2106.0
C-5	Cangzhou	38.32	116.87	17310.5	14303.0	25.0	1589.5	1393.0
C-6	Tangshan	39.63	118.18	127163.0	110064.5	793.0	13550.0	2755.5
C-7	Qinhuangdao	39.93	119.59	104212.0	88939.5	632.5	9074.5	5565.5
C-8	Nangong	37.36	115.37	14770.0	11570.0	0.0	2500.0	700.0
C-9	Shahe	36.85	114.50	17250.0	14750.0	0.0	1300.0	1200.0
C-10	Dingzhou	38.51	115.00	40359.5	38747.5	207.0	1280.0	125.0
C-11	Zhouxian	39.48	115.96	22200.0	19370.0	0.0	2123.0	707.0
C-12	Botou	38.07	116.57	14246.0	12713.0	103.0	533.0	897.0
C-13	Hengshui	37.73	115.70	6139.4	4549.4	0.0	800.0	790.0
C-14	Beijing	40.23	116.60	424300.0	219900.0	0.0	140400.0	64000.0
C-15	Tianjin	39.44	117.66	237776.0	161091.1	0.0	71267.7	25777.8

2.3.4 Boundary Conditions and Running the Simulation

At the upstream boundaries where no data is observed, the reflecting condition on the hydraulic head was used for the groundwater flow submodel on the supposition that no inflow occurs from the mountains in the opposite direction (Nakayama and Watanabe, 2004). At the eastern sea boundary (Bohai Sea), a constant head was set at 0 m. The hydraulic head values parallel to the ground level were input as the initial conditions for the groundwater flow submodel. In the 1747 river cells including the Yellow, Dugai (Tuhai), Majia, Fuyang, Hutuo, Ziya, Daqing, Yongding, and Hai (Haihe) rivers (Fig. 2.1), inflows or outflows from the riverbeds were considered depending on the difference in the hydraulic heads of the groundwater and the river. The time-series of observed river discharge at Huayuankou, Henan Province (R-13 in Table 2.3; 34.92°N, 113.65°E, mean elevation of 104 m), beside the lower reaches of the Yellow River, was also inputted into the model (China Institute for Geo-Environmental Monitoring, 2003). For the simulation of the groundwater trend, it can be assumed that the industrial water usage in 1959 was almost zero, along the lines of Nakayama *et al*. (2006). Although some water usage data beginning in 1992 were available, they were not as detailed as the statistical data contained in Table II. Therefore, the second-order curve of the year was estimated from the two periods between 1959 and 1987–1988 to represent a curve of economic conditions, such as GDP; the interpolated values were then applied to data for 1975 and 1992 (Nakayama *et al*., 2006). A constant chloride concentration of 34 psu was set at the first layer of the seabed and at the eastern boundary of the Bohai Sea for the saltwater simulation, as reported in a previous research (Zhang *et al*., 1990) (Fig. 2.1).

Table 2.3. Observation stations cited for validation.

No.	Point Name	Type	Lat. (°)	Lon. (°)	Elev. (m)
R-1	Haihezha (Hai River)	River Discharge	39.02	117.72	4.0
R-2	Yanqing Guanting Reservoir (Yongding River)	River Discharge	40.23	115.60	436.0
R-3	Yanchi (Yongding River)	River Discharge	40.03	115.88	314.0
R-4	Sanjiadian (Yongding River)	River Discharge	39.97	116.10	195.0
R-5	Xingaifang (Daqing River)	River Discharge	39.08	116.03	16.0
R-7	Luobaotan (Juma River)	River Discharge	39.57	115.72	93.0
R-10	Xianju (Ziya River)	River Discharge	38.23	116.10	15.0
R-11	Jiugaozhuang (Ziya River)	River Discharge	38.52	116.50	12.0
R-12	Yangliuqing (Ziya River)	River Discharge	39.13	117.00	5.0
R-13	Huayuankou (Yellow River)	River Discharge	34.92	113.65	104.0
R-14	Juancheng (Yellow River)	River Discharge	35.93	115.90	1.0
R-15	Lijin (Yellow River)	River Discharge	37.52	118.30	1.0
S-1	Luancheng	Soil Moisture	36.88	114.67	40.0
S-19	Xinxian	Soil Moisture	35.17	113.82	85.0
S-33	Zhengzhou	Soil Moisture	34.82	113.67	99.0
G-1	Luancheng	Groundwater Level	37.90	114.56	55.0
G-2	Handan City	Groundwater Level	36.60	114.41	85.0
G-3	Cangzhou	Groundwater Level	38.30	116.90	7.0
G-4	Daming	Groundwater Level	36.30	115.30	50.0
G-5	Nangong	Groundwater Level	37.20	115.60	38.0
G-6	Guangzong	Groundwater Level	36.90	115.20	40.0
G-7	Wuji	Groundwater Level	38.20	114.90	45.0
G-8	Rongcheng	Groundwater Level	39.00	116.00	7.0
G-9	Langfang	Groundwater Level	39.50	116.70	18.0
G-10	Bazhou	Groundwater Level	39.10	116.60	6.0
G-11	Xianxian	Groundwater Level	38.10	116.20	8.0
G-12	Huanghua	Groundwater Level	38.30	117.60	3.0
G-13	Shenzhou	Groundwater Level	37.90	115.70	16.0

The simulation area was 530 km in width by 840 km in length, with a grid spacing of 5 km in the Albers co-ordinates; this area covered almost the entire Hai River catchment and the lower reaches of the Yellow River. The vertical layer was discretized in thickness with depth, with each layer increasing in thickness by a factor of 1.1. The upper layer was set at a depth of 2 m, and the 20th layer was defined as an elevation of –400 m from the sea surface. The NICE-CNL simulation was performed on an NEC SX-6 supercomputer. The simulations were performed from January 1, 1987, through December 31, 1988. In agricultural fields, the NICE-CNL automatically simulated the winter wheat and maize rotations, following the sequence of 1987 winter wheat, 1987 maize, 1988 winter wheat, and 1988 maize. Automatic irrigation was chosen to simulate the theoretical water requirements of the two crops. This method calculates the theoretical water requirements at various sites on the basis of differences in soil conditions and local weather conditions, particularly precipitation. To determine a realistic amount of crop water usage, the author considered that the ratios of agricultural area to the total area and of the irrigated area to the total agricultural area obtained through published statistics (Governmental Office of Hebei Province, 1988, 1989; Hebei Department of Water Conservancy, 1987, 1988) would yield practical spatial water usage. The irrigated ratio was included at each grid point to input a more accurate amount of water usage into the NICE-CNL (Nakayama *et al*., 2006).

The first six months of the study were used as a warm-up period until equilibrium water levels were reached, and parameters were estimated by a comparison of simulated steady-state values in a steady-state condition with previously published observed values (Clapp and Hornberger, 1978; Rawls *et al*., 1982). A time step of Δt = 6 h was used. The simulations were validated by previously observed data for river discharge (12 points; Hai River and Yellow River Conservancy Committees, 1987, 1988), soil moisture (3 points of the Global Soil Moisture Data Bank; Entin *et al*., 2000; Robock *et al*., 2000), and groundwater level (13 points; China Institute for Geo-Environmental Monitoring, 2003) (Fig. 2.1 and Table 2.3). Moreover, the author calibrated and validated data for winter wheat in 1991–1992 and for maize in 1990 to develop genetic parameters for obtaining an accurate simulation of agricultural water usage in 1987–1988 (Nakayama *et al*., 2006).

2.4 Results and Discussion

2.4.1 River Discharge Affected by Dam and Canal Systems

Through previous comparison of simulated results for *LAI*, soil moisture, and irrigation water usage with the observed values for winter wheat and summer maize, the author showed that the NICE-AGR excellently reproduced the observed values (*Cor* = 0.97 for winter wheat, and *Cor* = 0.99 for summer maize) (Nakayama *et al*., 2006). In addition, to estimate spatial crop water usage, the simulated crop coefficients (K_c) for both crops were compared with the values observed in a previous research (Chen *et al*., 1995). This author's previous study suggested a relative reliability of the water usage simulated by the NICE-CNL (Nakayama, 2011a). This method is also effective for providing better evaluation of hydrological trends in longer periods including, the "evaporation paradox" (Roderick and Farquhar, 2002), together with observation networks because, depending on growing stage and type of crop, the model does not require a crop coefficient for the calculation of actual evaporation. In addition, simulation is direct and does not require detailed site-specific information or empirical relations to calculate effective precipitation (Nakayama, 2011a; Nakayama et al., 2006).

Fig. 2.3 compares the simulated river discharges with the observed values (Hai River and Yellow River Conservancy Committees, 1987, 1988) in the Hai and Yellow River catchments from January 1, 1987, to December 31, 1988. The correlation between the observed value and the simulated value *Cor* and the Nash–Sutcliffe Criterion *NS* (Nash and Sutcliffe, 1970) are also plotted in this figure. The model yields an excellent reproduction of the observed values in the lower reaches of the Yellow River, indicating that less water is discharged downstream mainly because more than 90% of the total withdrawal is for agriculture (Cai, 2006) (Fig. 2.3a; R-14 and 15 in Table 2.3; *Cor* = 0.83 and 0.96, *NS* = 0.66 and 0.90). At the downstream point at Lijin (R-15 in Table 2.3; 37.52°N, 118.30°E), the river discharge dries out during the spring mainly because most of the water is used for the irrigation of winter wheat. This finding is also related to the fact that groundwater cannot be used for irrigation because it is highly contaminated by total dissolved solids (TDS) and seawater intrusion (Brown and Halweil, 1998; Shimada, 2000; Liu *et al*., 2001; Chen *et al*., 2003; Nakayama *et al*., 2006), as described in the following section.

In the Hai River catchment, the simulated result correlates well with the observed value in the river where no dams are present upstream (Fig. 2.3b; R-7 in Table 2.3; *Cor* = 0.64, *NS* = 0.39). The simulated result for case-1, which includes only natural rivers, does not agree well with the observed value in the river where dams are constructed upstream (Fig. 2.3c; R-3 in Table 2.3; *Cor* = -0.48, *NS* = -3.81). The NICE-CNL result for case-2, which includes dam and canal systems, can excellently reproduce the observed value (*Cor* = 0.92, *NS* = 0.84). Although the simulated value agrees reasonably with the seasonal trend of the observed value in the main channel in the downstream area of the Hai River, the reproduction is less accurate (Fig. 2.3d; R-1 in Table 2.3; *Cor* =0.51, *NS* =0.20), indicating that the complicated processes of seasonal water withdrawal for irrigation and water transfer in the dam and canal systems, in addition to the natural rivers, can be generally reproduced. This difference is also related to the accuracy of the relatively scattered observation variety in base flow or mean flow data. This inaccuracy may be attributed to research differences and the method or standard of observation. The simulated result generally agrees well with the previous finding (Wang *et al*., 2004); in other words, flood resourcification ability is very high in the Hai River and less water enters the Bohai Sea (Nakayama, 2011a).

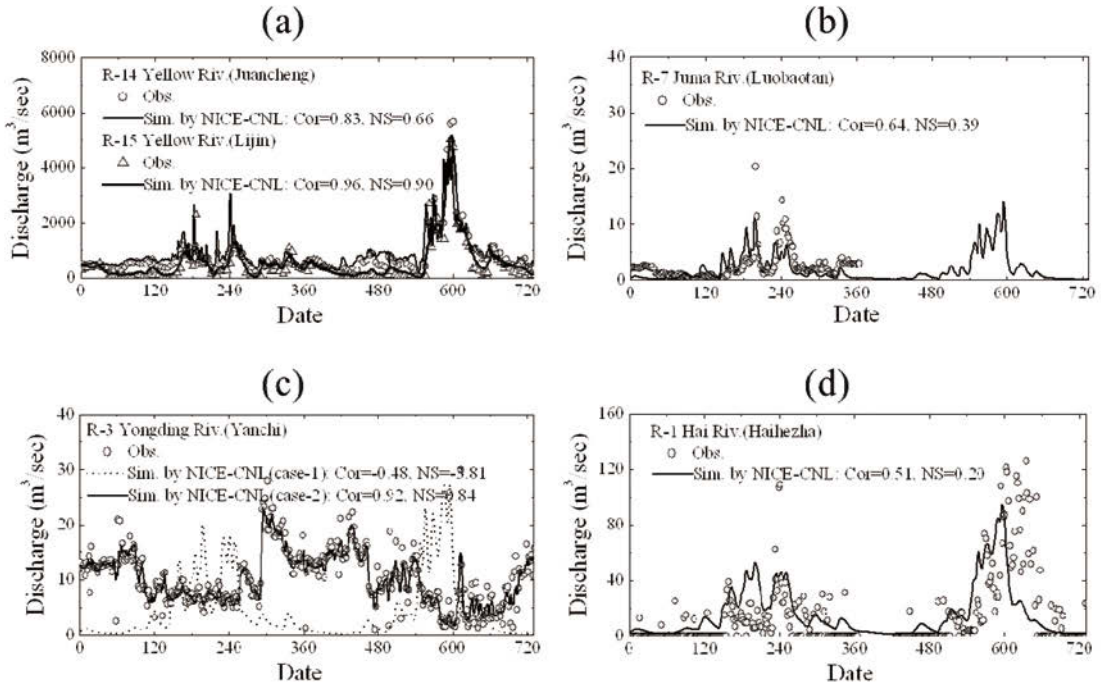

Fig. 2.3 Simulated and observed river discharges in the Hai and Yellow River catchments from January 1, 1987, to December 31, 1988, at (a) Juancheng and Lijin rivers downstream of the Yellow River (R-14 and 15 in Table 2.3), (b) the Luobaotan River (R-7 in Table 2.3), (c) the Yanchi River (R-3 in Table 2.3), and (d) the Haihezha River (R-1 in Table 2.3) at the Hai River catchment. Open circles and triangles represent observed values, and lines and dotted lines represent simulated values. *Cor* indicates the correlation between observed and simulated values, and *NS* indicates the Nash–Sutcliffe criterion.

2.4.2 Groundwater Level

The NICE-CNL simulates the changes in the groundwater levels over the previous half-century (Fig. 2.4). The NICE-AGR simulation used in a previous study (Fig. 2.4b) (Nakayama *et al*., 2006) excellently reproduced the observed groundwater levels (Fig. 2.4a) (Shimada, 2000) during the same period and showed a yearly decrease in water table levels; this is because the simulation included the effects of irrigation in the NCP. Hydraulic gradients were steeper near the Taihang and Yanshan mountains and were relatively flat in the plain area. Because the groundwater level is higher in the mountainous areas, groundwater constantly flows into the plain, and the mountainous area plays an important role as a recharge region. NICE-AGR was unable to reproduce cone depressions that occurred near major cities including Cangzhou, Hengshui, and Baoding because groundwater usage was excessive in 1975 and 1992, and this model does not consider industrial water usage in the area (Fig. 2.4b). The NICE-CNL more accurately reproduced these cone depressions because the new model explicitly includes processes for industrial and domestic water usage (Fig. 2.4c). Moreover, the NICE-CNL excellently reproduced observed groundwater fluctuations in a similar manner as that by NICE-AGR; these fluctuations are listed in Table 2.3 (China Institute for Geo-Environmental Monitoring, 2003) (Nakayama *et al.*, 2006). This is because this improved model can simulate both infiltration in non-agricultural periods and pumping in agricultural periods. Groundwater levels generally recede from March to June–July mainly as a result of winter wheat production. The levels begin to recover with the onset of the monsoons. The simulated groundwater levels accurately reproduce actual levels in both the mountainous and plain areas because the author used a 3-D groundwater submodel. In addition, SiB2 used for natural regions (Nakayama and Watanabe, 2004) and DSSAT for agricultural regions can correctly simulate the recharge rates in the upper layer, as described in Chapter 1 (Nakayama, 2011a; Nakayama *et al*., 2006).

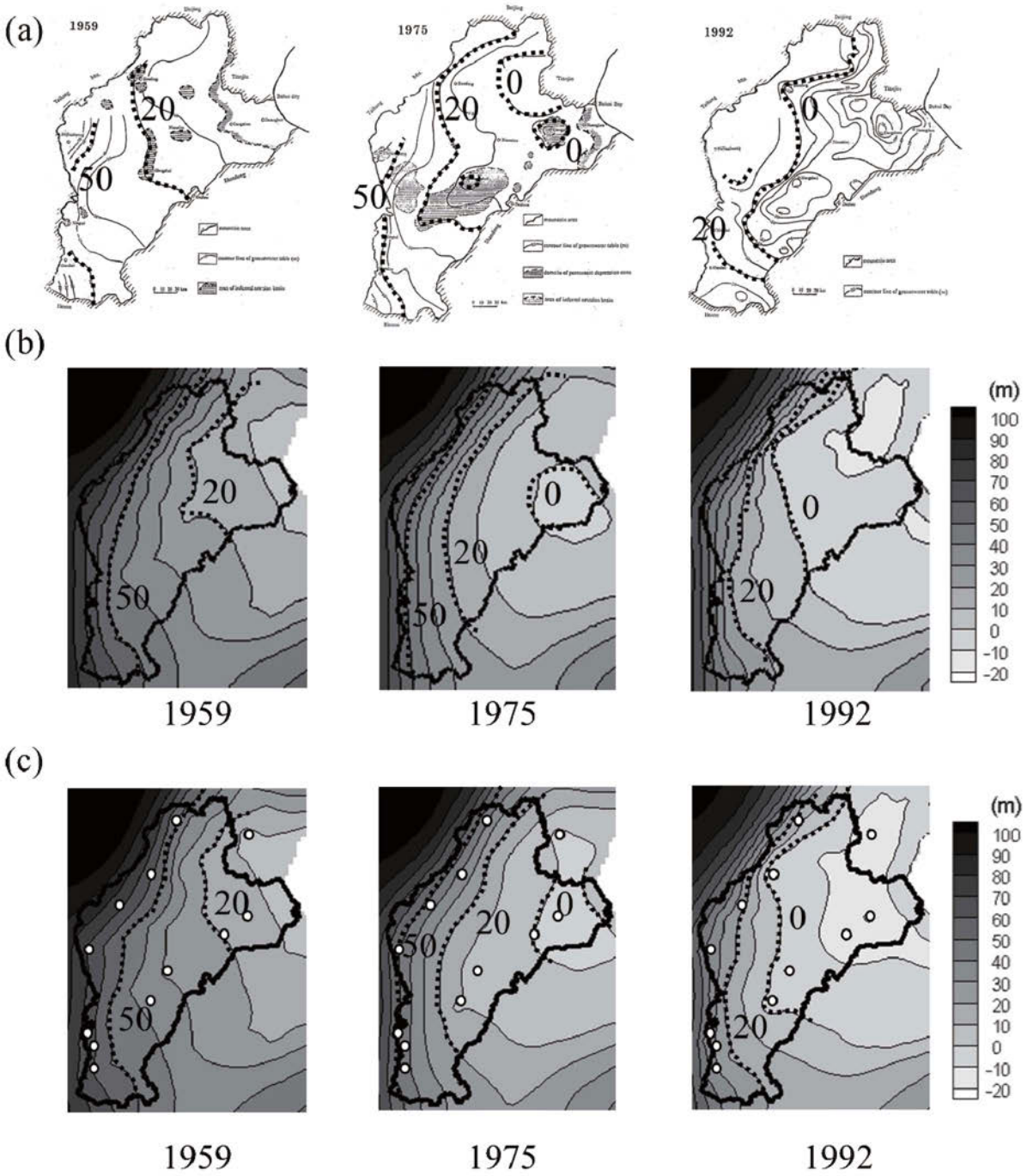

Fig. 2.4 Annually averaged groundwater levels in the NCP from 1959 to 1992 illustrating (a) observed value, (b) simulated result with only irrigation water usage, and (c) simulated result with irrigation and urban water usage. Bold lines represent the NCP borders, and dotted lines indicate the groundwater levels at 0 m, 20 m, and 50 m above sea level. In (c), circles represent the main cities where water usage in urban areas is predominant, as described in Table 2.2.

2.4.3 Hydrologic Changes and Ecosystem Degradation Caused by Human Intervention

Groundwater levels in the study area have receded dramatically over the previous half-century owing to over-pumping of groundwater. Therefore, seawater intrusion into the aquifers has a greater impact on agriculture near the coastal regions because saltwater cannot be used for agriculture or for domestic use (Brown and Halweil, 1998; Shimada, 2000; Liu *et al*., 2001; Chen *et al*., 2003; Nakayama *et al*., 2006). The tidal range in the Bohai Sea—where the difference in spring tide $M_2 + S_2 + K_1 + O_1$ is about 1 m at the mouth of the Yellow River and 4 m outside the Bohai Sea (Ogura, 1933),—also greatly affects this intrusion, particularly at spring tide. Therefore, if the area of seawater intrusion can be evaluated both qualitatively and quantitatively, the population will be able to use shallow and deep aquifers more efficiently to prevent groundwater degradation in this area. The NICE-CNL spatially simulates the intrusion of seawater in the NCP (Fig. 2.5). The simulated results are similar to previous data for the NCP (1:4,500,000) (Institute of Hydrogeology and Engineering Geology of the National Geology Bureau, 1980). The high concentration area in shallower groundwater expands to surround the Bohai Sea, which indicates a degradation of groundwater quality due to seawater intrusion. In addition, the results indicate that a wedge-shaped body of denser seawater develops beneath the lighter freshwater (Essaid, 1990). The simulated result shows that in addition to groundwater degradation, excessive groundwater use for agriculture, industry, and domestic purposes has a substantial effect on the intrusion of seawater in the aquifer.

The spatial distributions of NDVI calculated by using NOAA/AVHRR satellite images were similar to the results of previous research (NASA, 2006; data not shown). Because NDVI is linearly related to CGR (Calera *et al*., 2004; Nakayama, 2011b), the spatial distribution of this value is a good indicator of the rate of crop production. It is interesting that the NDVI in the cultivated field has a smaller value beside the Bohai Sea compared to the value inland, which is closely correlated with the higher regions of TDS observed in previous studies (Fei, 1997; Kondoh and Oyamada, 2000). To examine spatial patterns in NDVI trends in 1982–1999 in the NCP, the author further estimated the linear trend of monthly NDVI in the grain filling season for winter wheat in May over the study period using an ordinary least-squares regression method for each pixel (Fig. 2.6). The NDVI gradient was spatially heterogeneous, corresponding well to the regional distribution of water resources. The NDVI in irrigated and non-irrigated cultivated fields is smaller beside the Bohai Sea (Pt. I) than it is inland (Pt. II); this is because of several effects, including groundwater degradation (Fig. 2.4), seawater intrusion (Fig. 2.5), and rapid urbanization surrounding major cities (Kondoh and Oyamada, 2000), which has decreased the NDVI yearly owing to the decrease in river discharge. Mountainous and plain areas upstream of the Hai River have higher NDVI values than those observed in downstream areas. This tendency was also seen in the grain filling season for summer maize (August) (data not shown). This finding is closely connected to water shortages and seawater intrusion (Nakayama, 2011a) (Figs. 2.4 and 2.5), which have greatly reduced crop growth and production in coastal areas (Ayers and Westcot, 1985; Warrence *et al*., 2002).

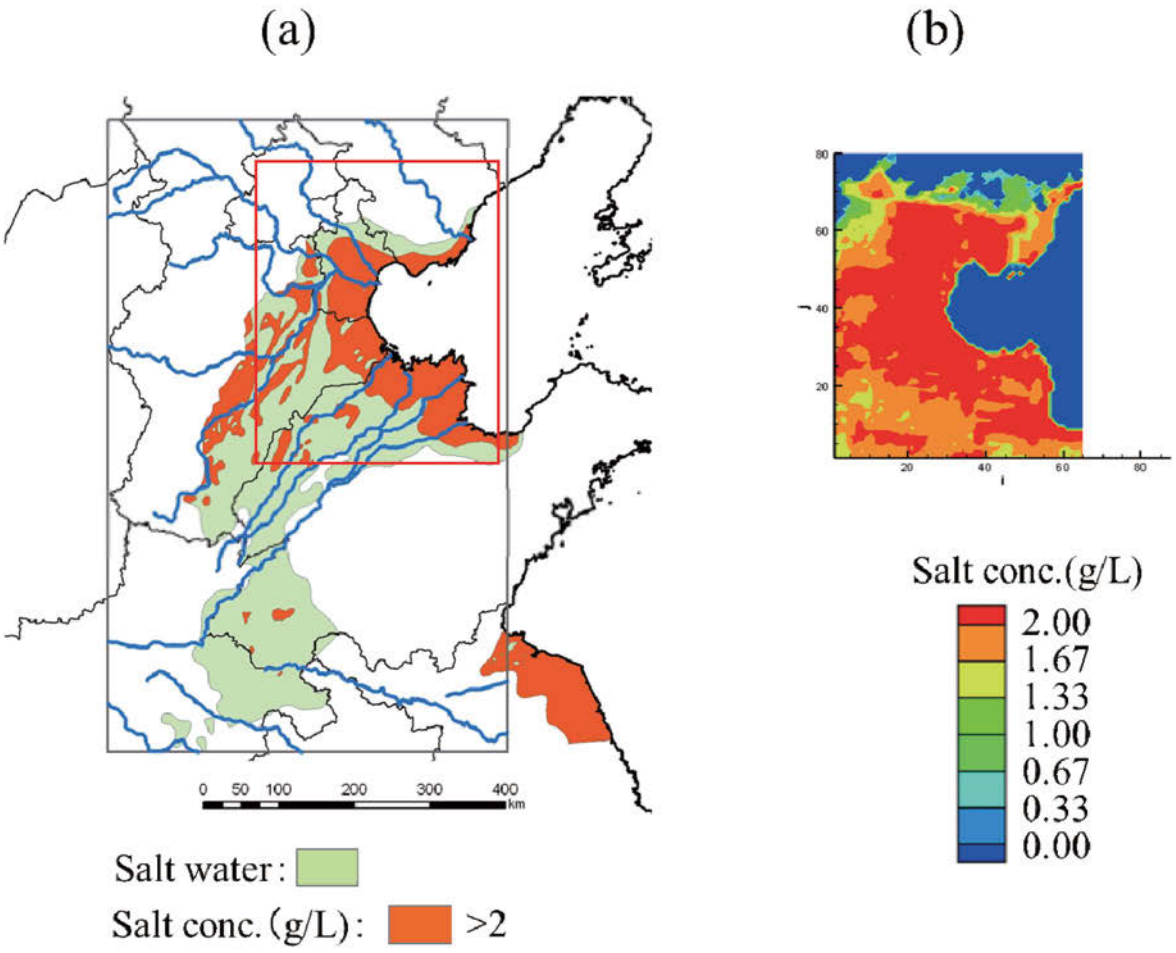

Fig. 2.5 Annually averaged contour of seawater intrusion in the NCP illustrating (a) observed value in the shallower groundwater. In (b), the annually averaged simulation result of NICE-CNL corresponds to the red square in (a).

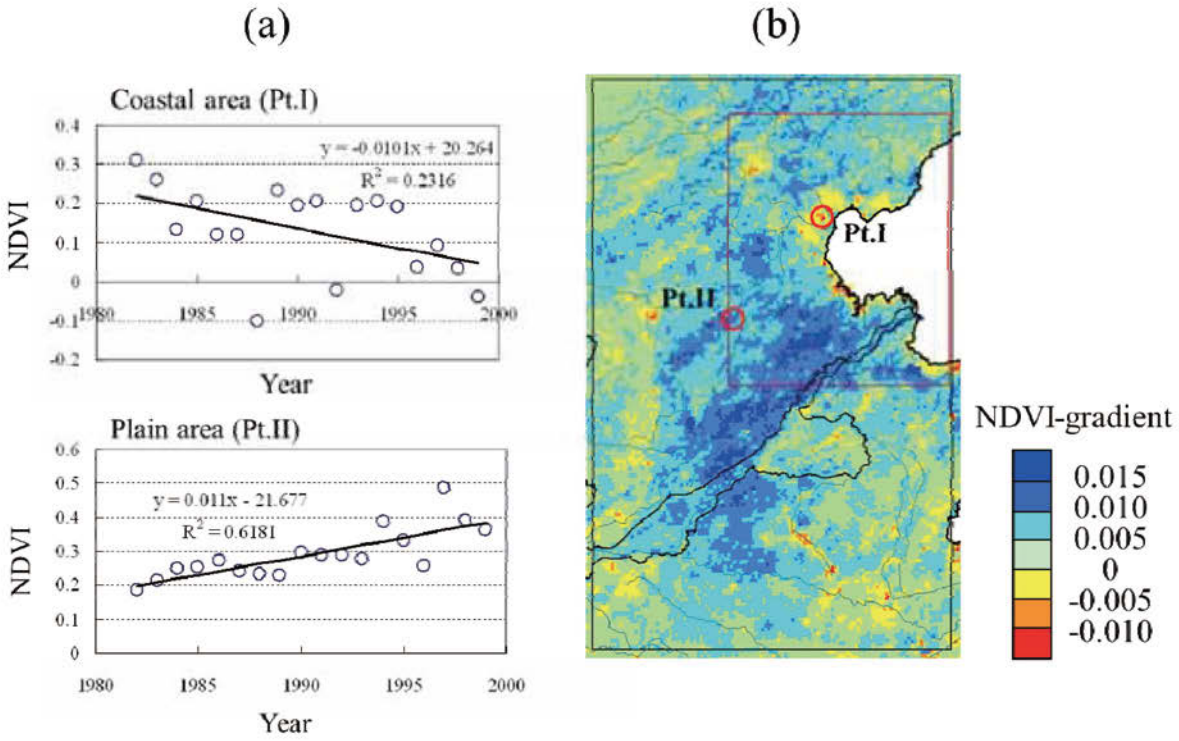

Fig. 2.6 NDVI in the NCP illustrating (a) the trend of NDVI in the grain filling season for winter wheat in May, both in the coastal (I) and plain (II) areas, and (b) spatial patterns in NDVI gradient in the NCP in 1982-1999. The bold line in (a) indicates a least-square regression line estimated from monthly NDVI in May (circle). In (b), the black square represents the border of the simulation area in a similar manner at that shown in Fig. 2.1; the red square represents the simulation area of seawater intrusion, as shown in Fig. 2.5.

2.5 Conclusion

Through simulation, this study addressed an important topic in a rather complicated and diverse water system in the NCP that included the hydrological processes of dried rivers, agricultural–urban water usage, groundwater pumping, seawater intrusion, and dam–canal effects. For the first time, the author combined the NICE model series with more complicated components such as urban water usage, saltwater simulation, and dam–canal systems (NICE-CNL) in order to simulate the effects of human intervention on hydrological changes in the catchments. This simulation clarified the relationship between the drying of rivers, groundwater degradation, seawater intrusion, and ecosystem degradation.

References

Ayers R.S., Westcot D.W. (1985) Water quality for agriculture. FAO Irrigation and Drainage Paper, 29, Food and Agriculture Organization of the United Nations, Rome, Italy. http://www.fao.org/DOCREP/003/T0234E/T0234E00.HTM#TOC.

Bacour C., Breon F.M., Maignan F. (2006) Normalization of the directional effects in NOAA–AVHRR reflectance measurements for an improved monitoring of vegetation cycles. Remote Sensing of Environment, 102, 402–413.

Brown L.R., Halweil B. (1998) China's water shortage could shake world food security. World Watch, 11(4), 10-18.

Cai X. (2006) Water stress, water transfer and social equity in Northern China: Implication for policy reforms. Human Development Report 2006, UNEP. http://hdr.undp.org/en/reports/global/hdr2006/papers/cai ximing.pdf.

Calera A., Gonzalez-Piqueras J., Melia J. (2004) Monitoring barley and corn growth from remote sensing data at field scale. International Journal of Remote Sensing, 25, 97-109.

Chen W. (1996) Preface. Geomorphology, 18, 1-4.

Chen J.Y., Tang C.Y., Sakura Y., Kondoh A., Shen Y.J. (2002) Groundwater flow and geochemistry in the lower reaches of the Yellow River: a case study in Shandang Province, China. Hydrogeology Journal, 10, 587-599.

Chen J.Y., Tang C.Y., Shen Y.J., Sakura Y., Kondoh A., Shimada J. (2003) Use of water balance calculation and tritium to examine the dropdown of groundwater table in the piedmont of the North China Plain (NCP). Environmental Geology, 44, 564-571.

Chen Y.M., Guo G.S., Wang G.X., Kang S.Z., Luo H.B., Zhang D.Z. (1995) Main crop water requirement and irrigation of China. Hydrologic and Electronic Press, Beijing, 73-102.

China Institute for Geo-Environmental Monitoring (CIGEM) (2003) China Geological Envoronment Infonet, Database of groundwater observation in the People's Republic of China. http://www.cigem.gov.cn.

Chinese Academy of Sciences (1988) Administrative division coding system of the People's Republic of China. Chinese Academy of Sciences, Beijing.

Clapp R.B., Hornberger G.M. (1978) Empirical equations for some soil hydraulic properties. Water Resources Research, 14, 601-604.

Entin J.K., Robock A., Vinnikov K.Y., Hollinger S.E., Liu S., Namkhai A. (2000) Temporal and spatial scales of observed soil moisture variations in the extratropics. Journal of Geophysical Research, 105(D9), 11865-11877.

Essaid HI. (1990) A multilayered sharp interface model of coupled freshwater and saltwater flow in coastal systems: model development and application. Water Resources Research, 26(7), 1431—1454.

Fei J. (1997) Groundwater of the North China Plain. Proceedings of International Symposium on Hydro-Environment in Asia. CEReS, China University, 25-32.

Geological Atlas of China (2002) Geological Publisher, Beijing (in Chinese).

Governmental Office of Hebei Province (1988) Hebei Agriculture Year Book in 1987. Economy Science Publishing House, Beijing (in Chinese).

Governmental Office of Hebei Province (1989) Hebei Agriculture Year Book in 1988. Economy Science Publishing House, Beijing (in Chinese).

Gower S.T., Kucharik C.J., Norman J.H. (1999) Direct and indirect estimation of Leaf Area Index, fAPAR, and net primary production of terrestrial ecosystems. Remote Sensing of Environment, 70, 29-51.
Guo H., Cai Y. (2000) Improving accomplishment of Hai river catchment in 50 years and view in future. Design of Water Resources & Hydroelectric Engineering (in Chinese).
Hai River Conservancy Committees (1987) Annual report of river discharge at Hai River. Interior report of the committee (in Chinese).
Hai River Conservancy Committees (1988) Annual report of river discharge at Hai River. Interior report of the committee (in Chinese).
Hebei Department of Water Conservancy (1987) Hebei year book of water conservancy for 1987. Department of Hebei Water Conservancy: Hebei, China (in Chinese).
Hebei Department of Water Conservancy (1988) Hebei year book of water conservancy for 1988. Department of Hebei Water Conservancy: Hebei, China (in Chinese).
Institute of Hydrogeology and Engineering Geology of the National Geology Bureau (1980) Hydrogeological map for the People's Republic of China. China Map Publishing House, Beijing (in Chinese).
Kogan F.N. (1990) Remote sensing of weather impacts on vegetation in non-homogeneous areas. International Journal of Remote Sensing, 11, 1405– 1419.
Kondoh A., Oyamada Y. (2000) Monitoring surface moisture and vegetation status by NOAA and GMS over north china plain. Advance in Space Research, 26(7), 1055-1058.
Lee T.M. (1996) Hydrogeologic controls on the groundwater interactions with an acidic lake in karst terrain, Lake Barco, Florida. Water Resources Research, 32, 831-844.
Liu C., Xia J. (2004) Water problems and hydrological research in the Yellow River and the Huai and Hai River basins of China. Hydrological Processes, 18, 2197-2210, doi:10.1002/hyp.5524.
Liu C., Yu J., Kendy E. (2001) Groundwater exploitation and its impact on the environment in the North China Plain. Water International, 26(2), 265-272.
Liu C., Zheng H. (2004) Changes in components of the hydrological cycle in the Yellow River basin during the second half of the 20th century. Hydrological Processes, 18, 2337-2345, doi:10.1002/hyp.5534.
Liu C.L., Xie G.D., Huang H.Q. (2006) Shrinking and Drying up of Baiyangdian Lake Wetland: A Natural or Human Cause? Chinese Geographical Science, 16, 314-319.
Liu L., Yang Z., Shen Z. (2003) Estimation of water renewal times for the middle and lower sections of the Yellow River. Hydrological Processes, 17, 1941-1950, doi:10.1002/hyp.1219.
Myneni R.B., Keeling C.D., Tucker C.J., Asrar G., Nemani R.R. (1997) Increased plant growth in the northern high latitudes from 1981 to 1991. Nature, 386, 698–702.
Nakayama T. (2008a) Factors controlling vegetation succession in Kushiro Mire. Ecological Modelling, 215, 225-236, doi:10.1016/j.ecolmodel.2008.02.017.
Nakayama T. (2008b) Shrinkage of shrub forest and recovery of mire ecosystem by river restoration in northern Japan. Forest Ecology and Management, 256, 1927-1938, doi:10.1016/j.foreco.2008.07.017.
Nakayama T. (2008c) Development of process-based NICE model and simulation of ecosystem dynamics in the catchment of East Asia (Part II), CGER's Supercomputer Monograph Report, 14, NIES, 91p., http://www-cger.nies.go.jp/publication/I083/i083.html.
Nakayama T. (2009) Simulation of ecosystem degradation and its application for effective policy-making in regional scale. In River pollution research progress, Mattia N. Gallo, Marco H. Ferrari (eds), 1-89 (Chapter 1), Nova Science Pub., Inc., New York.
Nakayama T. (2010) Simulation of hydrologic and geomorphic changes affecting a shrinking mire. River Research and Applications, 26(3), 305-321, doi:10.1002/rra.1253.
Nakayama T. (2011a) Simulation of complicated and diverse water system accompanied by human intervention in the North China Plain. Hydrological Processes, 25, 2679-2693, doi:10.1002/hyp.8009.
Nakayama T. (2011b) Simulation of the effect of irrigation on the hydrologic cycle in the highly cultivated Yellow River Basin. Agricultural and Forest Meteorology, 151, 314-327, doi:10.1016/j.agrformet.2010.11.006.
Nakayama T., Fujita T. (2010) Cooling effect of water-holding pavements made of new materials on water and heat budgets in urban areas. Landscape and Urban Planning, 96, 57-67, doi:10.1016/j.landurbplan.2010.02.003.
Nakayama T., Hashimoto S. (2011) Analysis of the ability of water resources to reduce the urban heat island in the Tokyo megalopolis. Environmental Pollution, 159, 2164-2173, doi:10.1016/j.envpol.2010.11.016.
Nakayama T., Watanabe M. (2004) Simulation of drying phenomena associated with vegetation change caused by invasion of alder (Alnus japonica) in Kushiro Mire. Water Resources Research, 40, W08402, doi:10.1029/2004WR003174.

Nakayama T., Watanabe M. (2006a) Simulation of spring snowmelt runoff by considering micro-topography and phase changes in soil layer. Hydrology and Earth System Sciences Discussions, 3, 2101-2144.
Nakayama T., Watanabe M. (2006b) Development of process-based NICE model and simulation of ecosystem dynamics in the catchment of East Asia (Part I), CGER's Supercomputer Monograph Report, 11, NIES, 100p., http://www-cger.nies.go.jp/publication/I063/I063.html.
Nakayama T., Watanabe M. (2008a) Missing role of groundwater in water and nutrient cycles in the shallow eutrophic Lake Kasumigaura, Japan. Hydrological Processes, 22, 1150-1172, doi:10.1002/hyp.6684.
Nakayama T., Watanabe M. (2008b) Role of flood storage ability of lakes in the Changjiang River catchment. Global and Planetary Change, 63, 9-22, doi:10.1016/j.gloplacha.2008.04.002.
Nakayama T., Watanabe M. (2008c) Modelling the hydrologic cycle in a shallow eutrophic lake. Verh International Verein Limnology, 30.
Nakayama T., Yang Y., Watanabe M., Zhang X. (2006) Simulation of groundwater dynamics in North China Plain by coupled hydrology and agricultural models. Hydrological Processes, 20(16), 3441-3466, doi:10.1002/hyp.6142.
Nakayama T., Watanabe M., Tanji K., Morioka T. (2007) Effect of underground urban structures on eutrophic coastal environment. Science of the Total Environment, 373(1), 270-288, doi:10.1016/j.scitotenv.2006.11.033.
Nakayama T., Sun Y., Geng Y. (2010) Simulation of water resource and its relation to urban activity in Dalian City, Northern China. Global and Planetary Change, 73, 172-185, doi:10.1016/j.gloplacha.2010.06.001.
Nakayama T., Hashimoto S., Hamano H. (in press) Multi-scaled analysis of hydrothermal dynamics in Japanese megalopolis by using integrated approach. Hydrological Processes.
NASA (2006) Visible earth. A catalog of NASA images and animations of our home planet. Drought in Northern China. http://visibleearth.nasa.gov/view_detail.php?id=17556.
Nash J.E., Sutcliffe J.V. (1970) Riverflow forecasting through conceptual model. Journal of Hydrology, 10, 282-290.
Ogura N. (1933) A tide inshore Japan. Japan Coast Guard's Report 7. Japan Coast Guard, Japan (in Japanese).
Piao S., Fang J., Zhou L. (2006) Variations in satellite derived phenology in China's temperate vegetation. Global Change Biology, 12, 672–685.
Rawls W.J., Brakensiek D.L., Saxton K.E. (1982) Estimation of soil water properties. Transactions of the ASAE, 25, 1316-1320.
Ritchie J.T., Singh U., Godwin D.C., Bowen W.T. (1998) Cereal growth, development and yield. In Understanding Options for Agricultural Production, Tsuji G.Y., Hoogenboom G., Thornton P.K. (eds). Kluwer, Great Britain, 79–98.
Robock A., Konstantin Y.V., Govindarajalu S., Jared K.E., Steven E.H., Nina A.S., Suxia L., Namkhai A. (2000) The global soil moisture data bank. Bulletin of the American Meteorological Society, 81, 1281-1299. http://climate.envsci.rutgers.edu/soil_moisture/.
Roderick M.L., Farquhar G.D. (2002) The cause of decreased pan evaporation over the past 50 years. Science, 298(15), 1410-1411.
Sato Y., Ma X., Xu J., Matsuoka M., Zheng H., Liu C., Fukushima Y. (2008) Analysis of long-term water balance in the source area of the Yellow River basin. Hydrological Processes, 22, 1618-1929. DOI:10.1002/hyp.6730.
Sellers P.J., Randall D.A., Collatz G.J., Berry J.A., Field C.B., Dazlich D.A., Zhang C., Collelo G.D., Bounoua L. (1996) A revised land surface prameterization (SiB2) for atomospheric GCMs. Part I : Model formulation. Journal of Climate, 9, 676-705.
Sellers P.J., Dickinson R.E., Randall D.A., Betts A.K., Hall F.G., Berry J.A., Collatz G.J., Denning A.S., Mooney H.A., Nobre C.A., Sato N., Field C.B., Henderson-Sellers A. (1997) Modeling the exchanges of energy, water, and carbon between continents and the atmosphere. Science, 275, 502-509.
Shimada J. (2000) Proposals for the groundwater preservation toward 21st century through the view point of hydrological cycle. Journal of Japan Association of Hydrological Sciences, 30, 63-72 (in Japanese).
Singh R.P., Roy S., Kogan F. (2003) Vegetation and temperature condition indices from NOAA AVHRR data for drought monitoring over India. International Journal of Remote Sensing, 24(22), 4393– 4402.
U.S. Geological Survey (1996) GTOPO30 Global 30 Arc Second Elevation Data Set. USGS. http://www1.gsi.go.jp/geowww/globalmap-gsi/gtopo30/gtopo30.html.
Wang Z., Wang X., Zhao F., Guo S., Hu S. (2004) The method of evaluation flood resources sustainable utilization capacity. Proceeding of Disaster Prevention Research Institute, Kyoto University. http://www.wrrc.dpri.kyoto-u.ac.jp/~aphw/APHW2004/proceedings/JSD/56-JSD-A616/56-JSD-A616(resubmit).pdf.

Warrence N.J., Bauder J.W., Pearson K.E. (2002) Basics of salinity and sodicity effects on soil physical properties. Department of Land Resources and Environmental Sciences, Montana State University – Bozeman. http://waterquality.montana.edu/docs/methane/basics.shtml#Salinity.

WebPaNDA (2008) NOAA AVHRR 10-days composite database over East Asia. University of Tokyo. http://webpanda.iis.u-tokyo.ac.jp/.

Xia J., Wang Z., Wang G., Tan G. (2004) The renewability of water resources and its quantification in the Yellow River basin, China. Hydrological Processes, 18, 2327-2336, doi:10.1002/hyp.5532.

Yang D., Li C., Hu H., Lei Z., Yang S., Kusuda T., Koike T., Musiake K. (2004) Analysis of water resources variability in the Yellow River of China during the last half century using historical data. Water Resources Research, 40, W06502, doi:10.1029/2003WR002763.

Yang L., Wylie B.K., Tieszen L.L., Reed B.C. (1998) An analysis of relationships among climate forcing and time-integrated NDVI of grasslands over the U.S. Northern and Central Great Plains. Remote Sensing of Environment, 65, 25-37.

Yellow River Conservancy Committees (1987) Annual report of river discharge at Yellow River. Interior report of the committee (in Chinese).

Yellow River Conservancy Committees (1988) Annual report of river discharge at Yellow River. Interior report of the committee (in Chinese).

Yin C.Q., Lan Z.W. (1995) The nutrient retention by ecotone wetlands and their modification for Baiyangdian Lake restoration. Water Science and Technology, 32, 159-167.

Zhang J., Huang W.W., Shi M.C. (1990) Huanghe (Yellow River) and its estuary: sediment origin, transport and deposition. Journal of Hydrology, 120, 203-223.

Zhou L.M., Tucker C.J., Kaufmann R.K., Slayback D., Shabanov N.V., Myneni R.B. (2001) Variations in northern vegetation activity inferred from satellite data of vegetation index during 1981 to 1999. Journal of Geophysical Research, 106(D17), 20069-0083.

Zhou L., Kaufmann R.K., Tian Y., Myneni R.B., Tucker C.J. (2003) Relation between interannual variations in satellite measures of vegetation greenness and climate between 1982 and 1999. Journal of Geophysical Research, 108(D1), 4004, doi:10.1029/2002JD002510.

Zhu Y. (1992) Comprehensive hydro-geological evaluation of the Huang-Huai-Hai Plain. Geological Publishing House of China, Beijing (in Chinese).

Chapter 3

Relation Between Water Resource and Urban Activity in Dalian

Abstract

The National Integrated Catchment-based Eco-hydrology (NICE) model was applied to the Biliu River catchment in northern China to estimate the relationship between its water resource and urban activity in the city of Dalian. NICE reasonably reproduced hydrologic budgets following the construction of a reservoir at the middle reach of the river, which is an important source of water for urban areas. Further, the model accurately backcasted the degradation of water resources in the form of river discharge and groundwater after the completion of the reservoir. The normalized difference vegetation index (NDVI) estimated from satellite data clearly showed vegetation degradation downstream of the reservoir. Statistical analysis of a decoupling indicator based on the simulated water-carrying capacity and satellite data of the vegetation index indicated that water-related stress in Dalian has increased in accordance with the environmental degradation below the reservoir, although Dalian's economy has grown rapidly since the completion of the reservoir. These results indicate a close relationship between water resources and economic growth, which has adversely affected the ecosystem to create a significant burden on the environment in the catchment and surrounding area. The simulated results highlight a close linkage between development in the urban area and sustainable water resource management. Moreover, this process-based model is important for the planning and execution of strategies to sustain social and economic development while ensuring ecosystem integrity.

Keywords: water stress, carrying capacity, ecosystem degradation, decoupling indicator, sustainable development, integrated catchment-based eco-hydrology model

3.1 Introduction

The demand for water in northern China has resulted in intensified water usage conflicts between upstream and downstream areas and between agricultural and municipal–industrial sectors (Nakayama *et al.*, 2006; Nakayama, 2011a). Several researchers have reported that China's demand for natural resources already exceeds the environment's capacity to sustain this densely populated land (Niu and Harris, 1996; Varis and Vakkilainen, 2001). In particular, more than 20,000 small catchments in China play important roles in supporting local development and maintaining local ecosystem functions (Shi *et al*., 2002; Geng *et al*., 2010). However, few studies have examined changes in water and heat dynamics, mainly because of a lack of data for quantifying complex phenomena related to human activities (Nakayama *et al.*, 2010).

The Biliu River catchment (2814 km^2), located in the southern region of Liaoning Province, is a heavy industrial base in northeast China (Fig. 3.1). Biliu, one of the largest rivers in southern Liaoning with a total length of 156 km, is the primary water source for Dalian, which has a population of more than 6 six million people and thousands of industries. Because Dalian is located at the southern tip of the Liaodong Peninsula, flanked on the East and West with the Yellow and Bohai seas, respectively, the region has limited access to fresh water. Therefore, its rapid economic growth has been supported by increased consumption of water transferred from remote fields (Fig. 3.2). The GDP increased relative to water consumption until 1991 (Fig. 3.2a), at which time the Dalian Municipal Government announced its new "Building an International City" policy (Dalian Planning Committee, 2001). Thereafter, Dalian entered a high-growth period, and the GDP increased more than tenfold in 1992–2007, which is attributed to overseas funding (Dalian Planning Committee, 2001). However, water consumption increased at a substantially slower rate. Although Dalian was the first city in China to receive an award from the United Nations Environment Programme's (UNEP) Global 500 Forum (UNEP, 2001) and was honored as a "Water-saving City" in 2002, the conflict between water supply and demand has exacerbated in recent years (Zhang and Xiong, 2006). The shortage of urban water has greatly influenced the development of the city and affected the lives of its residents, becoming the main obstruction to sustainable development of economy and society (Han *et al*., 2008). Most of the city's water (Fig. 3.2b) is drawn from Biliu Reservoir, in the middle of the river. Since the completion of the dam and reservoir in 1984, most of the water has been piped to Dalian, and the catchment has changed from water-rich to water-poor (Fig. 3.2c), as evidenced by the drying of the river downstream, receding of groundwater levels, and seawater intrusion, all of which have also been observed in other regions of northern China (Qian and Zhu, 2001; Ren *et al*., 2002; Nakayama *et al*., 2006; Nakayama, 2011a). To address the severe shortage of various natural resources, including water, a national policy known as Circular Economy was introduced in China around 2000 and was enacted into a law in 2008 (Ministry of Environmental Protection, 2008). Through this legislation, effective and efficient use and recycling of resources such as water and industrial waste were strengthened. In the city's 11th five-year plan for economic and social development in 2006, the Dalian government implemented a local circular economy plan that aimed to cut water consumption about 20% per million GDP (RMB) (Dalian City Government, 2006).

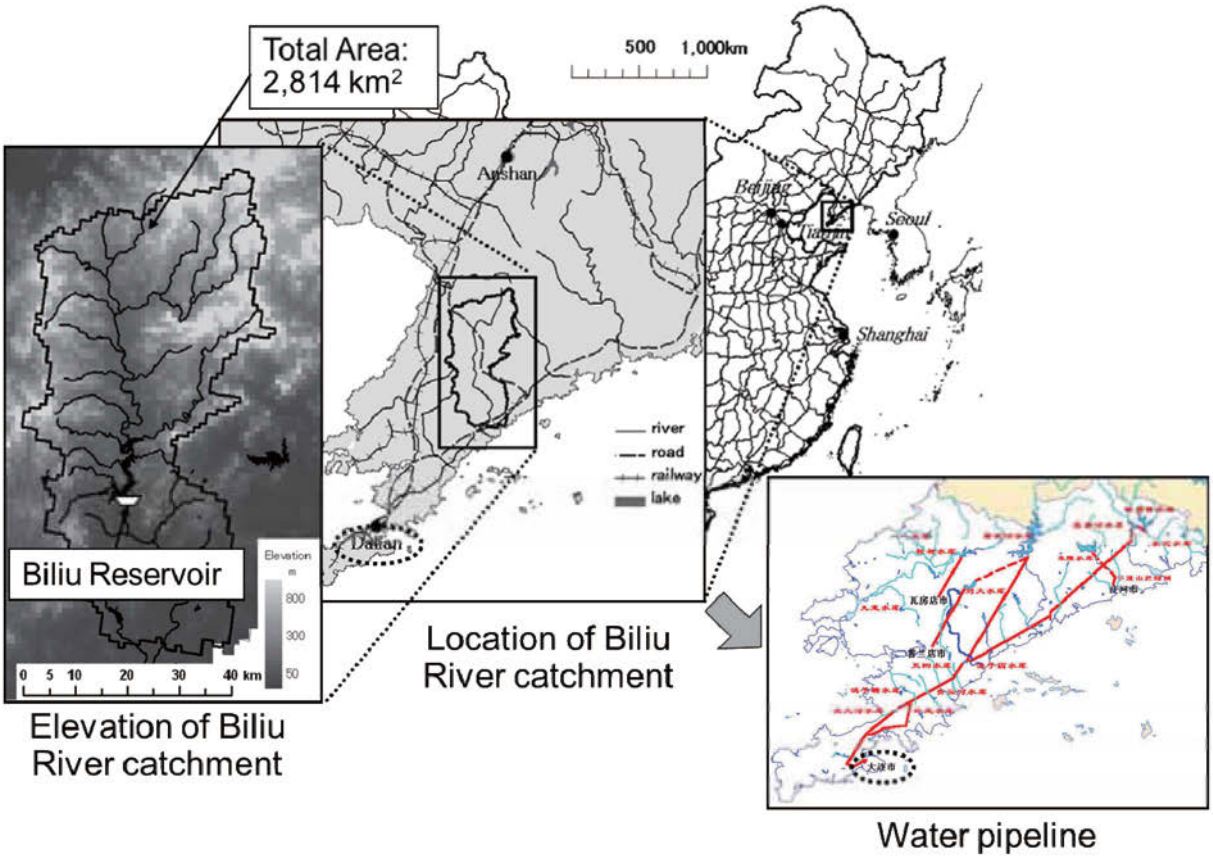

Fig. 3.1 Location of study area and elevation of the Biliu River catchment and Dalian. The bold black line represents the catchment border.

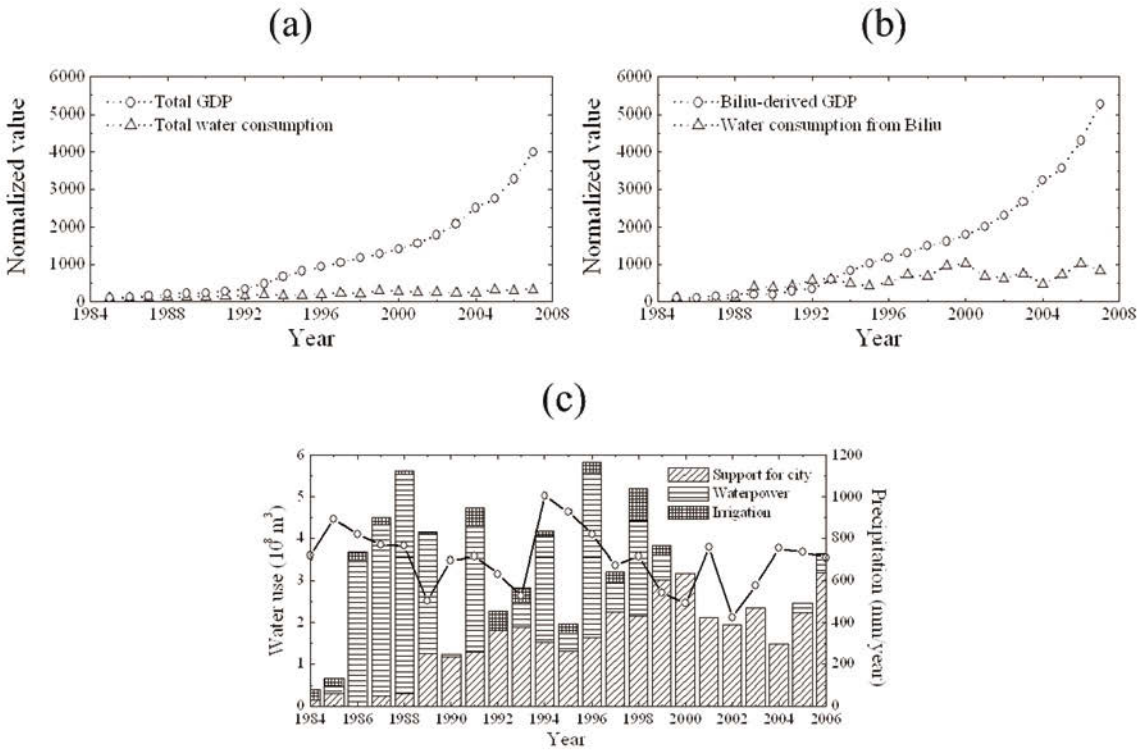

Fig. 3.2 Annual time series of GDP and water consumption in Dalian after the completion of Biliu Reservoir illustrating (a) GDP and water consumption in the entire city of Dalian, (b) GDP and water consumption in the urban area of the city, and (c) water intake from Biliu Reservoir. The values for GDP and water consumption were plotted on the basis of values reported in 1985 (value at 1985 = 100) in (a) and (b). Rainfall anomalies at the reservoir are plotted along the right-hand y-axis in (c).

Although remote sensing derived from satellite images has been used for decades to assess and monitor vegetation health in many regions of the world, few such studies have been conducted on northeast China, except for those that map cropping patterns in east China (Nagatani *et al*., 2002), infer forest phenological patterns from moderate resolution imaging spectroradiometer (MODIS) data in northeast China (Yu *et al*., 2005), and relate variations in the NDVI according to climate (Piao *et al.*, 2004, 2006). However, remote sensing has not been used to assess vegetation changes relative to water resources in the Biliu River catchment. The ability to meet the water demands of its swelling city and industries without undermining its own agriculture and the local ecosystem is the biggest challenge for the Dalian government. The integrated management of water quantity and quality, along with institutional arrangements and land-use planning, is essential for sustaining social and economic development while ensuring ecosystem integrity (He and Chen, 2001; Mitchell, 2005).

Decoupling analysis has become a popular approach that has been used widely among scholars and policy makers during the past decade (OECD, 2001). To identify the relationship between economic growth and environmental pressure, OECD (2001, 2002) explored a conceptual framework of decoupling indicators for the global economy related to climate change, air pollution, water quality, waste management, material use, and natural resources such as water, in addition to specific sectors in energy, transportation, agriculture, and manufacturing. Decoupling indicators are primarily intended to track various environmental problems for a single country or region such as Europe, the Pacific, and certain provinces and prefectures. OECD (2002) analyzed temporal changes in the relationship between environmental pressures and economic growth in those countries belonging to the organization. Moreover, the decoupling analyses of these parameters, including energy usage (Brown-Santirso and Thornley, 2006), transportation demands (Tight *et al*., 2004; OECD, 2004), carbon dioxide emissions (Lua *et al*., 2007), and metal consumption (Halada *et al*., 2007), were conducted in many developed countries. For example, Tachibana *et al*. (2008) performed a case study of material flow on a regional scale. For water resource environment analysis, Gleick (2000, 2002) decoupled economic development from increased water consumption in the United States. However, few decoupling analyses for economic growth, water consumption, and environmental degradation on a regional scale or for a catchment coupling with natural sciences are available.

The objective of this chapter is to evaluate the link between urban development in Dalian and sustainable water resource management in the Biliu River catchment (Nakayama *et al.*, 2010). The author first applied the process-based NICE model (Nakayama, 2008a, 2008b, 2008c, 2009, 2010, 2011a, 2011b; Nakayama and Fujita, 2010; Nakayama and Hashimoto, 2011; Nakayama and Watanabe, 2004, 2006a, 2006b, 2008a, 2008b, 2008c; Nakayama *et al*., 2006, 2007, 2010, in press) (Fig. 1.2) to the Biliu River catchment to estimate decadal changes in water resources since the completion of the Biliu Reservoir. The author then used NOAA/AVHRR satellite imagery analysis to evaluate the simulated result relative to the environmental degradation downstream of the reservoir in a similar manner as that described in Chapter 1. Finally, the author statistically analyzed a decoupling indicator based on the estimated water-carrying capacity to evaluate water-related stress against economic development in Dalian. This integrated assessment of the interactions between the water source and demand supports effective strategies and planning for sustainable development in the catchment (Nakayama *et al.*, 2010).

3.2 Methods

3.2.1 Hydrologic Budget

An accurate evaluation of the amount of water that can be drawn from Biliu Reservoir for use in Dalian is critical, as is an evaluation of the amount that can be retained for preserving the downstream ecosystem of the Biliu River. The hydrologic budget in the reservoir can be described by the following equation in a similar manner as that reported in the author's previous research (Pollman *et al*., 1991; Lee, 1996; Nakayama and Watanabe, 2008a):

$$\Delta V/\Delta t = P - E + Q_{sf} + Q_{ri} - Q_{ro} + Q_{gi} - Q_{go} - I + D, \tag{3.1}$$

where ΔV (m^3) is the change in reservoir volume for the period of interest, Δt (s); P (m^3/s) is the precipitation rate; E (m^3/s) is the evaporation rate; Q_{sf} (m^3/s) is the surface runoff flowing into the reservoir; Q_{ri} (m^3/s) is the inflow river discharge; Q_{ro} (m^3/s) is the outflow river discharge; Q_{gi} (m^3/s) is the volume of groundwater inflow; Q_{go} (m^3/s) is the volume of groundwater outflow; I (m^3/s) is the total volume of water piped to Dalian; and D (m^3/s) is the total drainage volume handled by wastewater treatment plants and public sewerage systems. Because Biliu Reservoir is located in a mountainous region, its river discharge, Q_{ro} (m^3/s), is evaluated as a residual term of the hydrologic budget, and the associated cumulative error is calculated from the variance of the total error in the measured components, assuming that some of the terms in Eq. (3.1) can be neglected ($Q_{sf} \approx 0$, $Q_{gi} \approx 0$, $Q_{go} \approx 0$, $D \approx 0$):

$$Q_{ro} = P - E + Q_{ri} - I - \Delta V/\Delta t \tag{3.2}$$

$$E_{ro} = \sqrt{e_P^2 + e_E^2 + e_{Q_{ri}}^2 + e_I^2 + e_{\Delta V}^2}\,, \tag{3.3}$$

where e_i represents the error inherent in measuring term i. Because the errors of each term are estimated by multiplying the budget value by the percentage error ascribed in the literature to the measurement technique (Winter, 1981), the error of Q_{ro} is the aggregate of the errors inherent in estimating each term in Eq. (3.2). This approach assumes that the measurement of each term is independent of the measurement of the other terms, and that no intercorrelations or covariances exist between measurement errors (Nakayama and Watanabe, 2008a). The budget-derived river discharge was used to validate the simulation results because data were unavailable downstream of the reservoir.

The author first estimated the water budget of the reservoir by the lumped method. We calculated the total river outflow from the observed river inflow data and the total precipitation at the reservoir collected by the Dalian Water Resource Bureau (2005–2006). Next, the author estimated the lake evaporation rate from the meteorological and water temperature data (Dalian Water Resource Bureau, 2005–2006) by the Priestley–Taylor method (Stewart and Rouse, 1976). The transfer of water to Dalian was calculated from statistical data on domestic and industrial water usage (Dalian Water Resource Bureau, 2007a). The change in reservoir volume was calculated from observed water level and bed elevation data (Dalian Water Resource Bureau, 2005–2006). The river discharge from the reservoir was finally estimated by the residuals of the total reservoir budget in Eq. (3.2) (Nakayama *et al.*, 2010).

3.2.2 Flood Resourcification Ability

Although floodwater usage for damming and irrigation is not a new concept, limited studies have been performed to evaluate the potential of flood resourcification, which describes flood resources development and utilization. From the perspective of flood resourcification, Wang *et al*. (2004) evaluated the capacity for floodwater capture as the difference between surface runoff and regional outflow downstream and out to sea:

$$w_f = w_s - w_o \,, \tag{3.4}$$

where w_f (m^3) is the flood resourcification ability; w_s (m^3) is the surface runoff; w_o (m^3) is the amount of outflow from the evaluation region, which includes water flowing downstream and into the sea. To secure the city's water supply, the Dalian government stated its intention to use floodwater capture to retain as much water as possible on land. Flood resourcification is expected to be a significant tool for increasing water supply. The quantity of water entering the sea, particularly during flood season, may show the flood resourcification potential in the entire catchment. A smaller amount of water entering the sea indicates greater potential for flood resourcification. The quantity of water entering the sea, particularly during flood season, is a good indicator for estimating the amount of water capture. The retained water can be used either directly or indirectly by transporting it to Dalian, storing it in reservoirs, or for recharging groundwater levels (Nakayama *et al.*, 2010).

3.2.3 Decoupling Indicator based on Water Consumption and Economic Growth

In Dalian, the author used a decoupling indicator procedure to analyze the effects of social activities, or driving force, on the environment and factors such as water consumption and economic growth. The author additionally decoupled water consumption from environmental degradation obtained from NDVI downstream of the catchment. The OECD has developed procedures to decouple environmental challenges from economic growth (OECD, 2002). Decoupling can be either absolute or relative. Absolute decoupling occurs when the environmental variable is stable, and it decreases when the economic driving force rises. Relative decoupling occurs when the economic variable rises more rapidly compared to the environmental variable (Brown-Santirso and Thornley, 2006).

The author first plotted two indexed time series on the same graph to express overall trends of the decoupling of pressure from the driving force (value at 1985 = 100). A time series of the ratio of the two was then analyzed for a numerical examination of annual decoupling trends by a decoupling indicator procedure (OECD, 2002). A decoupling indicator was calculated from the ratio of pressure to driving force at the end against the value at the start of a given time period:

$$Decoupling\ \ indicator = 1 - (EP/DF)_{\text{end of period}}/(EP/DF)_{\text{start of period.}} \tag{3.5}$$

Here, *EP* is environmental pressure, and *DF* is driving force. The decoupling indicator is zero or negative in the absence of decoupling, positive in relative decoupling, and has a maximum value of 1 when environmental pressure reaches zero, which describes absolute decoupling.

EP is the annual Biliu-derived water consumption in the entire city of Dalian or in its urban area in a time series from 1985 to 2007; this includes the industrial consumption of water derived from the Biliu River from 2001 to 2007. *DF* is the GDP in Dalian or in the

urban area during the same period, including industrial GDP. Various indicators of driving force exist in addition to GDP, such as population, standard of living, and urbanization. The main objective of this chapter is to evaluate the link among urban development, water resource management, and environmental degradation. Because the study area, Dalian, is a highly industrialized city in China, it is preferable, as an initial step, to use the GDP as a typical driving force. In our analysis of the impact of water abstraction from the Biliu River on the environment in the catchment, *EP* represents the NDVI as an index of environmental degradation, and *DF* is water supply from the Biliu River (Nakayama *et al.*, 2010).

3.3 Input Data and Boundary Conditions for Simulation

3.3.1 Meteorological Forcing Data

To create grid data with resolutions of 1 km, six-hour reanalysis data obtained by the European Centre for Medium-Range Weather Forecasts (ECMWF) with a resolution of 1° × 1° were assimilated with daily observation data of solar radiation, precipitation, temperature, humidity, and wind speed at a weather station operated by Dalian Water Resource Bureau (2005–2006) and Yingkou City Government (2005–2006) (Table 3.1). These data were inputted into each grid cell for a 2005–2006 simulation by interpolating the parameters in inverse proportion to the distance back-calculated in each cell. In particular, the daily precipitation data collected at 13 weather stations in the study area (R-1–R-13 in Table 3.1) were effective for the simulation because the ECMWF precipitation data had the least reliability, both spatially and temporally, and underestimated the observed values at the peak time (Nakayama and Watanabe, 2008b). This correction of ECMWF precipitation data by using observed data is critical because slight changes in precipitation will result in large variations in flood peaks and therefore are directly linked to the fluctuation of the water budget in the catchment. The calculated precipitation distribution for the simulation agreed well with previous research (Dalian Water Resource Bureau, 2005–2006; Yingkou City Government, 2005–2006), which shows higher rainfall in the eastern side of the study area (Fig. 3.3). Because the observed recharge rate data for natural regions are scarce, except for that using the chloride mass balance method (Lee, 1996), these values were simulated by NICE at each time step and were inputted into the groundwater submodel. Details are given in Nakayama and Watanabe (2004, 2008a).

Table 3.1. List of observation stations for validation.

No.	Point Name	Type	Lat.	Lon.	Elev. (m)
R-1	Xiao Shipeng	Rainfall Gauge	40°17.1'	122°27.0'	199.0
R-2	Meng Jiadian	Rainfall Gauge	40°14.6'	122°31.5'	191.0
R-3	Kuang Donggou	Rainfall Gauge	40°10.3'	122°43.0'	233.0
R-4	Taiping Zhuang	Rainfall Gauge	40°8.7'	122°44.0'	227.0
R-5	Xi Pashan	Rainfall Gauge	40°7.3'	122°32.3'	115.0
R-6	Biliu Reservoir	Rainfall Gauge	39°49.2'	122°29.5'	53.0
R-7	Guiyunhua Village	Rainfall Gauge	39°55.7'	122°35.9'	80.0
R-8	Daiiang Village	Rainfall Gauge	40°1.7'	122°42.6'	219.0
R-9	Shifogou Village	Rainfall Gauge	39°47.6'	122°38.4'	84.0
R-10	Tianyi	Rainfall Gauge	39°54.6'	122°26.4'	133.0
R-11	Shuangta Village	Rainfall Gauge	39°46.2'	122°28.7'	27.0
R-12	Xiaosongjia Village	Rainfall Gauge	39°34.3'	122°32.8'	9.0
R-13	Jian Chang	Rainfall Gauge	40°1.7'	122°32.3'	91.0
W-1	Gaizhou	Weather Data	40°23.7'	122°22.1'	8.0
W-2	Biliu Reservoir	Weather Data	39°49.2'	122°29.5'	53.0
W-3	Zhuanghe	Weather Data	39°42.0'	122°59.5'	3.0
W-4	Pulandian	Weather Data	39°23.7'	121°58.0'	2.0
W-5	Dalian	Weather Data	38°54.7'	121°36.1'	14.0
G-1	Jian Chang	Groundwater Level	40°1.7'	122°32.3'	91.0
G-2	Biliu Reservoir	Groundwater Level	39°49.2'	122°29.5'	53.0
G-3	Xiaosongjia Village	Groundwater Level	39°34.0'	122°33.0'	9.0
D-1	Jian Chang	River Discharge	40°1.7'	122°32.3'	91.0
D-2	Lingxi	River Discharge	39°55.7'	122°35.9'	80.0
D-3	Biliu Reservoir	River Discharge	39°49.2'	122°29.5'	53.0
D-4	Downstream of Biliu Reservoir	River Discharge (analyzed)	39°48.8'	122°29.6'	33.0
D-5	Xiaosongjia Village	River Discharge	39°34.3'	122°32.8'	9.0
S-1	Jian Chang	Soil Temp. & Moisture	40°1.7'	122°32.3'	91.0
T-1	Chengzitan	Tidal Level	39°29.2'	122°33.9'	5.0

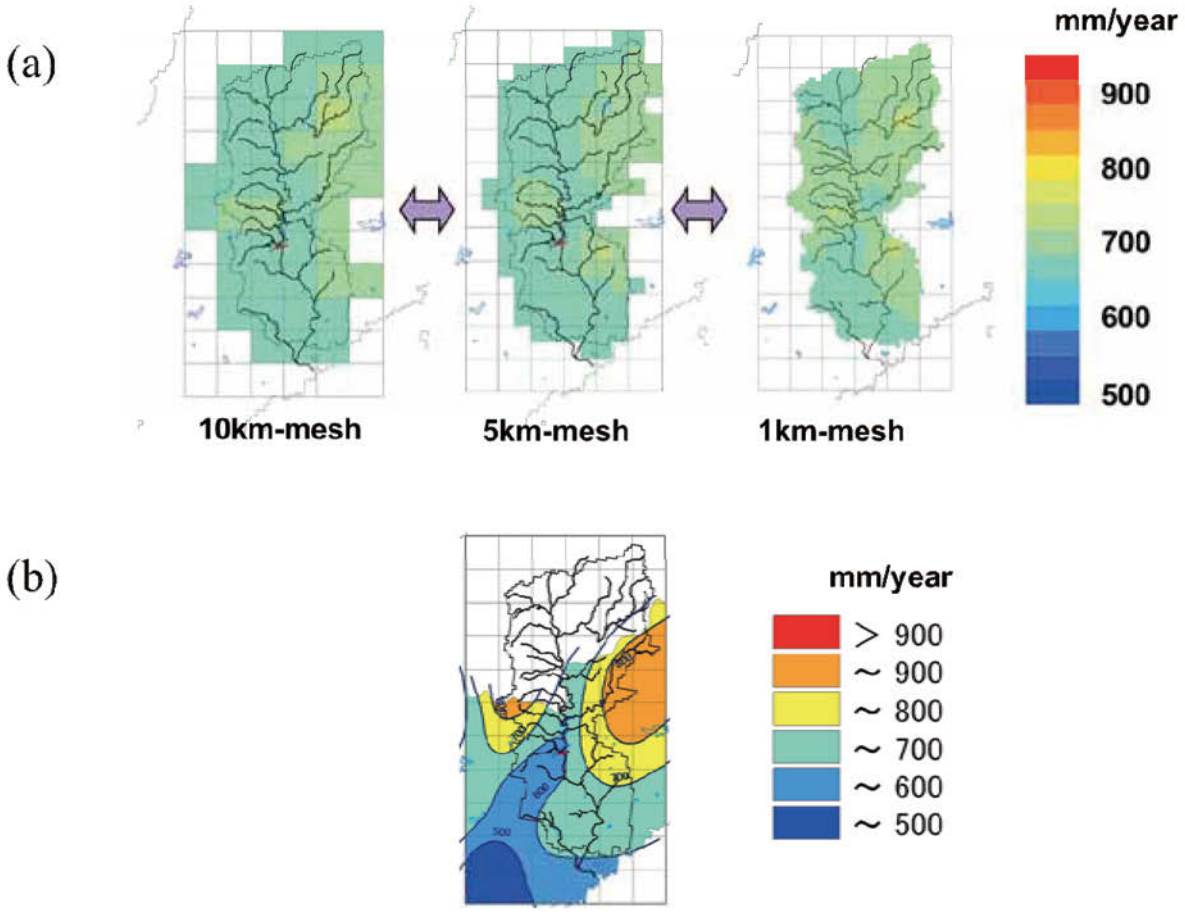

Fig. 3.3 Comparison between the forcing precipitation data created by 13 points of rain gauge data and previous research data: (a) rainfall anomalies (mm) in the forcing data and (b) rainfall anomalies (mm) in previous research data.

3.3.2 Vegetation and Geological Properties

The mean elevation of each 1-km grid cell was calculated by using the spatial average of a global digital elevation model (DEM; GTOPO30) with a horizontal grid spacing of 30 arc-seconds (approximately 1-km mesh) (US Geological Survey, 1996) throughout the Biliu River catchment (Fig. 3.1). Vegetation class and soil texture were categorized and digitized into 1-km mesh data from the Vegetation and Soil Maps of China (1:4,000,000) (Chinese Academy of Sciences, 1988) and the Soil Map of Dalian (1:100,000) (Liaoning Geology Investigation Agency, 2007b). These finer-resolution data were more accurate than data obtained from the International Satellite Land Surface Climatology Project (ISLSCP) with a resolution of 1°× 1° (Sellers *et al*., 1996). The geological structures were decided from scanned and digitized geological material (Liaoning Geology Investigation Agency, 2007a; Geological Atlas of China, 2002), which included core-sampling data at some points.

Geological structures were divided into four types with a resolution of 1 km in the horizontal direction and 20 layers in the vertical direction, K_h and K_v, respectively, on the basis of hydraulic conductivity, the specific storage of porous material (S_s), and specific yield (S_y), as described by Nakayama *et al*. (2006).

The NDVI was calculated from NOAA/AVHRR satellite data with a resolution of 1.1 km over East Asia during 1984–2007. The data area was selected from the original data to match the simulation area (39.35°N–40.50°N, 122.05°E–123.00°E). The important point of this study is that economic growth in the urban area, evaluated through water consumption, is closely related with environmental degradation in the water source area downstream of the Biliu River catchment, which is shown in the NDVI trend in the following section. Although a certain relationship exists between economic growth in Dalian and the city's NDVI value—such as the shrinkage of green areas inside the city accompanied by the expansion of urban areas and pollution—this factor is not the primary objective of this study because the NDVI value was evaluated for the Biliu River catchment rather than Dalian. Moreover, evaluation of the NDVI distribution inside the city requires the use of additional satellite data with higher resolution, such as data obtained by an advanced spaceborne thermal emission and reflection radiometer (ASTER).

3.3.3 Statistical Data on Water Resources and GDP

The consumption of water derived from the Biliu River during 1985–2007 was compiled from statistical data (Dalian Water Resource Bureau, 2007a), as was the total water consumption in Dalian during 2000–2007 (Dalian Water Resource Bureau, 2000–2007). Because official data on water consumption in Dalian from 1985 to 1999 was not available, we estimated the consumption for this period. The author first calculated the percentage of raw water consumption that was acquired from the environment and which was subsequently treated or purified in a water purification plant to produce potable water (Dalian Water Resource Bureau, 2000–2007) relative to the total water consumption in Dalian, and the percentage of Biliu-derived water consumption relative to total water consumption in a time series for the period 2000–2007. Because both annual-averaged percentages were nearly constant throughout the period, the author multiplied severally the two averages by raw water consumption in Dalian and water consumption from the Biliu River and estimated the two time series of water consumption in Dalian from 1985 to 1999. Finally, the author considered the 1985–1999 average to be representative of Dalian's total water consumption.

Annual GDP data during 1985–2007 was obtained from the Dalian Planning Committee (2001), the Dalian City Government (1990–2007), and the Dalian Bureau of Statistics (2002–2007). The annual GDP of the urban area (1985–2007) was estimated by multiplying the per-capita GDP of Dalian by the population of the urban area (Dalian City Government, 1990–2007). Because the rural–urban income disparity in eastern China was 54.4% in 1980 and 43.2% in 2000 (Wang and Ron, 2008), the author conducted a statistical analysis of decoupling indicators on the assumption that rural and urban incomes followed the same trend.

3.3.4 Boundary Conditions and Running the Simulation

Digital land cover data produced by the Institute of Remote Sensing Applications (IRSA) at the Chinese Academy of Sciences (CAS) (1988) based on Landsat TM data from the early 1990s (Liu, 1996) were categorized and divided into 1-km mesh data for the simulation.

Details are given in Nakayama and Watanabe (2008b). Land cover in the catchment (Liaoning Hydrology Bureau, 2007) was scanned and digitized to increase the accuracy of the IRSA data. Forest, grass, and scrub cover the mountainous and hilly areas in the upper catchment. Cultivated fields are widely distributed in the valley and lower regions. At the upstream boundaries, for which no observation data are available, the reflecting condition on the hydraulic head was used in the groundwater flow submodel on the supposition that there is no inflow from the mountains in the opposite direction (Nakayama and Watanabe, 2004). At the southern sea boundary (Yellow Sea), a variable head was set by using observed monthly data (T-1 in Table 3.1; Dalian Water Resource Bureau, 2005–2006). The hydraulic head values parallel to the ground level were input as the initial conditions for the groundwater flow submodel. The author used the digital river network produced by the IGSRR (1982) from 1:100,000 topographic maps covering the catchment. In 660 river cells, including the Biliu River, inflows into or outflows from the riverbed were simulated at each time step from the difference in the groundwater and river hydraulic heads.

The simulation area is 60 km wide by 110 km long on the basis of the Albers (WGS 1984) co-ordinates, covering almost the entire Biliu River catchment. The area was divided into a grid of 60 × 110 blocks with a grid spacing of 1 km in the horizontal direction and into 20 vertical layers with a weighting factor of 1.1; sediment was finer in the upper layers. The upper layer was set at a depth of 2 m, and the 20th layer was defined as an elevation of 200 m below sea level. The NICE simulation was conducted on a NEC SX-6 supercomputer. Simulations covering January 1, 2005, to December 31, 2006, were performed for calibration. The first six months of the study were used as a warm-up period until equilibrium water levels were reached, and parameters were estimated by comparison of simulated steady-state values with observed values that were previously published (Clapp and Hornberger, 1978; Rawls *et al*., 1982). A time step of Δt = 1 h was used. Simulations were validated against observed river discharge at five points, groundwater level at three points, and soil temperature and moisture at one point (Dalian Water Resource Bureau, 2005–2006; Yingkou City Government, 2005–2006) (Table 3.1).

3.4 Results and Discussion

3.4.1 Hydrologic Change Affected by the Reservoir Construction

The simulated results were calibrated for the Biliu River catchment during 2005–2006 (Fig. 3.4). The upper catchment is mountainous, and most of the cover is natural. The lower catchment comprises a vast, flat area covered mainly by paddy and other fields. The river discharge is greater from spring to fall because rainfall is higher in this period. The model showed a good reproductions of the observed river discharge from the upper to the lower regions, particularly around the reservoir (D-3 in Table 3.1) (*Cor* = 0.60). The *Cor* in the main upstream area (D-1 in Table 3.1) was as small as that observed downstream of the reservoir (D-4 in Table 3.1) mainly because the grid spacing in this simulation was slightly rough for similar reproduction of the river discharge as that reported in previous research (Nakayama and Watanabe, 2008b). In addition, inaccuracy of meteorological and other inputted data was possible, and the discharge downstream of the reservoir was greatly affected by the transfer of water to Dalian. Because there were no available observation data downstream of the reservoir (D-4 in Table 3.1), the author evaluated the outflow discharge from the reservoir by using a simple hydrologic budget (shown in Eq. (3.2)) (Nakayama and Watanabe, 2008a). This budget-derived value underestimates the simulated value, mainly by ignoring surface

runoff and groundwater seepage into the reservoir. The simulated values of groundwater levels were validated against actual groundwater level data (Fig. 3.5a). Since the author used a 3-D groundwater submodel, the simulated groundwater fluctuations agree strongly with the measured values, as shown in the values of *Cor*, *MV*, *SD*, and *CV*, which depend on precipitation, local topography, and water withdrawal. The groundwater level decreased rapidly with distance at the reservoir due to the rapid decrease of recharge; this is because surface runoff decreased rapidly below the reservoir (Fig. 3.5b). The groundwater level is significantly low in the middle and lower regions because of low elevation; therefore, it is sensitive to and greatly affected by tides and decreased discharge following the completion of the Biliu Reservoir. These results indicate that the simulation is highly effective for evaluating the link between urban development in Dalian and sustainable water resource management (Nakayama *et al.*, 2010).

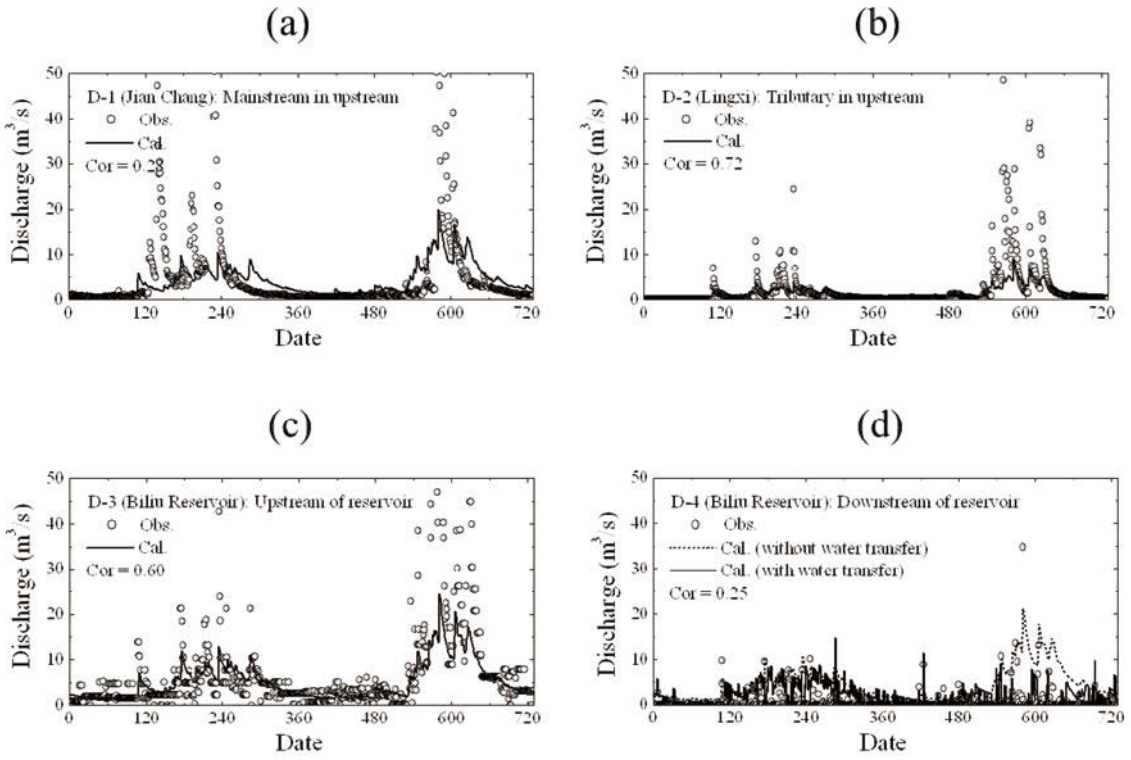

Fig. 3.4 Calibration in Biliu River catchment (D-1–D-4; Table 3.1). Circles represent observation data, and lines represent results simulated by NICE. Date = 0 on the horizontal axis corresponds to January 1, 2005. *Cor* shows the correlation between observed and simulated values. In (d), dotted and solid lines represent simulated discharges without and with the water transfer at Biliu Reservoir, respectively.

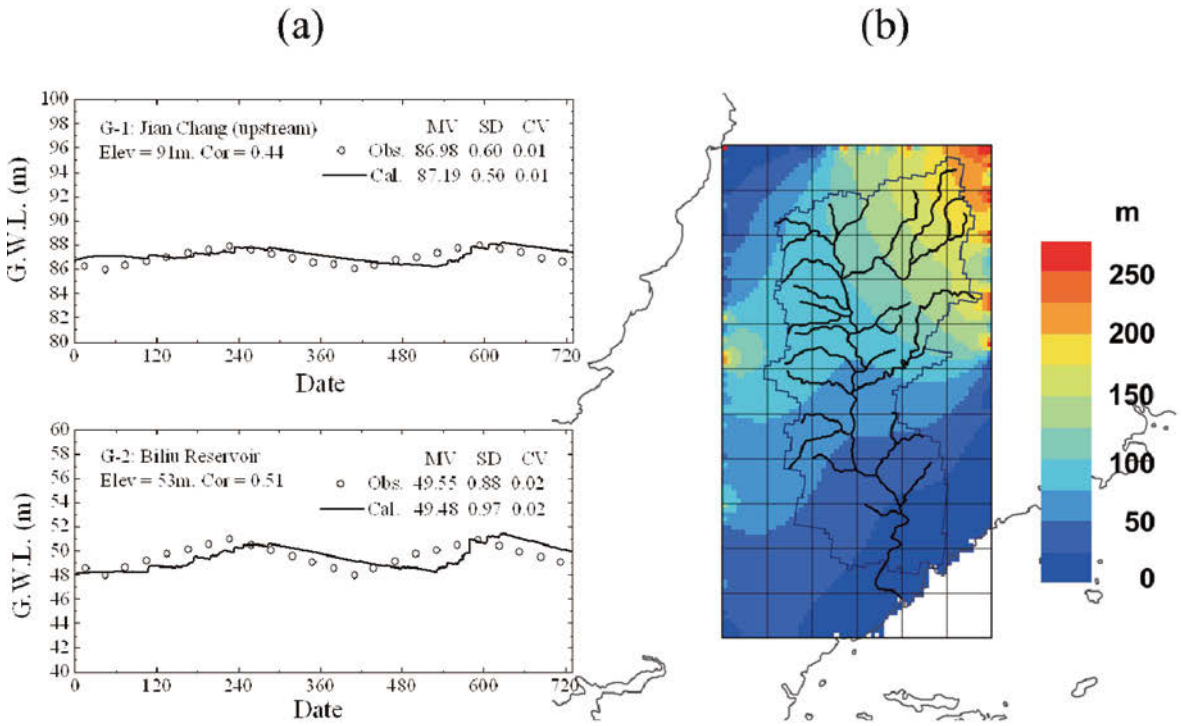

Fig. 3.5 Simulated results of annual-averaged groundwater levels in the Biliu River catchment illustrating (a) the comparison between simulated and observed values and (b) the simulated contour in the catchment. *Cor* shows the correlation between the observed value and the simulated value. *MV*, *SD*, *CV* represent mean value, standard deviation, and coefficient of variation (= *SD*/*MV*), respectively.

NICE backcasted the river discharge and flood resourcification ability downstream of the reservoir following its completion (Fig. 3.6). The simulated result clarified that the river discharge decreased yearly since the completion of the reservoir because water demand increased in the urban area (Fig. 3.6a). In particular, very little water was discharged into the waterway, and the river downstream became seasonal. In the dry autumn and winter seasons, the main waterway nearly dried out, while in the rainy season, it became a flood spillway. This trend is characteristic of catchments in northern China, where the downstream flow depends greatly on precipitation over the catchment and withdrawal from upstream (Qian and Zhu, 2001; Ren *et al*., 2002). It is evident that most of the water in the river was already being used at the beginning of this century, with the flood resourcification ability reaching a constant value (Fig. 3.6b). The degree of floodwater capture in this catchment is closely related to the history of water resource development, as is seen mainly in the construction of Biliu Reservoir. Because rapid development of industry and urbanization, in addition to the increase in farmland irrigation, has also pushed water demand to the limits of its carrying capacity (Varis and Vakkilainen, 2001), the groundwater table has receded in the floodplains of the river's downstream areas (Nakayama *et al.*, 2010) (Fig. 3.5).

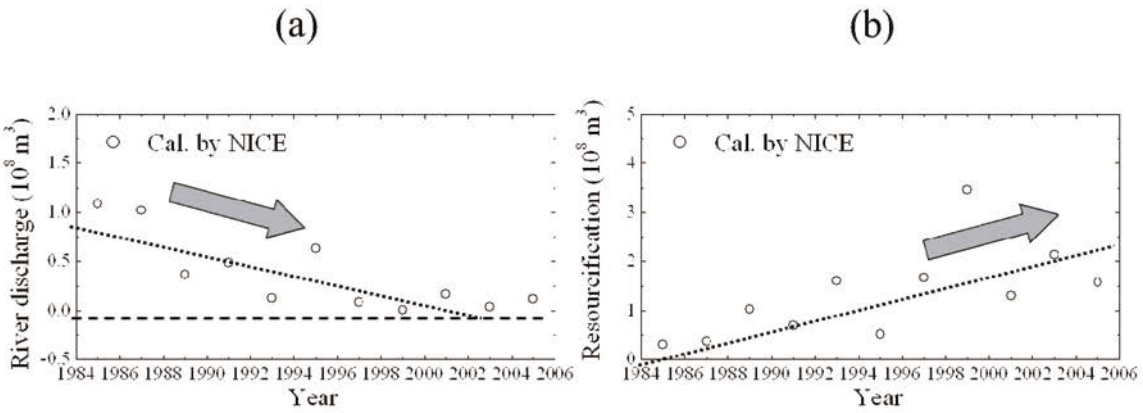

Fig. 3.6 Simulation result of water resources affected by the construction of Biliu Reservoir illustrating (a) river discharge downstream of the reservoir and (b) flood resourcification ability downstream of the reservoir.

3.4.2 Vegetation Change Affected by the Change in Water Resources

Trend analysis was used to study long-term vegetation trends (Fig. 3.7). The variation in annual NDVI corresponds to the variation in annual rainfall in the catchment (Fig. 3.7a). Along with a general decrease during the period of study, several fluctuations were observed. A closer examination revealed that since the construction of the reservoir in 1984, negative trends have predominated (1984–1994 and 2003–2007), whereas rainfall slightly increased during 1995–2002. The earlier decrease during 1984–1994 was associated with the conversion to farmland and a reduction in river flow. After the reservoir construction, large areas of native vegetation downstream of the floodplains were converted into farmland (Liu *et al*., 2005). Paddy fields were converted into dryland fields in direct response to water scarcity attributed to the cultivation of more farmland through the construction of reservoirs, which resulted in reduced river flow downstream. Low NDVI values during 1992–1994 were associated with the coldest and driest year in the 1990s (Piao *et al*., 2004). Increased values of NDVI can result from both a lengthened growing season and accelerated vegetation activity; Piao *et al*. (2004) suggested that a longer growing season is a primary contributor to increased NDVI.

The spatial pattern in the NDVI trend during 1984–2007 shows heterogeneity (Fig. 3.7b) that corresponds well to the regional distribution of water resources. A significant decrease in the NDVI occurred primarily downstream of the Biliu reservoir and downstream of the Zhujiaweizi and Liuda reservoirs, which were built in 1968 and 1971, respectively (Dalian City Government, 2003). Downstream of the Zhujiaweizi Reservoir and in its surrounding areas, the NDVI decreased as a result of several factors, including a reduction in water resources and rapid urbanization surrounding the city of Zhuanghe (Wang, 1997). In the coastal zone near Chengzitan, topographic depressions, most likely formed by fluvial processes, have shallow water tables and are susceptible to salinization. The low NDVI in this area is the result of high salt concentrations in the subsurface water (Kondoh and Oyamada, 2000). NDVI in cultivated fields is smaller beside the Yellow Sea than it is inland, which has increased yearly because of the decrease in river discharge. In addition, NDVI values showed the most rapid rate of decline near the Yellow Sea. Mountainous areas upstream of the Biliu Reservoir exhibit higher NDVI values than those observed in the downstream areas. This difference is closely related to the water shortage and seawater intrusion occurring since the construction of Biliu Reservoir (Nakayama *et al.*, 2010) (Fig. 3.5 and 3.6), which has greatly reduced crop growth and production in coastal areas.

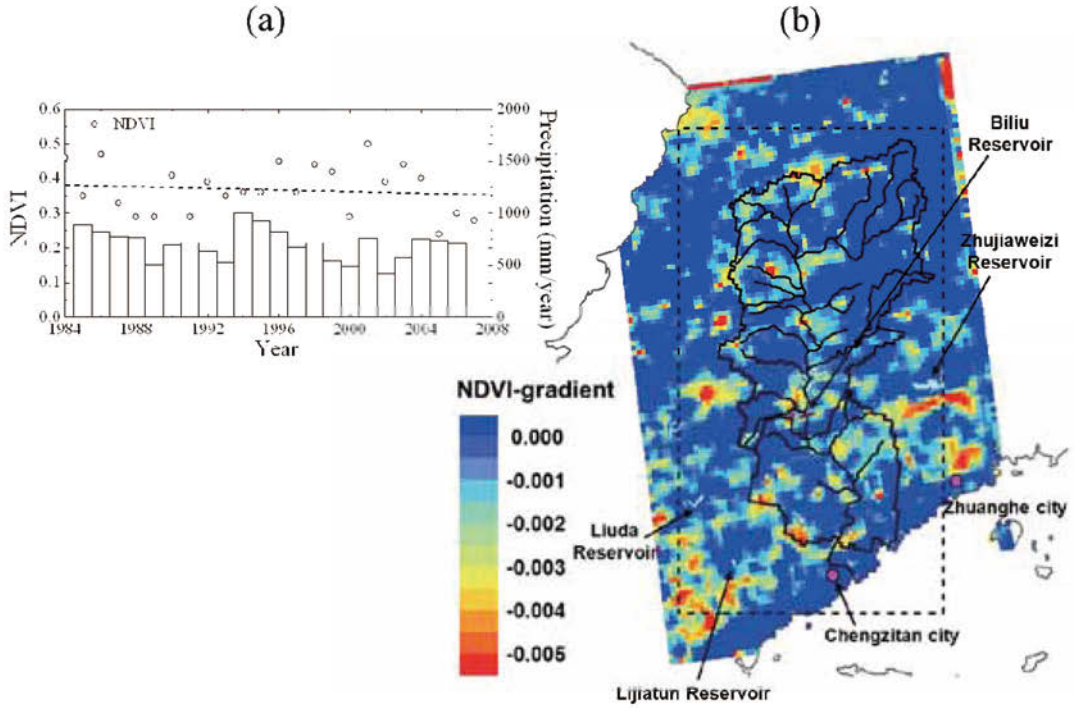

Fig. 3.7 NDVI with a resolution of 1.1 km mesh in the Biliu River catchment illustrating (a) the annual trend of NDVI downstream of Biliu Reservoir (circles). Rainfall anomalies at the reservoir are also plotted on the right-hand y-axis (bars). Dashed lines represent least-square regression lines estimated from NDVI data. (b) Spatial patterns in NDVI gradient in the entire catchment during 1984-2007 (image areas: 39.35°N–40.50°N, 122.05°E–123.00°E). The dashed square represents the border of the simulation area.

3.4.3 Relationship Between Water Resources and Urban Activity

Fig. 3.8a shows annual decoupling trends between water consumption and GDP in the entire city of Dalian. One noteworthy outcome is the relatively small decoupling indicators, although they are mostly positive. This result shows that environmental demand for water consumption in Dalian is higher than that in developed regions (OECD, 2002). An additional noteworthy outcome is the slight tendency of decline in the decoupling indicator from 1985 to 2007. The relative decoupling in this period was due to remarkable economic growth with a comparatively low increase in water consumption, although environmental demand for water consumption continues to increase with economic growth in Dalian.

The decoupling indicator value for the urban area was higher than that for the entire city of Dalian during some periods when the environmental demand from local areas was considerably less than that from Dalian; however, the values in 1985–1988 were irregular owing to the beginning of dam operation (Fig. 3.8b). The decoupling indicator values declined, were unstable, and were negative twice in eighty years (1998–1999 and 2004–2005),

although the Dalian government increased the water price several times to control consumption (Dalian Water Resource Bureau, 2007b). The value dropped from 0.43 in 1993–1994 to –0.37 in 1998–1999, became positive at 0.33 again in 2003–2004, and then declined. These trends show that the environmental demand for water has increased with economic growth in the urban area, although relative decoupling predominated, particularly when the decoupling indicator value was negative.

The impact of water withdrawal from Biliu Reservoir on environmental degradation of NDVI downstream is shown in Fig. 3.8c. The decoupling indicator value gradually decreased from 0.75 (relative decoupling) in 1988–1989 to –0.25 (no decoupling) in 2006–2007, although values were irregular in 1985–1988 due to the start of dam operation and inaccurate data. This result shows increasing environmental degradation with increasing abstraction of water from the Biliu River, which indicates that the environmental degradation in the Biliu River catchment will worsen with economic growth in the future (Nakayama *et al.*, 2010).

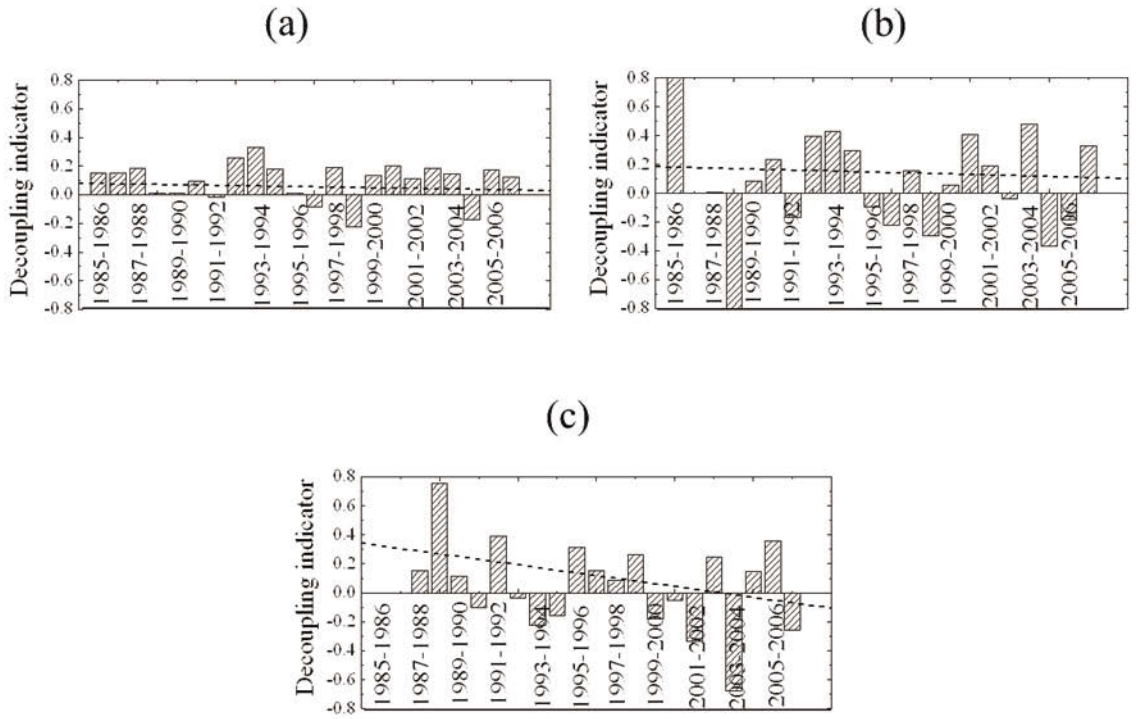

Fig. 3.8 Annual trends of decoupling indicators among (a) water consumption and GDP in the entire city of Dalian, (b) water consumption and GDP in the urban area of Dalian, and (c) NDVI and water consumption. Dashed lines represent least-square regression lines estimated from annual decoupling indicators (bars).

3.5 Conclusion

The author evaluated the hydrologic budget in Biliu Reservoir to estimate the relationship between water withdrawal and outflow from the dam. The NICE model appropriately reproduced river discharge, groundwater level, evapotranspiration, and crop productivity in the Biliu River catchment. Moreover, the model correctly backcasted the gradual decrease in water resources since the completion of the reservoir (in the middle of the catchment), showing reduced discharge into the Yellow Sea, the groundwater drop in the floodplain, and the reduced NDVI downstream of the reservoir. The statistical analysis of the decoupling indicators suggests that the limited water resources in the Biliu River catchment has degraded the environment and poses a threat to economic growth in the Dalian municipality, particularly in the central urban area. The results highlight the connection between urban development in Dalian and sustainable water resource management.

References

Brown-Santirso M., Thornley A. (2006) Decoupling economic growth and energy use in New Zealand. Statistics New Zealand. http://www.stats.govt.nz/NR/rdonlyres/CB3DE050-3163-4C6E-8871-AEF8014FD9E7/0/decouplingeconomicgrowthnzaepaperjun06.pdf.

Chinese Academy of Sciences (1988) Administrative division coding system of the People's Republic of China, Beijing.

Clapp R.B., Hornberger G.M. (1978) Empirical equations for some soil hydraulic properties. Water Resources Research, 14, 601-604.

Dalian Bureau of Statistics (2002-2007) Dalian statistical yearbook. China Statistics Press (in Chinese).

Dalian City Government (1990-2007) Dalian yearbook. Dalian Publisher (in Chinese).

Dalian City Government (2003) Reservoir projects in Dalian City. http://szb.dl.gov.cn/dlsz/003/004/005/12818_12883.htm (in Chinese).

Dalian City Government (2006) Outline of 11th five-year plan for Dalian City's economic and social development, 39 (in Chinese).

Dalian Planning Committee (2001) Strategic research on Dalian's tenth five-year plan. Dalian, China, Dongbei University of Finance & Economics Press. (in Chinese).

Dalian Water Resource Bureau (2000-2007) The water resources bulletin of Dalian City. http://www.swj.dl.gov.cn/info/info/fangxun.aspx?id=78 (in Chinese).

Dalian Water Resource Bureau (2005-2006) Annual report of weather, river discharge, groundwater level, tidal level, and soil characteristics at the Biliu River catchment. Interior report of the committee (in Chinese).

Dalian Water Resource Bureau (2007a) Five years water demand prediction. Official document, Dalian City Government (in Chinese).

Dalian Water Resource Bureau (2007b) The classification of the water rent and the collection. http://www.swj.dl.gov.cn/info/info/fangxun.aspx?id=81 (in Chinese).

Geng Y., Mitchell B., Fujita T., Nakayama T. (2010) Perspectives on small watershed management in China: the case of Biliu. International Journal of Sustainable Development and World Ecology, 17(2), 172-179, doi:10.1080/13504500903549528, 2010.

Geological Atlas of China (2002) Geological Publisher, Beijing, China (in Chinese).

Gleick P. (2000) The changing water paradigm: a look at twenty first century water resources development. Water International, 25, 127-138.

Gleick P. (2002) Water management: Soft water paths. Nature, 418, 373.

Halada K. ,Shimada M., Ijima K. (2007) Decoupling status of metal consumption from economic growth. Journal of the Japan Institute of Metals, 71(10), 823-830 (in Japanese, with Abstr. English).

Han Y., Xu S., Xu X. (2008) Modeling multisource multiuse water resources allocation. Water Resources Management, 22, 911-923.

He D., Chen J. (2001) Issues, perspectives and need for integrated watershed management in China. Environmental Conservation, 28(4), 368-377.
Kondoh A., Oyamada Y. (2000) Monitoring surface moisture and vegetation status by NOAA and GMS over north china plain. Advance in Space Research, 26(7), 1055-1058.
Lee T.M. (1996) Hydrogeologic controls on the groundwater interactions with an acidic lake in karst terrain, Lake Barco, Florida. Water Resources Research, 32, 831-844.
Liaoning Geology Investigation Agency (2007a) Geology Map of Dalian.
Liaoning Geology Investigation Agency (2007b) Soil Map of Dalian.
Liaoning Hydrology Bureau (2007) Land cover at the upstream area of Biliu River.
Liu J.Y. (1996) Macro-scale survey and dynamic study of natural resources and environment of China by remote sensing. Chinese Science and Technology Publisher, Beijing, ChiElsevier B.V.na. (in Chinese).
Liu Y., Wang D., Gao J., Deng W. (2005) Land use/cover changes, the environment and water resources in Northeast China. Environmental Management, 36(5), 691–701.
Lua I.J., Lin S.J., Lewisc C. (2007) Decomposition and decoupling effects of carbon dioxide emission from highway transportation in Taiwan, Germany, Japan and South Korea. Energy Policy, 35, 3226–3235.
Minstry of environmental protection of the people's republic of china (2008) Promotion law for circular economy, 4. http://www.sepa.gov.cn/law/law/200809/t20080901_128001.htm (in Chinese).
Mitchell B. (2005) Integrated water resource management, institutional arrangements, and land-use planning. Environmental Planning A, 37, 1335-1352.
Nagatani I., Saito G., Toritani H., Sawada H. (2002) Agricultural map of Asian region using time series AVHRR NDVI data. http://www.gisdevelopment.net/aars/acrs/2002/pos2/184.pdf
Nakayama T. (2008a) Factors controlling vegetation succession in Kushiro Mire. Ecological Modelling, 215, 225-236, doi:10.1016/j.ecolmodel.2008.02.017.
Nakayama T. (2008b) Shrinkage of shrub forest and recovery of mire ecosystem by river restoration in northern Japan. Forest Ecology and Management, 256, 1927-1938, doi:10.1016/j.foreco.2008.07.017.
Nakayama T. (2008c) Development of process-based NICE model and simulation of ecosystem dynamics in the catchment of East Asia (Part II), CGER's Supercomputer Monograph Report, 14, NIES, 91p., http://www-cger.nies.go.jp/publication/I083/i083.html.
Nakayama T. (2009) Simulation of ecosystem degradation and its application for effective policy-making in regional scale. In River pollution research progress, Mattia N. Gallo, Marco H. Ferrari (eds), 1-89 (Chapter 1), Nova Science Pub., Inc., New York.
Nakayama T. (2010) Simulation of hydrologic and geomorphic changes affecting a shrinking mire. River Research and Applications, 26(3), 305-321, doi:10.1002/rra.1253.
Nakayama T. (2011a) Simulation of complicated and diverse water system accompanied by human intervention in the North China Plain. Hydrological Processes, 25, 2679-2693, doi:10.1002/hyp.8009.
Nakayama T. (2011b) Simulation of the effect of irrigation on the hydrologic cycle in the highly cultivated Yellow River Basin. Agricultural and Forest Meteorology, 151, 314-327, doi:10.1016/j.agrformet.2010.11.006.
Nakayama T., Fujita T. (2010) Cooling effect of water-holding pavements made of new materials on water and heat budgets in urban areas. Landscape and Urban Planning, 96, 57-67, doi:10.1016/j.landurbplan.2010.02.003.
Nakayama T., Hashimoto S. (2011) Analysis of the ability of water resources to reduce the urban heat island in the Tokyo megalopolis. Environmental Pollution, 159, 2164-2173, doi:10.1016/j.envpol.2010.11.016.
Nakayama T., Watanabe M. (2004) Simulation of drying phenomena associated with vegetation change caused by invasion of alder (Alnus japonica) in Kushiro Mire. Water Resources Research, 40, W08402, doi:10.1029/2004WR003174.
Nakayama T., Watanabe M. (2006a) Simulation of spring snowmelt runoff by considering micro-topography and phase changes in soil layer. Hydrology and Earth System Sciences Discussions, 3, 2101-2144.
Nakayama T., Watanabe M. (2006b) Development of process-based NICE model and simulation of ecosystem dynamics in the catchment of East Asia (Part I), CGER's Supercomputer Monograph Report, 11, NIES, 100p., http://www-cger.nies.go.jp/publication/I063/I063.html.
Nakayama T., Watanabe M. (2008a) Missing role of groundwater in water and nutrient cycles in the shallow eutrophic Lake Kasumigaura, Japan. Hydrological Processes, 22, 1150-1172, doi:10.1002/hyp.6684.
Nakayama T., Watanabe M. (2008b) Role of flood storage ability of lakes in the Changjiang River catchment. Global and Planetary Change, 63, 9-22, doi:10.1016/j.gloplacha.2008.04.002.
Nakayama T., Watanabe M. (2008c) Modelling the hydrologic cycle in a shallow eutrophic lake. Verh International Verein Limnology, 30.

Nakayama T., Yang Y., Watanabe M., Zhang X. (2006) Simulation of groundwater dynamics in North China Plain by coupled hydrology and agricultural models. Hydrological Processes, 20(16), 3441-3466, doi:10.1002/hyp.6142.

Nakayama T., Watanabe M., Tanji K., Morioka T. (2007) Effect of underground urban structures on eutrophic coastal environment. Science of the Total Environment, 373(1), 270-288, doi:10.1016/j.scitotenv.2006.11.033.

Nakayama T., Sun Y., Geng Y. (2010) Simulation of water resource and its relation to urban activity in Dalian City, Northern China. Global and Planetary Change, 73, 172-185, doi:10.1016/j.gloplacha.2010.06.001.

Nakayama T., Hashimoto S., Hamano H. (in press) Multi-scaled analysis of hydrothermal dynamics in Japanese megalopolis by using integrated approach. Hydrological Processes.

Niu W.Y., Harris W.M. (1996) China: the forecast of its environmental situation in the 21st Century. J. Environmental Management, 47, 101-114.

OECD (2001) Decoupling: a conceptual overview. OECD paper No.10, OECD, Paris.

OECD (2002) Indicators to measure decoupling of environmental pressure from economic growth. http://www.olis.oecd.org/olis/2002doc.nsf/LinkTo/sg-sd(2002)1-final.

OECD (2004) Analysis of the links between transport and economic grow. Environment Directorate. http://www.oecd.org/dataoecd/29/37/31661238.pdf

Qian W., Zhu Y. (2001) Climate change in China from 1880 to 1998 and its impact on the environmental condition. Climatic Change, 50, 419-444.

Piao S., Fang J., Ji W., Guo Q., Ke J., Tao S. (2004) Variation in a satellite-based vegetation index in relation to climate in China. Journal of Vegetation Science, 15, 219-226.

Piao S., Fang J., Zhou L. (2006) Variations in satellite derived phenology in China's temperate vegetation. Global Change Biology, 12, 672–685.

Pollman C.D., Lee T.M., Andrews J.W., Sacks L.A., Gherini S.A., Munson R.K. (1991) Preliminary analysis of the hydrologic and geochemical controls on acid-neutralizing capacity in two acidic seepage lakes in Florida. Water Resources Research, 27, 2321-2335.

Rawls W.J., Brakensiek D.L., Saxton K.E. (1982) Estimation of soil water properties. Transactions of the ASAE, 25, 1316-1320.

Ren L., Wang M., Li C., Zhang W. (2002) Impacts of human activity on river runoff in the northern area of China. Journal of Hydrology, 261, 204-217.

Sellers P.J., Randall D.A., Collatz G.J., Berry J.A., Field C.B., Dazlich D.A., Zhang C., Collelo G.D., Bounoua L. (1996) A revised land surface prameterization (SiB2) for atomospheric GCMs. Part I : Model formulation. Journal of Climate, 9, 676-705.

Shi S.X., Zhang Z.Y., Li W.Z. (2002) Perspectives on small watershed's sustainable development, Beijing, Science Press. (in Chinese).

Stewart R.B., Rouse W.R. (1976) A simple equation for determining the evaporation from shallow lakes and ponds. Water Resources Research, 12, 623–628.

Tachibana J., Hirota K., Goto N., Fujie K. (2008) A method for regional-scale material flow and decoupling analysis: A demonstration case study of Aichi prefecture, Japan. Resources Conservation and Recycling, 52, 1382-1390.

Tight M.R., Delle-Site P., Meyer-Ruhile O. (2004) Decoupling transport from economic Growth: towards transport sustainability in Europe. European Journal of Transport and Infrastructure Research, 4(4), 381-404.

UNEP (2001) Global 500 forum. http://www.global500.org/default.asp.

U.S. Geological Survey (1996) GTOPO30 Global 30 Arc Second Elevation Data Set. USGS, http://www1.gsi.go.jp/geowww/globalmap-gsi/gtopo30/gtopo30.html.

Varis O., Vakkilainen P. (2001) China's 8 challenges to water resources management in the first quarter of the 21st Century. Geomorphology, 41, 93-104.

Wang M.Y.L. (1997) Urban growth and the transformation of rural China: the case of Southern Manchuria. Asia Pacific Viewpoint, 38(1), 1-18.

Wang X.L., Ron D.C. (2008) Rural-urban income disparity and WTO impact on China's agricultural sector: policy considerations. In: Chen, C., and Ron, D.C. (Eds.), Agriculture and food security in China. Asia Pacific Press, Australia, 85-103, http://epress.anu.edu.au/afsc/pdf/whole_book.pdf.

Wang Z., Wang X., Zhao F., Guo S., Hu S. (2004) The method of evaluation flood resources sustainable utilization capacity. Proceeding of Disaster Prevention Research Institute, Kyoto University, http://www.wrrc.dpri.kyoto-u.ac.jp/~aphw/APHW2004/proceedings/JSD/56-JSD-A616/56-JSD-A616(resubmit).pdf.

Yingkou City Government (2005-2006) Annual report of weather, river discharge, groundwater level, tidal level, and soil characteristics at the Biliu River catchment. Interior report of the committee (in Chinese).
Yu X., Zhuang D., Hou X., Chen H. (2005) Forest phenological patterns of Northeast China inferred from MODIS data. Journal of Geographical Sciences, 15(2), 239-246.
Zhang J., Xiong B.Y. (2006) Towards a healthy water cycle in China. Water Science and Technology, 53, 9-15.

Chapter 4

Ability of Water Resources to Reduce the Urban Heat Island in the Tokyo Megalopolis

Abstract

An innovative simulation procedure of the hydrothermal cycle integrated with multiple scales in horizontally regional–urban–point levels and in vertically atmosphere–surface–unsaturated–saturated layers was developed to estimate and predict the effects of urban geometry and anthropogenic exhaustion on the hydrothermal changes in the atmospheric–land regions and the interfacial areas of a Japanese megalopolis. The simulated results suggests that the latent heat flux in a new water-holding pavement, which consists of porous asphalt and a water-holding filler made of steel by-products based on silica compounds, has a strong impact on the hydrologic cycle and cooling temperatures in addition to a passive cooling effect of green areas in comparison with the observed heat budget. The author evaluated the relationship between the effects of groundwater usage as a heat sink to address the heat island and the effects of infiltration on the water cycle in the urban area. Moreover, the model predicted that hydrothermal change would affect the target and surrounding areas, implying the necessity of precise arrangement of a symbiotic urban scenario in the study area with neighboring administrations from a political perspective. These results indicate that effective management of water resources is important for ameliorating the heat island and recovering a sound hydrologic cycle. Further improvement in the process-based model is important for achieving a favorable solution for hydrothermal pollution in future eco-conscious societies.

Keywords: favorable solution, multi-scaled model, hydrothermal characteristics, heat island, imbalance of hydrologic cycle, symbiotic urban scenario

4.1 Introduction

Recently, a link has been found between environmental pollution and degradations of water and thermal environments and contamination in Asian urban areas (Endo, 1992; Taniguchi *et al*., 2009; Nakayama and Hashimoto, 2011; Nakayama *et al*., in press). In particular, urban heat islands have presented significant environmental challenges with the expansion of cities and industrial areas worldwide (Oke, 1987; Golden, 2003). Surfaces covered by concrete or asphalt can absorb a large amount of heat during the day and release this heat into the atmosphere at night. Many researchers have attempted to reproduce heat islands by using regional weather forecast models (Pielke *et al*., 1992; Dudhia, 1993; Skamarock *et al*., 2005). Zhang *et al*. (2008) used the Regional Atmospheric Modeling System (RAMS) coupled with a single-layer urban canopy model (UCM) (Kusaka *et al*., 2001; Kusaka and Kimura, 2004) to improve the reproducibility of a heat island; the original RAMS was unable to reproduce this environment accurately. Ichinose *et al.* (1999) investigated the impact of anthropogenic heat on heat islands compared with shortwave radiation. Ohashi *et al*. (2007) integrated building energy analysis models (BEM) into the UCM, which demonstrated the effect of anthropogenic heating on indoor workplaces to reproduce diurnal temperature variations during the workweek in Tokyo office settings.

The evaporation of water provides an important counterpoint to this effect; therefore, open parks and water surfaces in addition to green areas in urban settings are vital for creating cool islands (Spronken-Smith and Oke, 1999; Chang *et al*., 2007). The convective heat transfer of urban surfaces, defined as the sum of advective and diffusive transfer, is a crucial parameter for estimating the turbulent heat flux in urban areas, and this convective heat transfer should be estimated quantitatively (Hagishima *et al*., 2005). Several researchers have used process-based models to estimate the transport of water vapor and the regulation of temperature distribution above a paved surface (Grimmond and Oke, 1991; Asaeda and Ca, 1993; Dupont *et al*., 2006). Numerical models show that road hydrological behavior influences thermal exchange and evaporation creates significantly lower temperatures in bare soil than on covered surfaces (Asaeda and Ca, 1993). To aid the reduction of evapotranspiration from natural surfaces, Objective Hysteresis Model (OHM) (Grimmond and Oke, 1991) and Sub-Mesoscale Soil Model, Urbanized version (SM2-U) (Dupont *et al*., 2006) were used along with a submesoscale urban scheme to show that urban hydrological parameters determine the amount of water available for evaporation from artificial surfaces such as engineered pavements. However, in these models, a lack of accurate measured data on water infiltration into largely impermeable urban surfaces has led to the assumption by several urban hydrologists that infiltration is almost zero and runoff is 100% of rainfall, which could lead to overestimation of runoff and underestimation of groundwater recharge. Hollis and Ovenden (1988a, 1988b) and Ragab *et al*. (2003) showed that streets cannot be considered fully impermeable and that runoff also represents a significant source of pollution. In addition, it is important to assess the impacts of land use alteration scenarios on hydrology on the basis of observations, which are closely related to water resource management and the mitigation of heat islands (Alberti *et al*., 2007).

Permeable pavement and other stormwater control devices are increasingly being used to collect stormwater, which evaporates in fine weather (Andersen *et al*., 1999; Sansalone and Teng, 2005). Ramier *et al*. (2004) used a lysimeter to assess losses due to infiltration, evaporation, and runoff on engineered pavement. The promotion of vaporization by using water-holding pavement consisting of porous asphalt and water-holding filler made of steel by-products based on silica compounds would be an effective strategy for the mitigation of

heat islands when used in combination with light-colored and vegetated surfaces (Saaroni *et al*., 2000; Chang *et al*., 2007; Nakayama and Fujita, 2010). Because this thermal relaxation in newly symbiotic pavement is closely related to the heat capacity of water and the conductivity of the pavement, it is estimated that groundwater usage at nearly constant temperatures as a heat sink would be a highly effective measure for addressing the issue of heat islands (Ministry of Environment, 2003). A policy to promote infiltration into the aquifer is also important to prevent ground degradation, which has occurred in the past (Endo, 1992; Nakayama *et al*., 2007). The heat island related to the hydrologic cycle also differs between surface and street levels (Saaroni *et al*., 2000) and on local versus regional scales (Nichol and Wong, 2005), which makes evaluation difficult in actual urban regions. Therefore, it is critical to develop the process-based model and to evaluate the relationship between the effects of groundwater usage to ameliorate the heat island and the effect of infiltration on the hydrologic cycle in catchment areas and on a regional scale (Nakayama and Hashimoto, 2011; Nakayama *et al*., in press). Moreover, model simulation in a political scenario for effective selection and usage of ecosystem service sites (Millennium Ecosystem Assessment, 2005) would be a strong approach in the creation of thermally-pleasant environments and the achievement of sustainable development in megacities.

The objective of this chapter is to construct a simulation system of the hydrothermal cycle integrated with multi-scaled levels in horizontal regions of the urban area and in vertical atmosphere–surface unsaturated–saturated layers. The author has previously developed the National Integrated Catchment-based Eco-hydrology (NICE) model (Nakayama, 2008a, 2008b, 2008c, 2009, 2010, 2011a, 2011b; Nakayama and Fujita, 2010; Nakayama and Hashimoto, 2011; Nakayama and Watanabe, 2004, 2006a, 2006b, 2008a, 2008b, 2008c; Nakayama *et al*., 2006, 2007, 2010, in press) (Fig. 1.2), which was newly coupled with UCM (Nakayama and Fujita, 2010) and RAMS (Pielke *et al*., 1992) to simulate the effects of urban geometry and anthropogenic exhaustion on the change in water and heat cycles in the atmospheric–land and interfacial areas of the Japanese megalopolis (NICE-URBAN). Moreover, the author predicted hydrothermal changes for several political scenarios to reduce air temperatures above heat islands and to create thermally-pleasant environments in the megalopolis (Nakayama and Hashimoto, 2011; Nakayama *et al*., in press).

4.2 Study Area

The study area of Kawasaki with approximately 1.3 million inhabitants is in the Keihin industrial zone, the largest industrial area in Japan, located on the western shore of Tokyo Bay, halfway between the Tokyo metropolitan area and Yokohama (Nakayama and Hashimoto, 2011; Nakayama *et al*., in press) (Fig. 4.1). The bay is a eutrophic coastal area typical in Japan. The environment has changed extensively because of a rapid rise in the number of industries and residents, seashore concrete dikes and embankments built for reclamation and shipping from the tidal areas, and the construction of wastewater treatment plants and public sewerage systems. After heavy and chemical industry prosperity in the 1950s, the environmental amenity deteriorated, with air pollution reaching alarming levels in the early 1970s. The city government established a pollution prevention ordinance in 1972 and stipulated stricter standards than those mandated by Japan's 1967 Basic Law for Environmental Protection (Kawasaki City Government, 2004; van Berkel *et al*., 2009). As a result, pollution levels reduced gradually since the late 1970s. In addition, the city government issued policies to revitalize coastal industries and improve environmental amenities to compensate for the collapse of Japan's bubble economy in 1993.

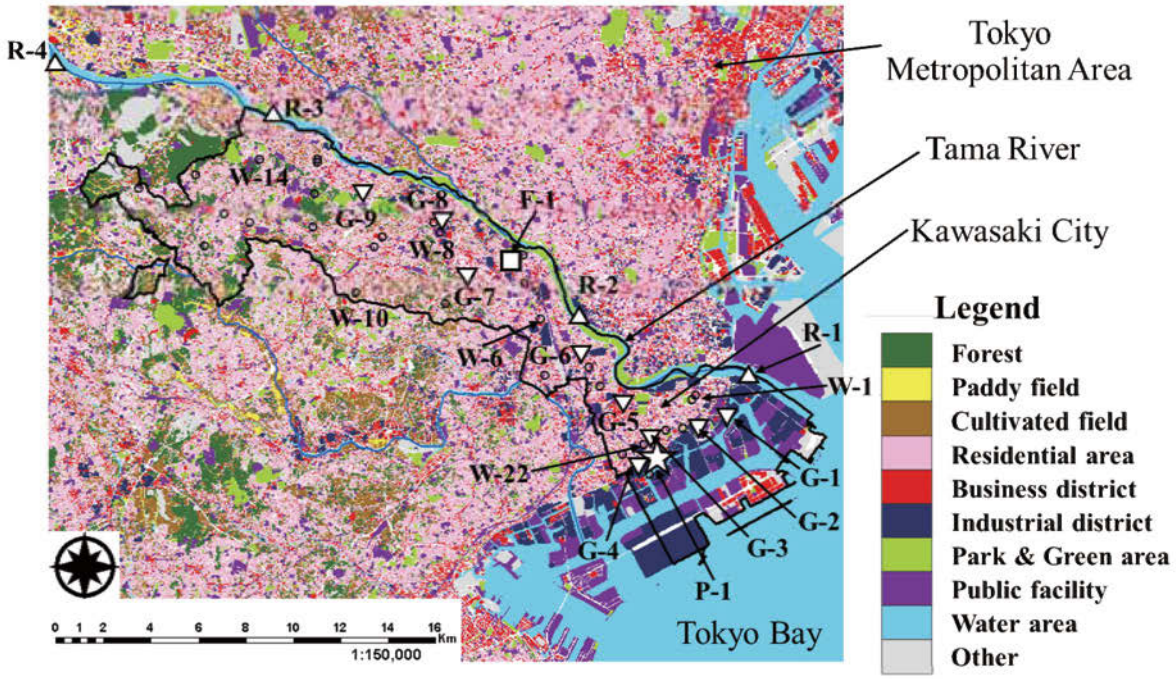

Fig. 4.1 Study area highlighting land cover in the city of Kawasaki and the Kanto Plain, including the Tokyo metropolitan area, Tokyo Bay, and the Tama River catchment (area: 1,240 km^2). Sampled data of 206 points of geological structures were used for input in the NICE-URBAN model. The observed data were as follows: 29 points of weather data (W; ○), 6 points of river discharge data (R; △), 9 points of groundwater level data (G; ▽) during 2004–2006, 1 point of flux tower data at the Todoroki car parking garage (F; □), and 1 point of various pavement blocks at the rooftop of the Keihin building (P; ☆). The data points were used for validation of the model (Table 4.1).

Various environmental degradations such as groundwater level depression, ground subsidence, and seawater intrusion became serious issues resulting from the intensive utilization of groundwater as an important water resource for industries during the period of rapid development from the 1970s to the 1980s (Endo, 1992; Nakayama *et al*., 2007). The government has since prohibited such groundwater usage, which has allowed groundwater levels to recover substantially. However, this measure has created further complications marked by the "floating" of subways, stations, and buildings (Ministry of Environment, 2004a). The study area is currently one of the most severe heat island regions intermingled with hydrologic cycle imbalance. Government officials have taken various measures to mitigate the effects of the heat island by changing and rearranging surface layers via albedo and emissivity and installing elements such as sky views, ventilation or wind paths, and rooftop gardens. Other undertakings are the use of light-colored surfaces and highly infrared reflective coating, reconstruction of elderly buildings and urban geometry by spatially adequate arrangement, and green-infrastructure systems in parks and flood plains, in addition to increasing energy efficiency and managing traffic–transportation systems (Ministry of Environment, 2003; Kawasaki City Government, 2008).

The city is situated on an alluvial plain in the lower Tama River and has the Shimosueyoshi upland in the middle. The city is comprised of residential (40%), commercial–industrial (28%), and other (32%) areas. Lowland areas are covered by alluvial delta clay with a thickness of 10–40 m, which is underlain by alternating layers of silt, sand, and gravel to constitute a semi-confined aquifer system. The northern region borders the Musashino upland, and the western region lies on the Tama hills, which are generally covered by relatively permeable volcanic ash known as Kanto loam (thickness of 5–10 m) (Arai and Sun, 1996). The river, recently considered an important source for flood control, drinking water, and irrigation, is also an environmental amenity in the Japanese megalopolis. In particular, the roles of water resources such as rivers, lakes, seas, and groundwater are important in the mitigation of urban heat islands.

4.3 Materials and Methods

4.3.1 Developing a Process-based Model Applicable to Urban Areas (NICE-URBAN)

In this chapter, the NICE model was newly combined with the UCM to include the effects of the hydrothermal cycle on various engineered pavements and with the RAMS to include the water–heat interaction between land and atmosphere regions (NICE-URBAN) (Nakayama and Hashimoto, 2011; Nakayama *et al*., in press) (Fig. 4.2). The general equations for the atmospheric model (RAMS) are standard hydrostatic Reynolds-averaged primitive equations (Pielke *et al*., 1992) consisting of motion, thermodynamics, water species mixing ratio continuity, mass continuity, and hydrostatic equations. Downward short- and long-wave radiation, precipitation, atmospheric pressure, air temperature, air humidity, and wind speed simulated by the atmospheric model were inputted into the UCM, whereas momentum, sensible, latent, and long-wave flux simulated by the UCM were inputted into the atmospheric model at each time step. This procedure ensures that the feedback process on water and heat transfers between atmospheric regions and land surfaces are implicitly included in the simulation process (Fig. 4.2). Moreover, one-dimensional equations of momentum, heat, and vapor (wind velocity, air temperature, and specific humidity) inside the boundary layer between buildings were coupled with the UCM by considering the influence of buildings on diffusing potentials. In this process, anthropogenic heat emissions were also simulated automatically by coupling with a building energy analysis model on the assumption that all emissions originated from the buildings and depended on the difference between the outside air temperature and the temperature inside the buildings. The heat source data evaluated by the GIS data were also inputted directly as the forcing data in another simulation for verification of the simulated anthropogenic heat emissions. Although this scheme simplifies the anthropogenic heat calculation by coupling the urban canopy and atmospheric models, the model can automatically simulate the feedback processes of hydrothermal cycles between the outdoor conditions and each urban building and is instrumental in predicting future hydrothermal changes, as described in Nakayama *et al*. (in press). A horizontal momentum equation was then solved, preserving the continuity equation at each time step. In addition, the author expanded specific heat conductivity and heat conductivity for natural soil (Sellers *et al*., 1996) into those for engineered pavement by including the effect of the amount of water on the heat characteristics in materials; heat capacity is an important factor for reproducing the amplitude and phase of the diurnal cycle (Nakayama and Fujita, 2010; Nakayama and Hashimoto, 2011; Nakayama *et al*., in press) (Fig. 4.2).

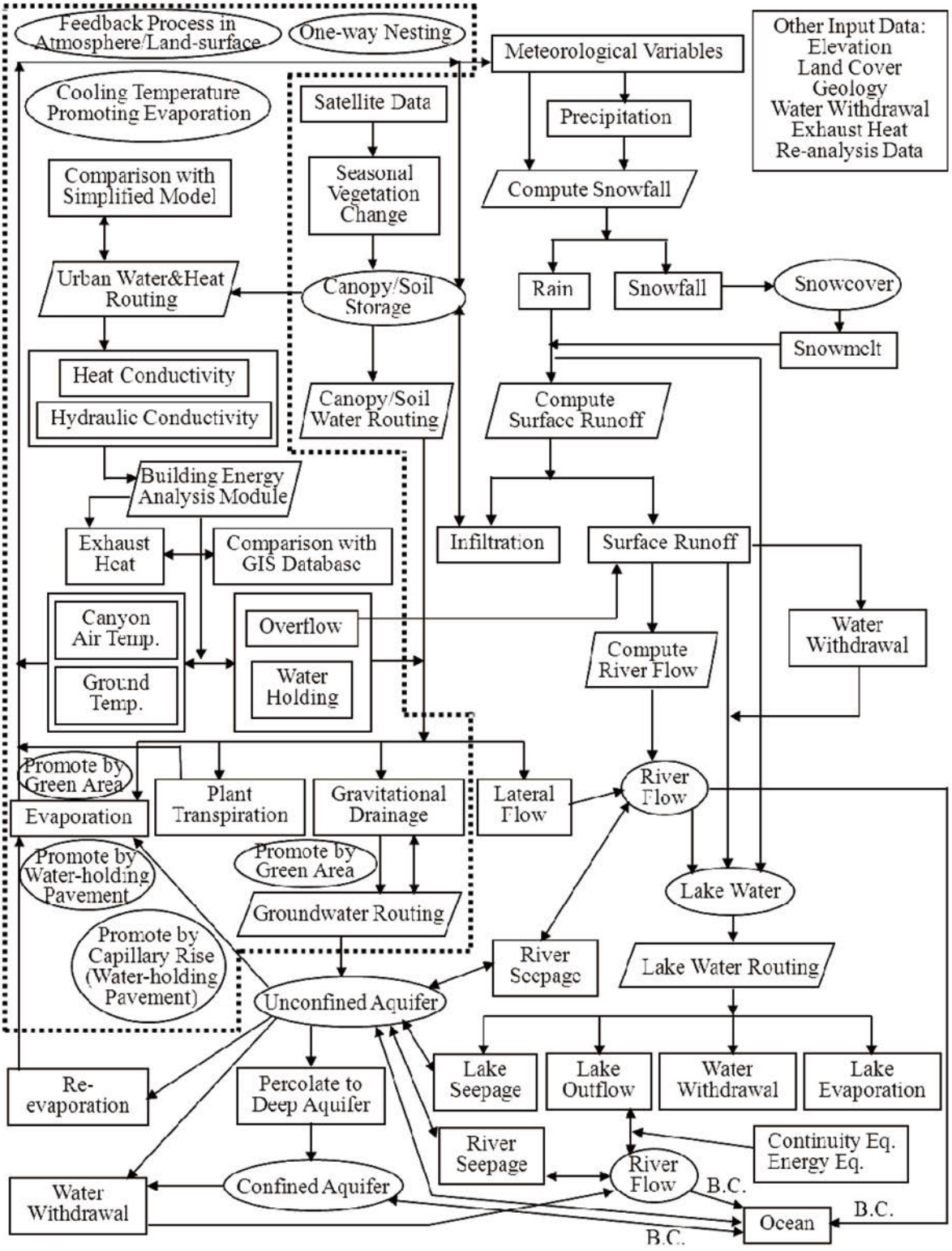

Fig. 4.2 Flow diagram of the NICE-URBAN model. Dotted frames indicate the newly developed processes used in this study.

4.3.2 Input Data and Boundary Conditions

Hourly observation data obtained from the Automated Meteorological Data Acquisition System (AMeDAS) (Japan Meteorological Agency, 2005–2006a) at 126 points were assimilated with NICE-URBAN. Artificial augmentation of waterworks and sewerage systems discharging into the sea was inputted to the model using statistical data for domestic and industrial water usage (Digital National Land Information GIS Data of Japan, 2002). Annual groundwater-use data covering the Kanto Plain (Digital National Land Information GIS Data of Japan, 2002) were digitized and inputted into the model. The rate of water withdrawal in the surrounding (western) area of the Kawasaki district was about 149,000 ton/day in 2004 (Kawasaki City Government, 2004–2006).

Vertical geological structures were divided into 10 layers with a weighting factor of 1.1 by using a 206-sample database and a digital elevation model (DEM) (Geographical Survey Institute of Japan, 1999). The upper layer was set at a depth of 2 m, and the 10th layer was defined by an elevation of –500 m. The geological structure was divided into four types on the basis of hydraulic conductivity (K_h and K_v), specific storage (S_s), and specific yield (S_y) (Nakayama *et al*., 2007). Approximately 50 vegetation and soil parameters were calculated on the basis of vegetation class and soil texture obtained from the Digital National Land Information GIS data of Japan (2002).

At the upstream boundaries, conditions affecting the hydraulic head were used for the model on the supposition that no inflow occurs from the opposite direction of the mountains. A time series of tidal levels was inputted as a constant head at the sea boundary (Nakayama *et al*., 2007). At the lateral boundaries of the region, meteorological data such as temperature, humidity, wind speed, altitude, and sea surface temperatures obtained by the European Centre for Medium-Range Weather Forecasts (ECMWF) were inputted into the model with a resolution of 1° × 1°; similar data obtained from the Meso Scale Model (MSM) with a resolution of 10 km × 10 km were also inputted (Japan Meteorological Agency, 2005–2006b).

4.3.3 Building Structure and Anthropogenic Heat Source in Urban Areas

The anthropogenic exhaustion heat generated by energy consumption considering differences in sensible and latent heat was analyzed by using the GIS database for fundamental investigation of urban planning in the study area (Kawasaki City Government, 1994; Tokyo Metropolitan Government, 2001; Yokohama City Government, 2003) (Fig. 4.3). Because several studies have reported that the main sources of anthropogenic heat emission are buildings and factories in Kawasaki, both of which are located at the center of the Keihin industrial area, the anthropogenic sensible and latent heats generated by buildings such as offices and homes, and factory smokestacks were analyzed according to anthropogenic heat per unit. The anthropogenic sensible, latent, and sewage heats at each mesh (200 m resolution) were calculated every hour by multiplying the area of each building-use and land-use with unit energy consumption in eight types of land—detached houses, apartment houses, offices, businesses, hotels, schools, factories, and other—reported previously (Ministry of Environment, 2004b). The calculated heat results were inputted into each layer of the model including the vertical direction of a vent and an exhaust fan within an average building height as often as possible because this type of location differs significantly from buildings and factories. These calculated heat results were also used to calibrate and validate the anthropogenic heat emissions that were automatically simulated by the feedback process of NICE-URBAN (Nakayama *et al*., in press) (Fig. 4.2).

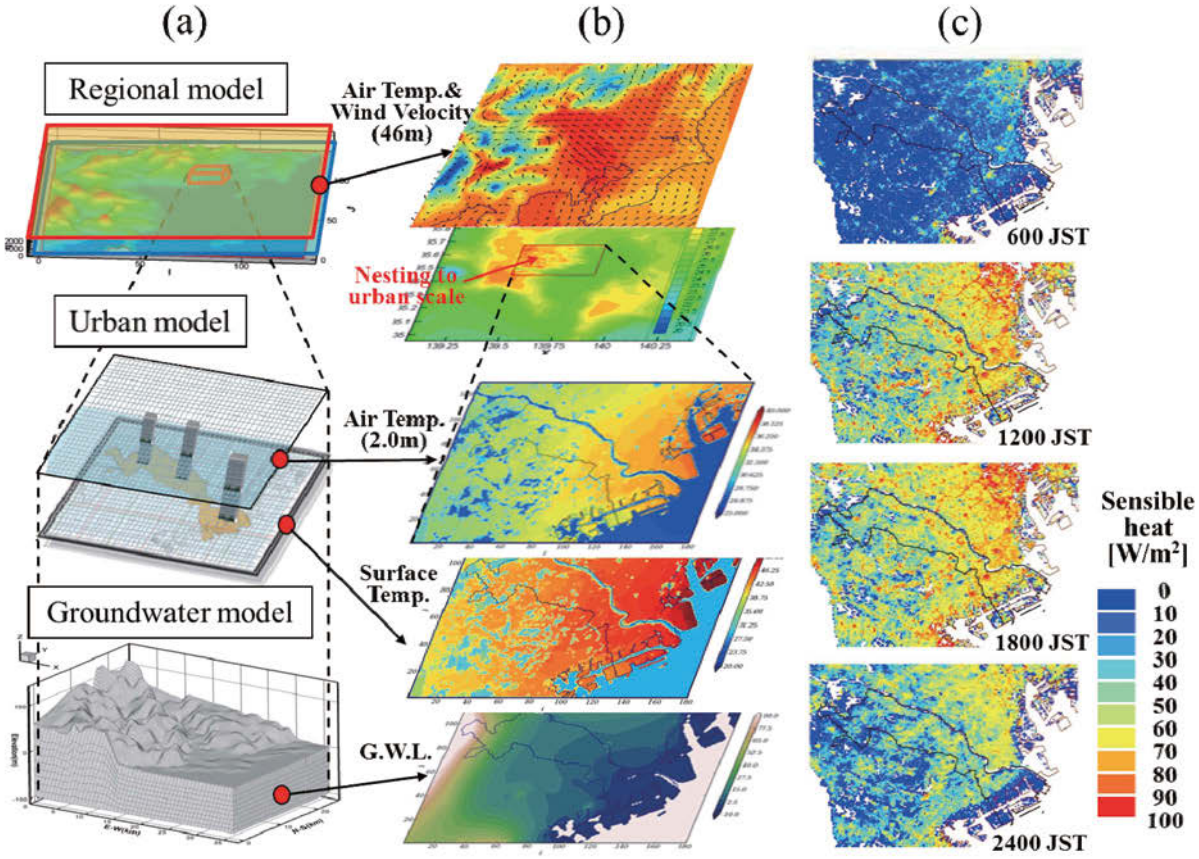

Fig. 4.3 Schematic representation of multi-scaled model illustrating (a) multi-layers in the vertical direction, (b) an example of simulated values, and (c) the diurnal cycle of anthropogenic heat emission estimated by the GIS database.

4.3.4 Simulation and Prediction for Political Scenarios

The simulation was conducted with multi-scale levels in a horizontal regional area (260 km wide by 260 km long with a grid spacing of 2 km covering the Kanto region) nesting one way to an urban area (36 km wide by 26 km long with 200 m grid covering Kawasaki) (Nakayama *et al*., 2007) and in vertical atmosphere–surface unsaturated–saturated layers (Fig. 4.3) for three years from January 1, 2004, to December 31, 2006. There was a six-month warm-up period until equilibrium was reached. A time step of the simulation was changed from Δt = 1.5 s to 1 h depending on spatial scale and submodel. Observed data of groundwater levels, river discharge, air temperature, and humidity (Kanto Regional Development Bureau, 2005–2006; Kawasaki City Government, 2004–2006) were used to validate the simulations (Fig. 4.1 and Table 4.1).

Table 4.1. Lists of observation stations used for validation.

No.	Point Name	Type	Lat.	Lon.	Elev. (m)
W-1	Daishi-1	Weather Data	35°32'1"	139°44'8"	1.0
W-2	Sakamoto	Weather Data	35°31'14"	139°43'19"	-1.0
W-3	Oda	Weather Data	35°30'41"	139°42'6"	1.0
W-4	Minamigawara	Weather Data	35°32'14"	139°41'27"	2.0
W-5	Ogura	Weather Data	35°32'28"	139°39'56"	3.0
W-6	Kariyado	Weather Data	35°33'45"	139°39'49"	6.0
W-7	Nishimaruko	Weather Data	35°35'12"	139°39'19"	8.0
W-8	Hisamoto	Weather Data	35°35'43"	139°37'0"	14.0
W-9	Hisasue	Weather Data	35°34'5"	139°37'9"	45.0
W-10	Nishiarima	Weather Data	35°34'19"	139°34'38"	51.0
W-11	Sugao	Weather Data	35°35'50"	139°33'27"	44.0
W-12	Miyazakidai	Weather Data	35°35'36"	139°35'23"	37.0
W-13	Noborito	Weather Data	35°37'22"	139°33'34"	21.0
W-14	Minamisuge	Weather Data	35°37'22"	139°31'57"	62.0
W-15	Nagasawa	Weather Data	35°35'55"	139°31'40"	83.0
W-16	Chiyogaoka	Weather Data	35°36'60"	139°30'9"	108.0
W-17	Shinpukuji	Weather Data	35°35'23"	139°30'25"	47.0
W-18	Kurikidai	Weather Data	35°36'41"	139°28'35"	83.0
W-19	Ougimachi	Weather Data	35°30'14"	139°42'52"	2.0
W-20	Ikuta	Weather Data	35°36'35"	139°33'30"	78.0
W-21	Daishi-2	Weather Data	35°31'55"	139°44'2"	1.0
W-22	Tajima	Weather Data	35°30'54"	139°42'42"	1.0
W-23	Kawasaki	Weather Data	35°31'53"	139°42'11"	2.0
W-24	Saiwai	Weather Data	35°32'39"	139°41'9"	3.1
W-25	Nakahara	Weather Data	35°34'34"	139°39'21"	8.0
W-26	Takatsu	Weather Data	35°35'56"	139°36'50"	13.0
W-27	Miyamae	Weather Data	35°35'22"	139°35'10"	45.9
W-28	Tama	Weather Data	35°37'19"	139°33'33"	23.0
W-29	Asao	Weather Data	35°36'8"	139°30'56"	104.0

Table 4.1. Lists of observation stations used for validation (continued).

No.	Point Name	Type	Lat.	Lon.	Elev. (m)
G-1	Chidoricyo	Groundwater Level	35°31'21"	139°45'11"	2.0
G-2	Kannongawa	Groundwater Level	35°31'24"	139°44'10"	0.0
G-3	Tajima	Groundwater Level	35°31'02"	139°42'52"	0.0
G-4	Watada	Groundwater Level	35°30'38"	139°42'40"	1.0
G-5	Rokugou	Groundwater Level	35°32'9"	139°42'15"	2.0
G-6	Komuki	Groundwater Level	35°32'46"	139°41'16"	3.0
G-7	Shinjyo	Groundwater Level	35°34'51"	139°37'53"	9.0
G-8	Sakado	Groundwater Level	35°35'45"	139°37'23"	12.0
G-9	Inada	Groundwater Level	35°36'48"	139°34'44"	18.0
R-1	Tamagawakakou	River Level	35°32'12"	139°46'1"	2.0
R-2	Denencyofu	River Level	35°35'21"	139°39'57"	8.0
R-3	Ishihara	River Discharge and Level	35°38'39"	139°31'40"	35.0
R-4	Takahatabashi	River Discharge and Level	35°39'52"	139°24'37"	67.0
R-5	Hinobashi	River Discharge and Level	35°41'1"	139°24'49"	83.0
R-6	Cyofubashi	River Discharge and Level	35°46'52"	139°16'0"	182.0
F-1	Todoroki	Flux Tower	35°35'10"	139°39'0"	9.0
P-1	Keihin	Pavement Block	35°30'38"	139°43'1"	2.0

Scenario-based analyses have been used extensively since the 1940s for better understanding of the effectiveness of alterative policies and technology options under uncertain situations (Kahyaogˇlu-Koracˇin *et al*., 2008). In this study, the author prepared two types of land cover scenarios to reduce air temperature. The first is a technology-oriented approach that introduces a water-retaining pavement to promote positive cooling through evaporative latent heat effects (Nakayama and Fujita, 2010). In contrast, the second scenario is a natural-restoration-oriented approach that introduces new green areas or expands existing ones to promote passive cooling effects through plant evapotranspiration (Nakayama *et al*., 2007). These scenarios were designed to follow the techno-garden and adapting-mosaic scenarios, both of which were developed for the Millennium Ecosystem Assessment project (Millennium Ecosystem Assessment, 2005). Using the GIS database originally developed for city planning, these two scenarios were applied to all vacant spaces of building sites and to open spaces like parks in Kawasaki (Table 4.2); these areas were identical to the target areas of existing land use legislation enacted to restore nature and to create amenities (Kawasaki City Government, 2008). Identification of cooling effects would assist policymakers in prioritizing alternatives or deciding which approach to adopt as a countermeasure against heat islands (Nakayama and Hashimoto, 2011; Nakayama *et al*., in press).

Table 4.2. Present land use and available vacant space considered in the scenario simulation.

Land use	Area (km^2)	Available vacant space (km^2)
Industrial sites	18.4	13.5
Low-rise residential areas (general)	40.0	12.8
Low-rise residential areas (high-density)	0.5	0.1
Medium-to-high-rise residential areas	17.0	5.6
Commercial and business areas	4.8	3.0
Parks and green areas	2.2	1.9
Public institution areas	16.6	5.3
Roads	10.8	N/a
Forests	9.9	N/a
Rice paddy fields	0.1	N/a
Cultivated land	2.2	N/a
Rivers and lakes	6.3	N/a
Sea	8.8	N/a
Other	6.7	N/a
Total	144.4	42.1

4.4 Results and Discussion

4.4.1 Multi-scaled Characteristic in Hydrothermal Cycle

The simulated air temperature was compared with values observed across the Kawasaki region from August 15–31, 2006 (Kawasaki City Government, 2006) (Fig. 4.4a). Despite better reproduction of cloud cover, the simulated air temperature underestimates conditions in August 16–19 and overestimates conditions in August 24–27 mainly because of an inaccurate precipitation simulation by RAMS when nesting with one way to local scale (Pielke *et al*., 1992). The simulated air temperatures in NICE-URBAN are generally in good agreement with the observed values at various land covers such as cultivated fields, residential areas, business districts, and industrial areas. This is evident by the high correlation (r^2 = 0.70 – 0.80) and relatively high accuracy (root-mean-square error; RMSE = 1.6–2.1 °C), similar to those observed in previous cases (Nakayama *et al*., 2007; Nakayama and Fujita, 2010). The simulated heat-flux budget was compared to the analyzed value at the water-holding pavement in the Todoroki car parking area (F-1 in Table 4.1) from August 3 to August 7, 2007 (Fig. 4.4b). The water-holding pavement exhibited a surface temperature about 10.0 °C lower than that of the infiltration pavement, which is closely associated with the promotion of vaporization and the higher surface reflectance (0.48) of this material; this result continued for five days after the saturation of the water-holding pavement (Nakayama and Fujita, 2010). In the field experiment, these heat fluxes were estimated by using the bulk method and, following water irrigation of about 5.4 liter per 1 m^2 on August 3, the errors in the cumulative heat flux ranged from –0.2% to 1.2% in the daytime (Nakayama *et al*., in press). The simulated maximum sensible and latent heat fluxes in the water-holding pavement recorded just after water irrigation were 130 W/m^2 and 345 W/m^2, respectively, which had relatively good approximations of 161 W/m^2 and 337 W/m^2, respectively, in observed values and in previous research (Yamagata *et al*., 2008). The simulated result shows that the newly symbiotic pavement is a highly effective in promoting cooler temperatures (Nakayama and Hashimoto, 2011; Nakayama *et al*., in press).

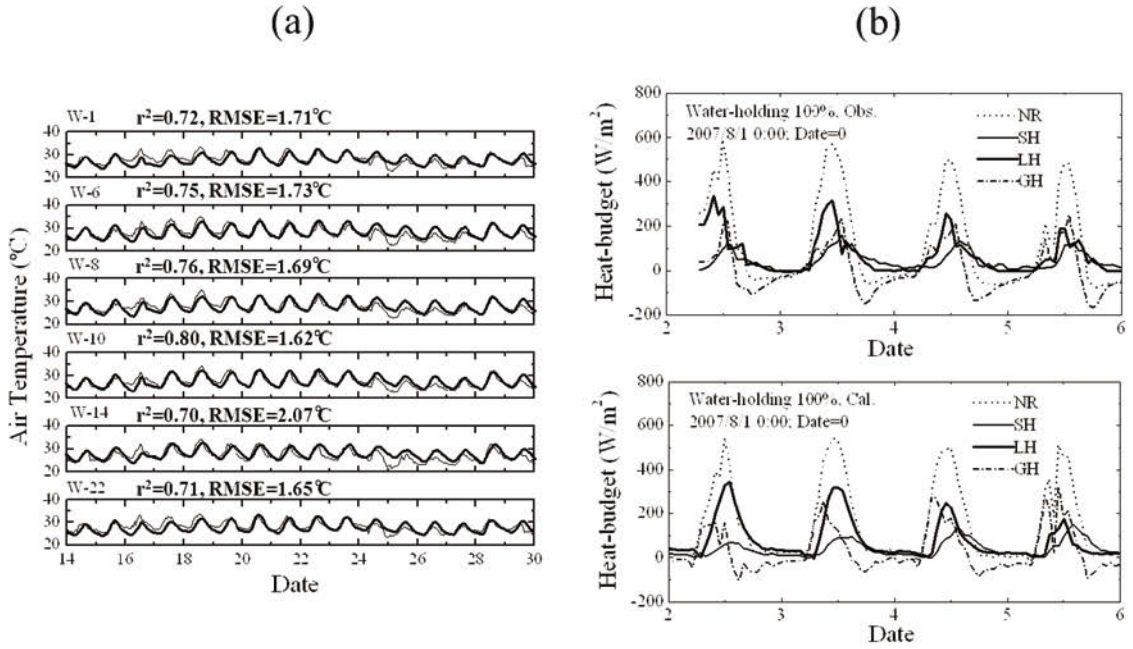

Fig. 4.4 Verification of heat flux in the interfacial area: (a) comparison of simulated air temperature with observed value 2.0 m above the ground surface at points W-1 to W-29 in Table 4.1; (b) validation of heat-flux budget in the symbiotic water-holding pavement after water irrigation at point F-1 in Table 4.1. In (a), the solid line represents observation data, and the bold line represents the results simulated by NICE-URBAN. Date = 14 on the horizontal axis corresponds to August 15, 2006. r^2 and *RMSE* represent correlation between observed value and simulated value, and root-mean-square error, respectively. In (b), the dotted line represents net radiation (NR); solid line, sensible heat flux (SH); bold line, latent heat flux (LH); and dash-dotted line, ground transfer heat flux (GH). Date = 0 on the horizontal axis corresponds to August 1, 2007.

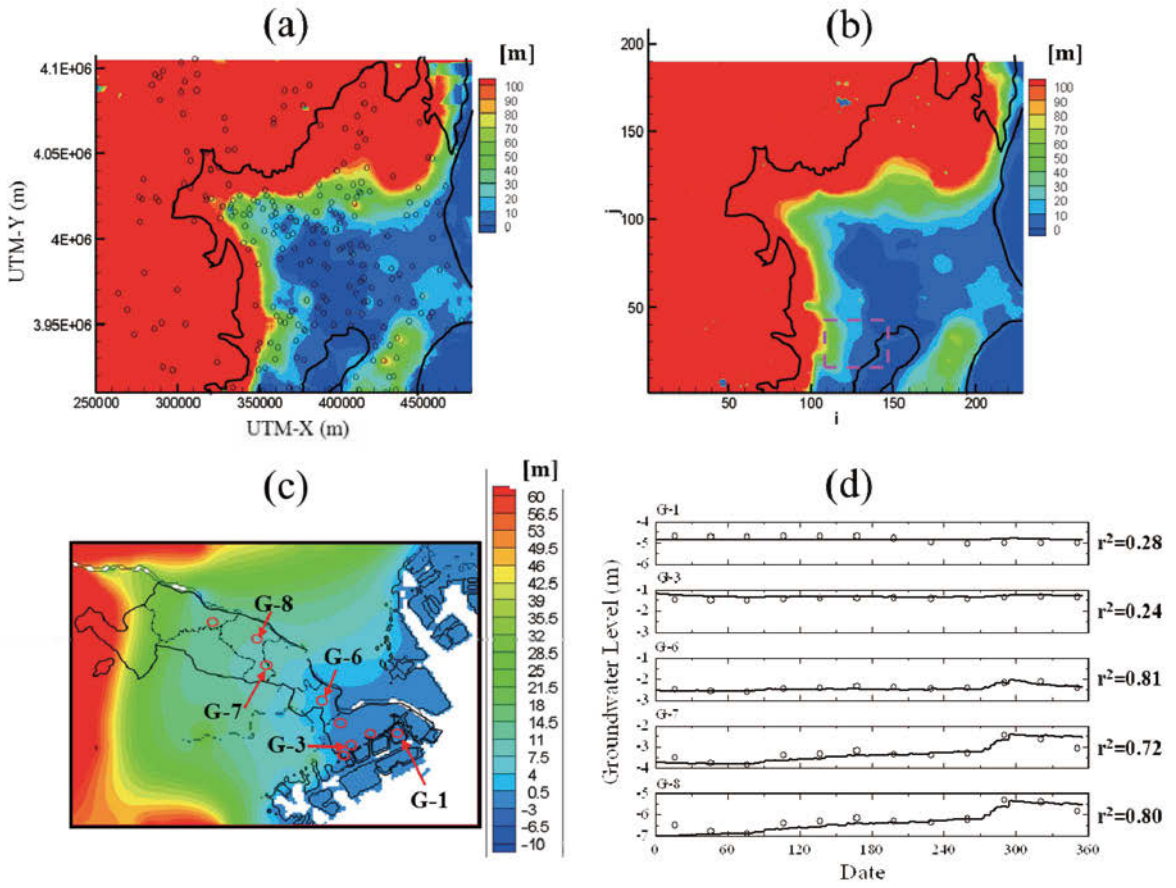

Fig. 4.5 Verification of hydrologic cycle from regional to urban scales: (a) annual-averaged groundwater level in the regional scale (Kanto Plain) interpolated by using the observed value; (b) simulated value in the regional scale; (c) simulated value in the urban area downscaled from the regional scale in (b); and (d) comparison of simulated groundwater level with observed value at points G-1 to G-9 in Table 4.1. In (a), the dotted circle represents the observed locations of 247 points. In (b), the dotted purple frame represents the urban area simulated in (c). In (d), circles represent observation data, and lines represent results simulated by NICE-URBAN. Date = 0 on the horizontal axis corresponds to January 1, 2004.

4.4.2 Prediction of Hydrothermal Changes in the Symbiotic Urban Scenario

As described in Section 4.3.4, the author predicted hydrothermal changes in the symbiotic urban scenario (Fig. 4.6). The previous research showed that in addition to air temperature above the surface, the water content of the block also affects the surface temperature (Nakayama and Fujita, 2010). Because the model estimates an air temperature at the water-holding pavement 1–2 °C lower than that at the lawn and 3–5 °C lower than that at the building rooftop as the surface level (Saaroni *et al*., 2000), this material is instrumental for proving the positive cooling effects when combined with lawns for passive cooling at the surface level in addition to the street level and at the regional scale (Nakayama and Fujita, 2010; Nakayama *et al*., 2007). Because the air temperature was relatively high with no rainfall, the temperature on the heat island was severe at 1500 JST on August 5, 2006; these conditions are effective in demonstrating the cooling effects of the water-holding pavement in addition to green areas. The simulated surface temperature in the scenario of the water-holding pavement showed a dramatic decrease in the entire city of Kawasaki (Figure 10b). In particular, the business district area beside the sea (Fig. 4.6a), where the urban heat island is predominant—because of the paved surfaces (Fig. 4.1) and a larger amount of anthropogenic heat sources (Fig. 4.3)—underwent effective cooling in this scenario. The simulation shows that the scenario of a natural zone and green area was also effective for cooling temperatures in the study area (Fig. 4.6c).

The predicted groundwater level change in August is interesting in contrast to the previously simulated air temperature (Fig. 4.6d-e). In the water-holding-pavement scenario, all the water required to saturate the water-holding pavement was automatically simulated by considering the difference between precipitation and evaporation, and withdrawn from subsurface groundwater in the NICE-URBAN model, which indicates that the pavement remained saturated. The increase in recharge rate and the consequent groundwater level increase in the scenario of natural zones and green areas are also very effective in promoting groundwater resources in urban areas covered by impermeable pavements (Nakayama *et al*., 2007). In the scenario of the water-holding pavement, the groundwater level decreased dramatically, particularly in the commercial and industrial areas beside the sea; the level also decreased in the inland residential areas as a consequence of dramatic cooling in the corresponding and surrounding areas. Because these phenomena are closely related to the heat capacity of water and the conductivity of the pavement, the subsurface water temperature is an additional important factor for effective cooling. Because the water temperature in an aquifer remains nearly constant throughout the year, the use of groundwater as a heat sink is a highly effective tool for addressing the urban heat island phenomenon, particularly during the summer (Ministry of Environment, 2003; Nakayama and Fujita, 2010). Generally, predicted temperatures and groundwater levels in the business districts of Kawasaki and the Tokyo metropolitan area are greatly affected. This factor is critical from a political perspective and highlights the importance of greater precision when estimating the arrangement of symbiotic urban scenarios in the study area together with neighboring administrations (Nakayama and Hashimoto, 2011; Nakayama *et al*., in press).

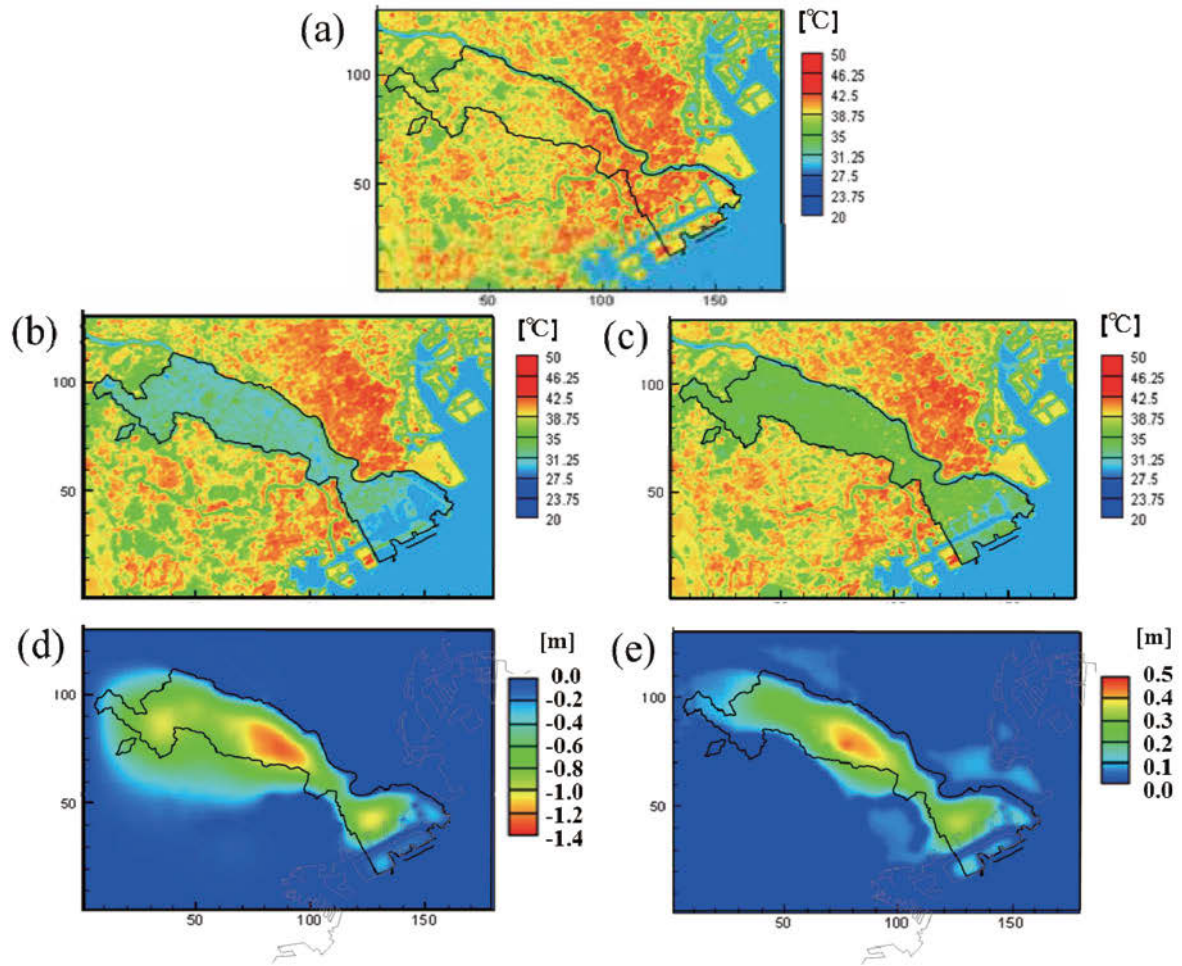

Fig. 4.6 Prediction of hydrothermal changes at 1500 JST on August 5, 2006, in the symbiotic urban scenario: (a) present surface temperature; (b–c) prediction of surface temperature considering water-holding pavement and green areas, respectively; and (d–e) prediction of monthly-averaged groundwater level change considering water-holding pavement and green areas, respectively.

4.4.3 Heterogeneity of Hydrothermal Cycles in Urban Areas

Simulated groundwater levels relative to the surface clearly indicate the heterogeneity of water resources as a slight imbalance of the hydrologic cycle in the urban and surrounding areas (Fig. 4.7a). The levels become deeper in the northern part of Kawasaki and Kanto, where extensive groundwater extraction continues through the cultivation of spring water around the foot of the mountain. This cultivation of spring water takes place because regulated areas are few and regulatory standards are relatively less severe (Hayashi *et al*., 2009). For these reasons, land subsidence remains a serious environmental issue. In addition to the thermal environment, water contamination also shows some relation to the heterogeneity of water resources (Fig. 4.7b). For example, higher nitrogen concentrations in groundwater exceed environmental standards (10 mg/L) in some areas (Ministry of Environment, 2000; Nakayama *et al*., 2007; Nakayama and Watanabe, 2008a), creating substandard drinking water that could threaten human health and the ecosystem (Ministry of Environment, 2004a). These contaminants could leach into the water supply and also play an important role in eutrophication, which indicates that groundwater is a relatively large source of nitrogen loading to aquatic regions, even though the seepage is not as large as the overland flow (Nakayama *et al*., 2007; Nakayama and Watanabe, 2008a; Taniguchi *et al*., 2009). In addition, nitrogen concentration varies according to the hydrologic cycle and water temperature through complex chemical reactions. Therefore, it is necessary to further evaluate water resources, heat islands, and contamination issues relative to environmental pollution (Nakayama *et al*., 2007; Nakayama and Watanabe, 2008a; Nakayama and Hashimoto, 2011).

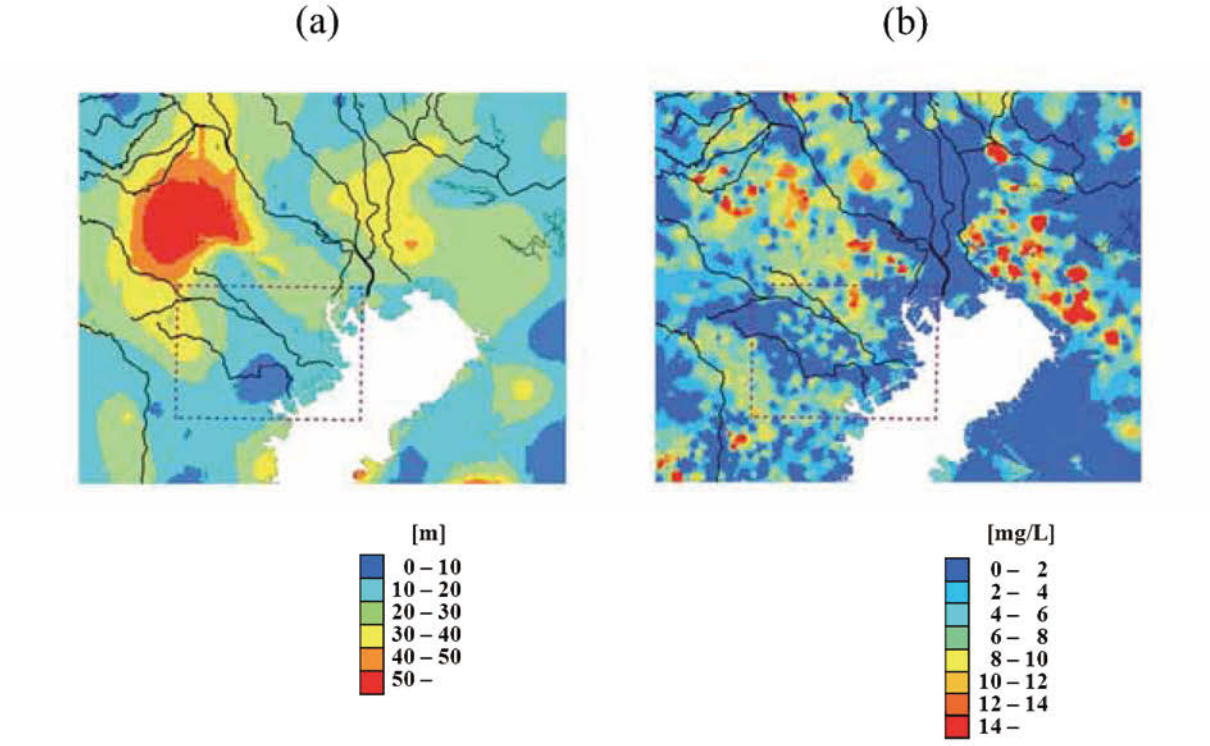

Fig. 4.7 Environmental pollution in urban and surrounding areas: (a) simulated groundwater level relative to the ground surface; (b) annual-averaged groundwater nitrogen concentration (mg/L) interpolated by observed data. Urban and cultivated fields are plotted together in the figures. Dotted frames represent urban areas similar to those described in Fig. 4.5. The northeastern region of the urban area represents the Tokyo metropolitan area.

4.5 Conclusion

The process-based NICE model was coupled with the UCM and RAMS models to simulate the effects of urban structures and anthropogenic emission on hydrothermal change in the Japanese megalopolis (NICE-URBAN). The simulation, which integrated multi-scale horizontal regional–urban–point levels and vertical atmosphere–surface unsaturated–saturated layers, was created to predict the effect of urban geometry and anthropogenic exhaustion on hydrothermal changes in the atmospheric–land and the interfacial areas of the Japanese megalopolis. The results suggest that the latent heat flux in the novel water-holding pavement—consisting of porous asphalt and water-holding filler made of steel by-products based on silica compounds—strongly affects the hydrologic cycle and cooling temperatures in comparison with the observed heat budget. The author further evaluated the relationship between the effects of groundwater used as a heat sink to address the temperatures on the heat island and the effects of infiltration on the water cycle in urban areas. The results indicate that effective water resource management is instrumental for cooling heat islands and recovering a sound hydrologic cycle.

References

Alberti M., Booth D., Hill K., Coburn B., Avolio C., Coe S., Spirandelli D. (2007) The impact of urban patterns on aquatic ecosystems: an empirical analysis in Puget lowland sub-basin. Landscape and Urban Planning, 80, 345-361.

Andersen C.T., Foster I.D.L., Pratt C.J. (1999) The role of urban surfaces (permeable pavements) in regulating drainage and evaporation: development of a laboratory simulation experiment. Hydrological Processes, 13, 597-609.

Arai T., Sun S. (1996) The Kanto plain and the Yangtze delta. Kokon-Shoin Co. Ltd., Tokyo, 163 pp.

Asaeda T., Ca V.T. (1993) The subsurface transport of heat and moisture and its effect on the environment: a numerical model. Boundary-Layer Meteorology, 65, 159-179.

Chang C.R., Li M.H., Chang S.D. (2007) A preliminary study on the local cool-island intensity of Taipei city parks. Landscape and Urban Planning, 80, 386-395.

Deardorff J.W. (1978) Efficient prediction of ground surface temperature and moisture with inclusion of a layer of vegetation. Journal of Geophysical Research, 83, 1889-1903.

Digital National Land Information GIS Data of Japan (2002) Database of groundwater in Japan. Ministry of Land Infrastructure and Transport of Japan. http://www.nla.go.jp/ksj/.

Dudhia J. (1993) A nonhydrostatic version of the Penn State-Ncar mesoscale model: Validation tests and simulation of an atlantic cyclone and cold front. Monthly Weather Review, 121, 1493-1513.

Dupont S., Mestayer P.G., Guilloteau E., Berthier E., Andrieu H. (2006) Parameterization of the urban water budget with the submesoscale soil model. Journal of Applied Meteorology and Climatology, 45, 624-648.

Endo T. (1992) Confined groundwater system in Tokyo. Environmental Geology and Water Sciences, 20, 21-34.

Ferguson G., Woodbury A.D. (2004) Subsurface heat flow in an urban environment. Journal of Geophysical Research, 109, B02402, doi:10.1029/2003JB002715.

Geographical Survey Institute of Japan (1999) Digital map 50m grid (elevation), Nippon-II. CD-ROM.

Golden J.S. (2003) The built environment induced urban heat island effect in rapidly urbanizing arid regions – A sustainable urban engineering complexity. Environmental Sciences, 4, 321-349.

Grimmond C.S.B., Oke T.R. (1991) An evapotranspiration-interception model for urban areas. Water Resources Research, 27(7), 1739-1755.

Hagishima A, Tanimoto J, Narita K. (2005) Intercomparisons of experimental convective heat transfer coefficients and mass transfer coefficients of urban surfaces. Boundary-Layer Meteorology, 117, 551-576, doi:10.1007/s10546-005-2078-7.

Hayashi T., Tokunaga T., Aichi M., Shimada J., Taniguchi M. (2009) Effects of human activities and urbanization on groundwater environments: An example from the aquifer system of Tokyo and the surrounding area. Science of the Total Environent, 407, 3165-3172, doi:10.1016/j.scitotenv.2008.07.012.

Hollis G.E., Ovenden J.C. (1988a) One year irrigation experiment to assess losses and runoff volume relationships for a residential road in Hertfordshire, England. Hydrological Processes, 2, 61-74.
Hollis G.E., Ovenden J.C. (1988b) The quantity of stormwater runoff from ten stretches of road, a car park and eight roofs in Hertfordshire, England during 1983. Hydrological Processes, 2, 227-243.
Ichinose T., Shimodozono K., Hanaki K. (1999) Impact of anthropogenic heat on urban climate in Tokyo. Atmospheric Environment, 33, 3897-3909.
Japan Meteorological Agency (JMA) (2005-2006a) AMeDAS (Automated Meteorological Data Acquisition System) Annual Reports 2005-2006. Japan Meteorological Business Support Center (CD-ROM).
Japan Meteorological Agency (JMA) (2005-2006b) MSM (Meso Scale Model) Objective Analysis Data 2005-2006. Japan Meteorological Business Support Center (CD-ROM).
Kahyaogˇlu-Koracˇin J., Bassett S., Mouat D., Gertler A. (2008) Application of a scenario-based modeling system to evaluate the air quality impacts of future growth. Atmospheric Environment, 43(5), 1021-1028, doi:10.1016/j.atmosenv.2008.04.004.
Kanto Regional Development Bureau (2000-2001) Observation data of river discharge, groundwater level, river quality, and groundwater quality.
Kanto Regional Development Bureau (2005-2006) Observation data of river discharge and level at Tama River 2005–2006.
Kawasaki City Government (1994) GIS database about building-use and land-use. Fundamental investigation for urban planning.
Kawasaki City Government (2004) Eco-industrial revolution underway in Kawasaki - Kawasaki Model (in Japanese).
Kawasaki City Government (2004-2006) Observation data of groundwater level, air temperature, and humidity 2004-2006.
Kawasaki City Government (2008) Implementation plan for open space planning (in Japanese).
Kusaka H., Kimura F. (2004) Coupling a single-layer urban canopy model with a simple atmospheric mode: Impact on urban heat island simulation for an idealized case. Journal of Meteorological Society of Japan, 82, 67-80.
Kusaka H., Kondo H., Kikegawa Y., Kimura F. (2001) A simple single-layer urban canopy model for atmospheric models: Comparison with multi-layer and slab models. Boundary-Layer Meteorology, 101, 329-358.
Millennium Ecosystem Assessment (2005) Strengthening capacity to manage ecosystems sustainability for human well-being. http://www.millenniumassessment.org/en/index.aspx.
Ministry of Environment (2000) Observation data of groundwater nitrogen concentration in the Kanto district.
Ministry of Environment (2003) Research report about the effect of heat island phenomena on surrounding environments. http://www.env.go.jp/air/report/h15-02/ (in Japanese).
Ministry of Environment (2004a) Present condition and provision against groundwater pollution by nitrate nitrogen. In: Japan Environment Association (Ed) Environment 29: 14-20 (in Japanese).
Ministry of Environment (2004b) Report on heat-island measures by controlling anthropogenic exhaustion heat in the urban area. http://www.env.go.jp/air/report/h16-05/ (in Japanese).
Nakayama T. (2008a) Factors controlling vegetation succession in Kushiro Mire. Ecological Modelling, 215, 225-236, doi:10.1016/j.ecolmodel.2008.02.017.
Nakayama T. (2008b) Shrinkage of shrub forest and recovery of mire ecosystem by river restoration in northern Japan. Forest Ecology and Management, 256, 1927-1938, doi:10.1016/j.foreco.2008.07.017.
Nakayama T. (2008c) Development of process-based NICE model and simulation of ecosystem dynamics in the catchment of East Asia (Part II), CGER's Supercomputer Monograph Report, 14, NIES, 91p., http://www-cger.nies.go.jp/publication/I083/i083.html.
Nakayama T. (2009) Simulation of ecosystem degradation and its application for effective policy-making in regional scale. In River pollution research progress, Mattia N. Gallo, Marco H. Ferrari (eds), 1-89 (Chapter 1), Nova Science Pub., Inc., New York.
Nakayama T. (2010) Simulation of hydrologic and geomorphic changes affecting a shrinking mire. River Research and Applications, 26(3), 305-321, doi:10.1002/rra.1253.
Nakayama T. (2011a) Simulation of complicated and diverse water system accompanied by human intervention in the North China Plain. Hydrological Processes, 25, 2679-2693, doi:10.1002/hyp.8009.
Nakayama T. (2011b) Simulation of the effect of irrigation on the hydrologic cycle in the highly cultivated Yellow River Basin. Agricultural and Forest Meteorology, 151, 314-327, doi:10.1016/j.agrformet.2010.11.006.

Nakayama T., Fujita T. (2010) Cooling effect of water-holding pavements made of new materials on water and heat budgets in urban areas. Landscape and Urban Planning, 96, 57-67, doi:10.1016/j.landurbplan.2010.02.003.

Nakayama T., Hashimoto S. (2011) Analysis of the ability of water resources to reduce the urban heat island in the Tokyo megalopolis. Environmental Pollution, 159, 2164-2173, doi:10.1016/j.envpol.2010.11.016.

Nakayama T., Watanabe M. (2004) Simulation of drying phenomena associated with vegetation change caused by invasion of alder (Alnus japonica) in Kushiro Mire. Water Resources Research, 40, W08402, doi:10.1029/2004WR003174.

Nakayama T., Watanabe M. (2006a) Simulation of spring snowmelt runoff by considering micro-topography and phase changes in soil layer. Hydrology and Earth System Sciences Discussions, 3, 2101-2144.

Nakayama T., Watanabe M. (2006b) Development of process-based NICE model and simulation of ecosystem dynamics in the catchment of East Asia (Part I), CGER's Supercomputer Monograph Report, 11, NIES, 100p., http://www-cger.nies.go.jp/publication/I063/I063.html.

Nakayama T., Watanabe M. (2008a) Missing role of groundwater in water and nutrient cycles in the shallow eutrophic Lake Kasumigaura, Japan. Hydrological Processes, 22, 1150-1172, doi:10.1002/hyp.6684.

Nakayama T., Watanabe M. (2008b) Role of flood storage ability of lakes in the Changjiang River catchment. Global and Planetary Change, 63, 9-22, doi:10.1016/j.gloplacha.2008.04.002.

Nakayama T., Watanabe M. (2008c) Modelling the hydrologic cycle in a shallow eutrophic lake. Verh International Verein Limnology, 30.

Nakayama T., Yang Y., Watanabe M., Zhang X. (2006) Simulation of groundwater dynamics in North China Plain by coupled hydrology and agricultural models. Hydrological Processes, 20(16), 3441-3466, doi:10.1002/hyp.6142.

Nakayama T., Watanabe M., Tanji K., Morioka T. (2007) Effect of underground urban structures on eutrophic coastal environment. Science of the Total Environment, 373(1), 270-288, doi:10.1016/j.scitotenv.2006.11.033.

Nakayama T., Sun Y., Geng Y. (2010) Simulation of water resource and its relation to urban activity in Dalian City, Northern China. Global and Planetary Change, 73, 172-185, doi:10.1016/j.gloplacha.2010.06.001.

Nakayama T., Hashimoto S., Hamano H. (in press) Multi-scaled analysis of hydrothermal dynamics in Japanese megalopolis by using integrated approach. Hydrological Processes.

Nichol J., Wong M.S. (2005) Modeling urban environmental quality in a tropical city. Landscape and Urban Planning, 73, 49-58.

Ohashi Y., Genchi Y., Kondo H., Kikegawa Y., Yoshikado H., Hirano Y. (2007) Influence of air-conditioning waste heat on air temperature in Tokyo during summer: Numerical experiments using an urban canopy model coupled with a building energy model. Journal of Applied Meteorology and Climatology, 46, 66-81.

Oke T.R. (1987) Boundary layer climates. Methuen Press, London.

Pielke R.A., Cotton W.R., Walko R.L., Tremback C.J., Lyons W.A., Grasso L.D., Nicholls M.E., Moran M.D., Wesley D.A., Lee T.J., Copeland J.H. (1992) A comprehensive meteorological modeling system-RAMS. Meteorology and Atmospheric Physics, 49, 69-91.

Ragab R., Rosier P., Dixon A., Bromley J., Cooper J.D. (2003) Experimental study of water fluxes in a residential area: 2. Road infiltration, runoff and evaporation. Hydrological Processes, 17, 2423-243, doi:10.1002/hyp.1251.

Ramier D., Berthier E., Andrieu H. (2004) An urban lysimeter to assess runoff losses on asphalt concrete plates. Physics and Chemistry of the Earth, 29, 839-847, doi:10.1016/j.pce.2004.05.011.

Saaroni H., Ben-Dor E., Bitan A., Potchter O. (2000) Spatial distribution and microscale characteristics of the urban heat island in Tel-Aviv, Israel. Landscape and Urban Planning, 48, 1-18.

Sansalone J.J., Teng Z. (2005) Transient rainfall-runoff loadings to a partial exfiltration system: implications for urban water quantity and quality. Journal of Environmental Engineering-ASCE, 131(8), 1155-1167.

Sellers P.J., Randall D.A., Collatz G.J., Berry J.A., Field C.B., Dazlich D.A., Zhang C., Collelo G.D., Bounoua L. (1996) A revised land surface prameterization (SiB2) for atomospheric GCMs. Part I : Model formulation. Journal of Climate, 9, 676-705.

Skamarock W., Klemp J.B., Dudhia J., Gill D., Barker D., Wang W., Powers J. (2005) A description of the advanced research wrf version 2. NCAR Tech. Note NCAR/TN-468 STR, 88pp.

Spronken-Smith R.A., Oke T.R. (1999) Scale modeling of nocturnal cooling in urban parks. Boundary-Layer Meteorology, 93, 287-312.

Taniguchi M., Burnett W.C., Ness G.D. (2009) Integrated research on subsurface environments in Asian urban areas. Science of the Total Environent, 407, 3076-3088, doi:10.1016/j.scitotenv.2009.02.001.

Tokyo Metropolitan Government (2001) GIS database about building-use and land-use. Fundamental investigation for urban planning.

van Berkel R., Fujita T., Hashimoto S., Fujii M. (2009) Quantitative assessment of urban and industrial symbiosis in Kawasaki, Japan. Environmental Science and Technology, 43, 1271-1281.

Yamagata H., Nasu M., Yoshizawa M., Miyamoto A., Minamiyama M. (2008) Heat island mitigation using water retentive pavement sprinkled with reclaimed wastewater. Water Science and Technology, 57, 763-771, doi:10.2166/wst.2008.187.

Yokohama City Government (2003) GIS database about building-use and land-use. Fundamental investigation for urban planning.

Zhang H., Sato N., Izumi T., Hanaki K., Aramaki T. (2008) Modified rams-urban canopy model for heat island simulation in chongqing, china. Journal of Applied Meteorology and Climatology, 47, 509-524.

Chapter 5

Final Conclusions and Future Work

5.1 Final Conclusions

In a previous work, the author developed the National Integrated Catchment-based Eco-hydrology (NICE) model, which is a 3-D, grid-based eco-hydrology model that includes interactions among surface water, canopies, unsaturated water, aquifers, lakes, and rivers (Nakayama, 2008a, 2008b, 2008c, 2009, 2010, 2011a, 2011b; Nakayama and Fujita, 2010; Nakayama and Hashimoto, 2011; Nakayama and Watanabe, 2004, 2006a, 2006b, 2008a, 2008b, 2008c; Nakayama *et al*., 2006, 2007, 2010, in press) (Fig. 1.2). In this monograph (Part III), NICE was enhanced to couple human and natural systems and to assess the impact of water degradation on ecosystem changes in urban areas.

In Chapter 2, an integrated approach including the process-based model showed a close relationship among water resources, economic growth, and ecosystem degradation in the environment. Although water resources are vital for human activity, overexploitation causes severe hydrologic changes such as drying up of rivers, receding groundwater levels, and seawater intrusion (Nakayama, 2011a, 2011b; Nakayama *et al*., 2006).

In Chapter 3, the results indicated a close relationship between water resources and economic growth, which strongly affects ecosystem degradation and places a significant burden on the environment in catchment areas. In addition, the simulated results highlighted the association between urban development and sustainable water resource management (Nakayama *et al*., 2006, 2010).

The results of Chapter 4 indicate that effective water resource management is instrumental to the planning and execution of sustainable development strategies; the author also suggests the potential for recovering a sound hydrologic cycle in addition to creating thermally pleasant environments (Nakayama and Hashimoto, 2011; Nakayama *et al*., 2007, in press).

These above results are crucial for clarifying the effect of human activity on ecosystem degradation caused by water–heat–mass cycle changes. The improved model and the prediction of ecosystem dynamics in these catchments are effective for achieving favorable solutions to hydrothermal pollution challenges in future eco-conscious societies.

5.2 Future Work

This monograph suggests that effective water resource management is instrumental to the mitigation of heat islands. This indicates the potential for achieving favorable solutions to hydrothermal pollution challenges in an eco-conscious society (Fig. 5.1). An estimation of the cooling effects of water resources and areas through image analysis including remote sensing, satellite data, and aerial images would be based on quantification through high-resolution imaging of spatio-temporally cooling effects. In addition, the identification of hot spots in hydrothermal cycles through down-scaling is necessary through assimilation with ground-truth networking systems. An initiative to assess alterative policies and technological options can then lead to a more powerful integrated assessment system. The evaluation of hydrothermal interactions by flux observation systems (Nakayama *et al*., in press), isotope analysis (Nakayama and Watanabe, 2008a), and tracer techniques, in addition to the employment of existing databases, can become a more viable solution. Appropriate combinations among the establishment of a network system and the up-scaling method, development of cross-referencing databases of heat sinks and sources, and estimation of potential thermal relaxation of water resources are necessary. Visualization and assessment through an integrated multi-scaled model is the final goal in creating thermally pleasant environments and achieving sustainable development in urban regions. This ideal necessitates

the construction of a highly accurate integrated management model, the reproduction of hydrothermal cycles on the basis of flow and stock mechanisms, and the identification of ecosystem vulnerability and sustainability. These procedures to construct an integrated assessment system for favorable solutions would be beneficial for adaptation to climate changes and urbanization on a global scale, proposal of sustainability index, and the creation of an eco-conscious society (Ministry of Environment, 2004; Nakayama and Hashimoto, 2011; Nakayama *et al*., 2007, in press). Moreover, the construction of an integrated assessment system would provide visualization of hydrothermal feedback about thermal pollution in air, on land, and in marine areas (Nakayama, 2011c).

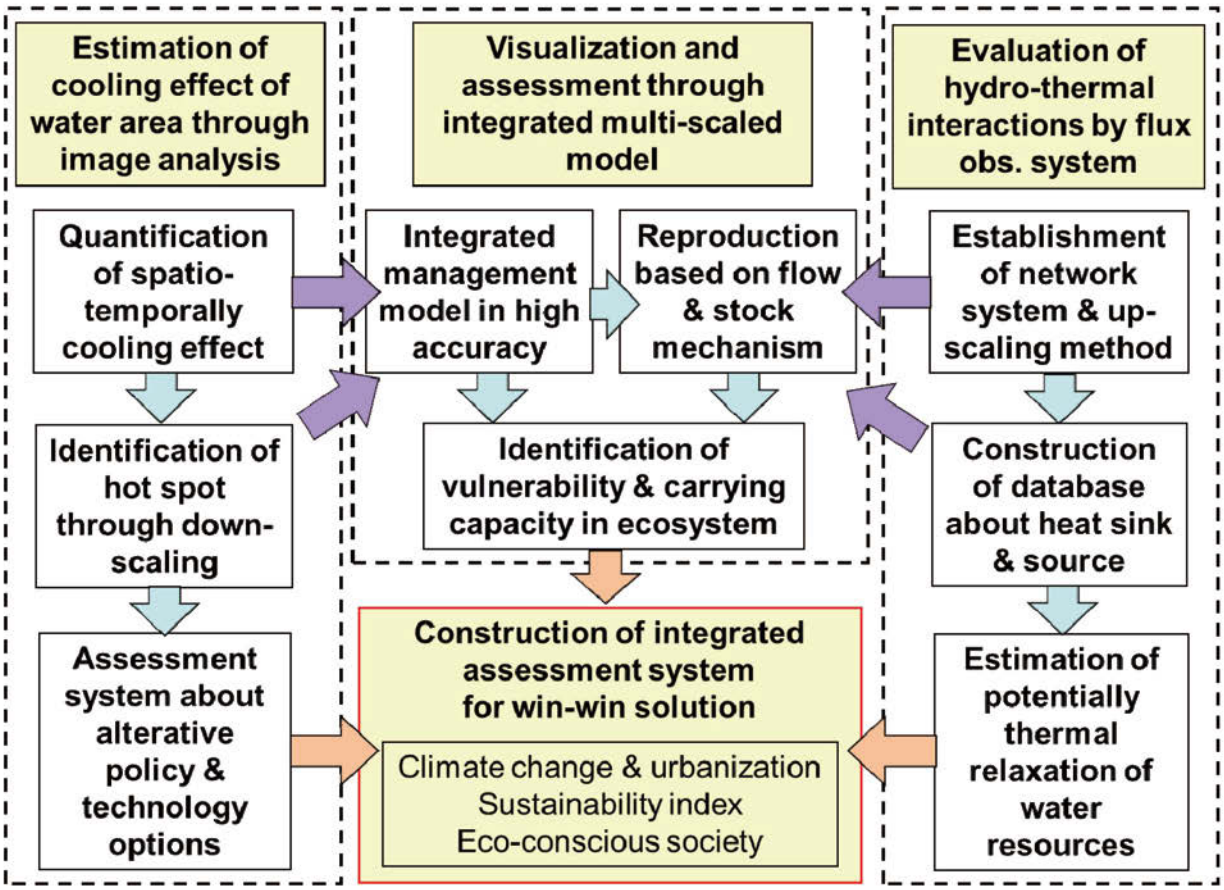

Fig. 5.1 Framework for visualization of hydrothermal interactions for favorable solutions.

Further evaluation of the water–heat–mass cycle in China is also necessary relative to the national security of Japan and international contributions (Nakayama, 2011a, 2011b; Nakayama and Watanabe, 2008b; Nakayama *et al*., 2006, 2010). The Changjiang (Yangtze), Yellow (Huanghe), and Huaihe rivers (Fig. 5.2) are among the "seven big rivers" of China. Their lower reaches are affected by severe flooding nearly every year, which causes significant damage to surrounding towns and farms. In China, the hydroclimate between the North and South is diverse. The semi-arid North is heavily irrigated, which, combined with increased food demands and diminishing water availability, creates substantial pressure in the region of the Yellow River (Brown and Halweil, 1998; Yang et al., 2004; Nakayama *et al*.,

2006, 2010; Nakayama, 2011a,b). However, the flood storage ability around lakes has decreased, and the impact of the Three Gorges Dam (TGD) on flood occurrences in Changjiang downstream against the dam's original purpose is an increasing problem in the humid South region (Shankman and Liang, 2003; Zhao *et al*., 2005; Nakayama and Watanabe, 2008b). Moreover, China is accelerating preparatory work on its ambitious project for transferring water from the Changjiang to the Yellow River (South-to-North Water Transfer Project; SNWTP) (Yang and Zehnder, 2001; Li *et al*., 2007). Although it is estimated that the TGD and SNWTP would remove these imbalances as far as possible (Yang and Zehnder, 2001; Li *et al*., 2007), there is an urgent need to clarify the relations of these two extremes affected by human activity, develop a process-based model, and present an integrated approach for appropriate water resource management to achieve sustainable development on a regional scale (Nakayama, 2011d; Nakayama and Shankman, 2011a, 2011b). Therefore, accurate evaluation of the optimum amount of transferred water, and socioeconomic and environmental consequences are essential in both basins. Future installments of this study will evaluate water–heat–mass dynamics using the NICE model to simulate the changes caused by human activity and to aid accurate estimation on the amount of water to be transferred between catchments.

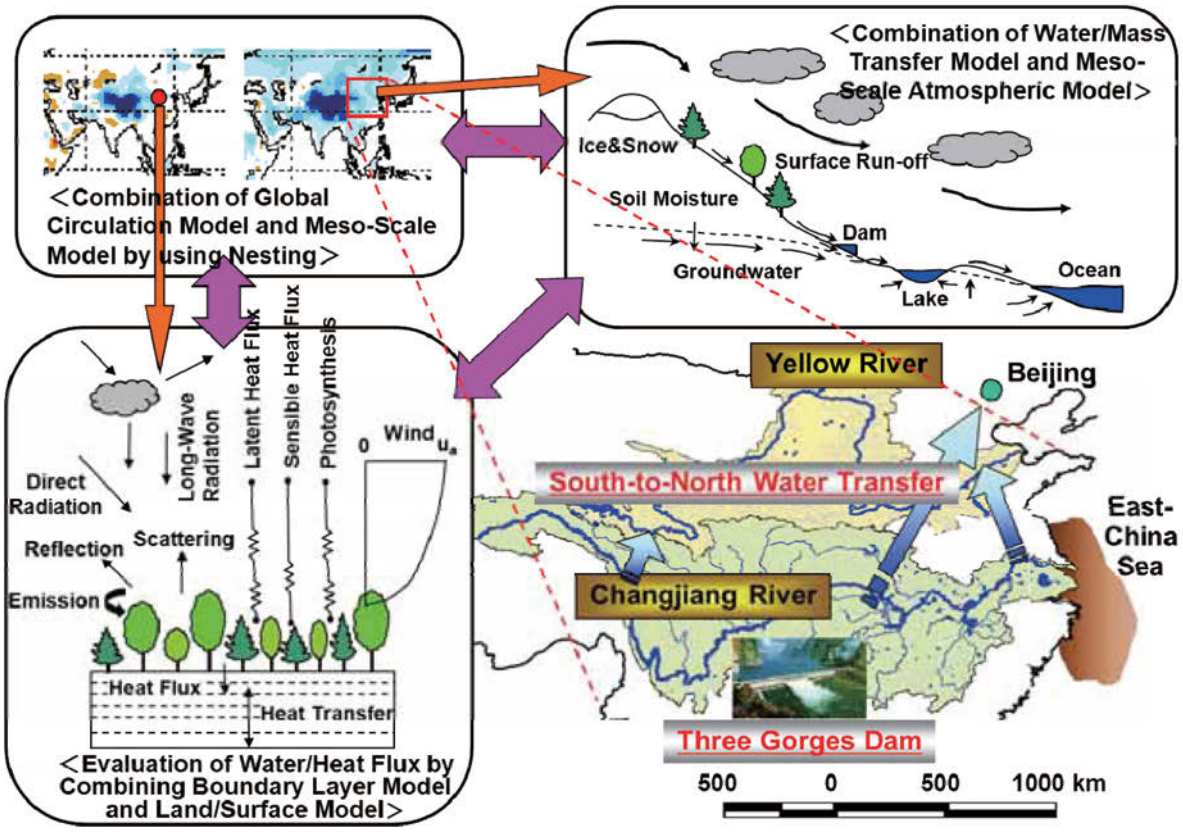

Fig. 5.2 Dynamics of water–heat–mass cycles in the Changjiang and Yellow River basins obtained by the combined land–atmosphere model.

The author has also researched the mutual interaction and feedback of hydro-geomorphology and vegetation dynamics in the ecosystem to further explain the positive feedback between geomorphology and eco-hydrology on irregular slopes and in heterogeneous vegetation, whereas most previous studies have considered regular slopes and their relation to string or maze patterns. The heterogeneous vegetation succession was evaluated in relation to self-organization and regime shift. These results suggest the effectiveness of river restoration in conservation plans for mire recovery and the importance of the process-based model in assessing the connection between hydrologic change and vegetation succession (Nakayama, 2011e). On the basis of this dispatch, the author is currently attempting to re-evaluate the ecosystem in the catchment from the perspective of a "meta-ecosystem" by considering global–local interaction and hydrology–ecology connections (Fig. 5.3). In addition, the author plans to assess the impact of water–heat–material cycle changes through human activities on ecosystem function, analysis environmental impact and limiting factor accompanied by the change in ecosystem function. Moreover, a quantitative estimation is planned for more effective measures and available technologies as alternative scenarios for the final objective of sustainable development under the constraint of global security in addition to environmental degradation. The author's goal is to develop integrated modeling-system flexibly available to various-scaled ecosystems consisting of urban areas, forests, grasslands, cultivated fields, paddy fields, wetlands, rivers, lakes, groundwater, oceans, and atmosphere on the basis of integrations between numerical simulation, satellite data, and ground-truth observation on a global scale, as described in the following objectives:

(A) Construction of assessment models in multiple scales, including dynamism in regional scales, impact assessment of urban activities on regional water–heat–material cycles, quantification of potential capacity in the ecosystem, numerical simulation in the scenario of technology for environmental improvement, and integration of modeling and political scenarios through an evaluation of sustainability.

(B) Impact assessment of various stress factors on a multi-scaled ecosystem, development of a modeling system including the multi-scaled aspect between global–regional–micro (genetic) levels and a feedback mechanism between hydrology and ecology, and evaluation of vulnerability in ecosystem functions.

(C) Impact assessment to contribute to global security relative to (A) and (B), up-scaling and down-scaling procedures focusing on urban, agricultural, and natural areas, re-evaluation of natural energy and environmental resources, and objective-oriented research combined with political scenarios and decision making on the basis of multiple criteria.

The author intends to report this research in a succeeding monograph (Part IV) in the near future.

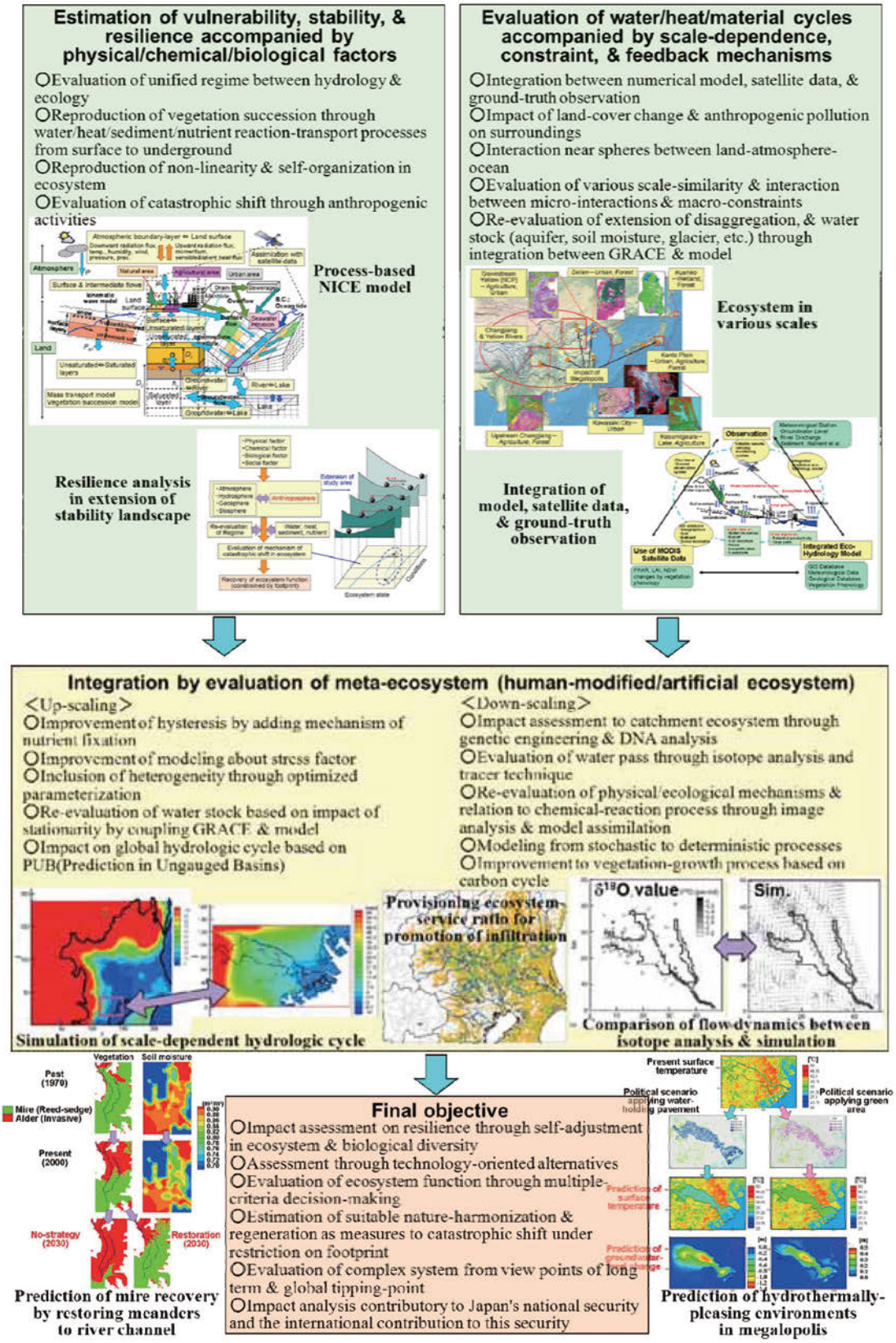

Fig. 5.3 Integrated procedures through meta-ecosystem analysis.

References

Brown L.R., Halweil B. (1998) China's water shortage could shake world food security. World Watch, 11(4), 10-18.

Li Q., Zou Z., Xia Z., Guo J., Liu Y. (2007) Impacts of human activities on the flow regime of the Yangtze River. Changes in Water Resources Systems: Methodologies to Maintain Water Security and Ensure Integrated Management, IAHS Publication 315, 266-275.

Ministry of Environment (2004) Report on heat-island measures by controlling anthropogenic exhaustion heat in the urban area. http://www.env.go.jp/air/report/h16-05/ (in Japanese).

Nakayama T. (2008a) Factors controlling vegetation succession in Kushiro Mire. Ecological Modelling, 215, 225-236, doi:10.1016/j.ecolmodel.2008.02.017.

Nakayama T. (2008b) Shrinkage of shrub forest and recovery of mire ecosystem by river restoration in northern Japan. Forest Ecology and Management, 256, 1927-1938, doi:10.1016/j.foreco.2008.07.017.

Nakayama T. (2008c) Development of process-based NICE model and simulation of ecosystem dynamics in the catchment of East Asia (Part II), CGER's Supercomputer Monograph Report, 14, NIES, 91p., http://www-cger.nies.go.jp/publication/I083/i083.html.

Nakayama T. (2009) Simulation of ecosystem degradation and its application for effective policy-making in regional scale. In River pollution research progress, Mattia N. Gallo, Marco H. Ferrari (eds), 1-89 (Chapter 1), Nova Science Pub., Inc., New York.

Nakayama T. (2010) Simulation of hydrologic and geomorphic changes affecting a shrinking mire. River Research and Applications, 26(3), 305-321, doi:10.1002/rra.1253.

Nakayama T. (2011a) Simulation of complicated and diverse water system accompanied by human intervention in the North China Plain. Hydrological Processes, 25, 2679-2693, doi:10.1002/hyp.8009.

Nakayama T. (2011b) Simulation of the effect of irrigation on the hydrologic cycle in the highly cultivated Yellow River Basin. Agricultural and Forest Meteorology, 151, 314-327, doi:10.1016/j.agrformet.2010.11.006.

Nakayama T. (2011c) Visualization of missing role of hydrothermal interactions in Japanese megalopolis for win-win solution. Water Science and Technology (submitted).

Nakayama T. (2011d) Impact of anthropogenic activity on eco-hydrological process in continental scales. Procedia Environmental Sciences (accepted).

Nakayama T. (2011e) Feedback and regime shift of mire ecosystem in northern Japan. Hydrological Processes (revised).

Nakayama T., Fujita T. (2010) Cooling effect of water-holding pavements made of new materials on water and heat budgets in urban areas. Landscape and Urban Planning, 96, 57-67, doi:10.1016/j.landurbplan.2010.02.003.

Nakayama T., Hashimoto S. (2011) Analysis of the ability of water resources to reduce the urban heat island in the Tokyo megalopolis. Environmental Pollution, 159, 2164-2173, doi:10.1016/j.envpol.2010.11.016.

Nakayama T., Shankman D. (2011a) Impact of the Three-Gorges Dam and water transfer project on Changjiang floods. Global and Planetary Change (revised).

Nakayama T., Shankman D. (2011b) Effect of two extremes on ecosystem variation in continental scale. Hydrological Processes (submitted).

Nakayama T., Watanabe M. (2004) Simulation of drying phenomena associated with vegetation change caused by invasion of alder (Alnus japonica) in Kushiro Mire. Water Resources Research, 40, W08402, doi:10.1029/2004WR003174.

Nakayama T., Watanabe M. (2006a) Simulation of spring snowmelt runoff by considering micro-topography and phase changes in soil layer. Hydrology and Earth System Sciences Discussions, 3, 2101-2144.

Nakayama T., Watanabe M. (2006b) Development of process-based NICE model and simulation of ecosystem dynamics in the catchment of East Asia (Part I), CGER's Supercomputer Monograph Report, 11, NIES, 100p., http://www-cger.nies.go.jp/publication/I063/I063.html.

Nakayama T., Watanabe M. (2008a) Missing role of groundwater in water and nutrient cycles in the shallow eutrophic Lake Kasumigaura, Japan. Hydrological Processes, 22, 1150-1172, doi:10.1002/hyp.6684.

Nakayama T., Watanabe M. (2008b) Role of flood storage ability of lakes in the Changjiang River catchment. Global and Planetary Change, 63, 9-22, doi:10.1016/j.gloplacha.2008.04.002.

Nakayama T., Watanabe M. (2008c) Modelling the hydrologic cycle in a shallow eutrophic lake. Verh International Verein Limnology, 30.

Nakayama T., Yang Y., Watanabe M., Zhang X. (2006) Simulation of groundwater dynamics in North China Plain by coupled hydrology and agricultural models. Hydrological Processes, 20(16), 3441-3466, doi:10.1002/hyp.6142.

Nakayama T., Watanabe M., Tanji K., Morioka T. (2007) Effect of underground urban structures on eutrophic coastal environment. Science of the Total Environment, 373(1), 270-288, doi:10.1016/j.scitotenv.2006.11.033.

Nakayama T., Sun Y., Geng Y. (2010) Simulation of water resource and its relation to urban activity in Dalian City, Northern China. Global and Planetary Change, 73, 172-185, doi:10.1016/j.gloplacha.2010.06.001.

Nakayama T., Hashimoto S., Hamano H. (in press) Multi-scaled analysis of hydrothermal dynamics in Japanese megalopolis by using integrated approach. Hydrological Processes.

Shankman D., Liang Q. (2003) Landscape changes and increasing flood frequency in China's Poyang Lake region. Professional Geographer, 55(4), 434-445.

Yang H., Zehnder A. (2001) China's regional water scarcity and implications for grain supply and trade. Environmental Planning A, 33, 79-95.

Yang D., Li C., Hu H., Lei Z., Yang S., Kusuda T., Koike T., Musiake K. (2004) Analysis of water resources variability in the Yellow River of China during the last half century using historical data. Water Resources Research, 40, W06502, doi:10.1029/2003WR002763.

Zhao S., Fang J., Miao S., Gu B., Tao S., Peng C., Tang Z. (2005) The 7-decade degradation of a large freshwater lake in central Yangtze River, China. Environmental Science and Technology, 39, 431-436.

Appendix

Publications and Presentations

Original Papers and Reviews:

Nakayama T. (2008a) Factors controlling vegetation succession in Kushiro Mire. Ecological Modelling, 215, 225-236., doi: 10.1016/j.ecolmodel.2008.02.017.
Nakayama T. (2008b) Shrinkage of shrub forest and recovery of mire ecosystem by river restoration in northern Japan. Forest Ecology and Management, 256, 1927-1938, doi: 10.1016/j.foreco.2008.07.017.
Nakayama T. (2010a) Simulation of hydrologic and geomorphic changes affecting a shrinking mire. River Research and Applications, 26(3), 305-321, doi: 10.1002/rra.1253.
Nakayama T. (2011a) Simulation of complicated and diverse water system accompanied by human intervention in the North China Plain. Hydrological Processes, 25, 2679-2693, doi: 10.1002/hyp.8009.
Nakayama T. (2011b) Simulation of the effect of irrigation on the hydrologic cycle in the highly cultivated Yellow River Basin. Agricultural and Forest Meteorology, 151, 314-327, doi: 10.1016/j.agrformet.2010.11.006.
Nakayama T. (2011c) Visualization of missing role of hydrothermal interactions in Japanese megalopolis for win-win solution. Water Science and Technology (submitted).
Nakayama T. (2011d) Impact of anthropogenic activity on eco-hydrological process in continental scales. Procedia Environmental Sciences (accepted).
Nakayama T. (2011e) Feedback and regime shift of mire ecosystem in northern Japan. Hydrological Processes (revised).
Nakayama T., Fujita T. (2010) Cooling effect of water-holding pavements made of new materials on water and heat budgets in urban areas. Landscape and Urban Plannin, 96, 57-67, doi: 10.1016/j.landurbplan.2010.02.003.
Nakayama T., Hashimoto S. (2011) Analysis of the ability of water resources to reduce the urban heat island in the Tokyo megalopolis. Environmental Pollution, 159, 2164-2173, doi: 10.1016/j.envpol.2010.11.016.
Nakayama T., Shankman D. (2011a) Impact of the Three-Gorges Dam and water transfer project on Changjiang floods. Global and Planetary Change (revised).
Nakayama T., Shankman D. (2011b) Effect of two extremes on ecosystem variation in continental scale. Hydrological Processes (submitted).
Nakayama T., Watanabe M. (2004) Simulation of drying phenomena associated with vegetation change caused by invasion of alder (Alnus japonica) in Kushiro Mire. Water Resources Research, 40, W08402, doi: 10.1029/2004WR003174.
Nakayama T., Watanabe M. (2006a) Simulation of spring snowmelt runoff by considering micro-topography and phase changes in soil layer. Hydrology and Earth System Sciences Discussions, 3, 2101-2144.
Nakayama T., Watanabe M. (2008a) Missing role of groundwater in water and nutrient cycles in the shallow eutrophic Lake Kasumigaura, Japan. Hydrological Processes, 22, 1150-1172, doi: 10.1002/hyp.6684.
Nakayama T., Watanabe M. (2008b) Role of flood storage ability of lakes in the Changjiang River catchment. Global and Planetary Change, 63, 9-22, doi: 10.1016/j.gloplacha.2008.04.002.
Nakayama T., Watanabe M. (2008c) Modelling the hydrologic cycle in a shallow eutrophic lake. Verh International Verein Limnology, 30.
Nakayama T., Yang Y., Watanabe M., Zhang X. (2006) Simulation of groundwater dynamics in North China Plain by coupled hydrology and agricultural models. Hydrological Processes, 20(16), 3441-3466, doi: 10.1002/hyp.6142.
Nakayama T., Watanabe M., Tanji K., Morioka T. (2007) Effect of underground urban structures on eutrophic coastal environment. Science of the Total Environment, 373(1), 270-288, doi: 10.1016/j.scitotenv.2006.11.033.
Nakayama T., Sun Y., Geng Y. (2010) Simulation of water resource and its relation to urban activity in Dalian City, Northern China. Global and Planetary Change, 73, 172-185, doi: 10.1016/j.gloplacha.2010.06.001.
Nakayama T., Hashimoto S., Hamano H. (in press) Multi-scaled analysis of hydrothermal dynamics in Japanese megalopolis by using integrated approach. Hydrological Processes.

Books:

Nakayama T. (2008c) Development of process-based NICE model and simulation of ecosystem dynamics in the catchment of East Asia (Part II), CGER's Supercomputer Monograph Report, 14, NIES, 91p., http://www-cger.nies.go.jp/publication/I083/i083.html.

Nakayama T. (2009a) Simulation of ecosystem degradation and its application for effective policy-making in regional scale. In River pollution research progress, Mattia N. Gallo, Marco H. Ferrari (eds), pp.1-89 (Chapter 1), Nova Science Pub., Inc., New York.
Nakayama T. (2009b) Evaluation of intertwined relations between water stress and crop productivity in grain-cropping plain area by using process-based model. In Agricultural runoff, coastal engineering and flooding, Christopher A. Hudspeth, Timothy E. Reeve (eds), pp.107-136 (Chapter 5), Nova Science Pub., Inc., New York.
Nakayama T. (2010b) Evaluation of flood storage ability of Dongting and Poyang Lakes in Yangtze River by using process-based model, In River Deltas: Types, Structures & Ecology, Paul E. Schmidt (ed), pp.69-94 (Chapter 4), Nova Science Pub., Inc., New York.
Nakayama T. (2011f) Multi-level evaluation of hydrologic cycle in the catchment including shallow eutrophic lake, In Advances in Environmental Research, Volume 11, Justin A. Daniels (ed), pp.1-37 (Chapter 1), Nova Science Pub., Inc., New York.
Nakayama T. (2011g) Impact of water degradation on ecosystem change and adaptation strategy for sustainable development, In Water and Society, D. W. Pepper and C. A. Brebbia (eds), pp.139-150, WIT Press, doi: 10.2495/WS110131.
Nakayama T. (in press) Impact of irrigation on hydrologic change in highly cultivated basin, In Evapotranspiration / Book 1, A. Irmak (ed), InTech, Croatia.
Nakayama T., Watanabe M. (2006b) Development of process-based NICE model and simulation of ecosystem dynamics in the catchment of East Asia (Part I), CGER's Supercomputer Monograph Report, 11, NIES, 100p., http://www-cger.nies.go.jp/publication/I063/I063.html.
Nakayama T., Sun Y., Geng Y. (2011) Relation between river management and economic growth in urban regions, In River Ecosystems: Dynamics, Management and Conservation, Hannah S. Elliot, Lucas E. Martin (eds), pp.301-312 (Chapter 9), Nova Science Pub., Inc., New York.

Conference Reports:

Nakayama T., Watanabe M. (2006) Simulation of 1998-big flood in Changjiang River Catchment, China, paper number H23D-24, AGU Joint Assembly 2006, Baltimore, USA, 23 – 26 May (CD-ROM).
Nakayama T., Watanabe M., Tanji K., Morioka T. (2006) Effect of underground urban structures on hydrologic budget in Tokyo metropolitan area, Japan, session number TS-C04, ASLO 2006 Summer Meeting, Victoria, Canada, 4 – 9 June (CD-ROM).
Nakayama T. (2006) Influence of river channelization and re-meandering on vegetation change in Kushiro Mire, ICEM2006, Yamaguchi, Japan, 28 August – 1 September (CD-ROM).
Nakayama T. (2006) Development of process-based NICE model and simulation of ecosystem dynamics in the East Asia, Wuhee-NIES Joint Meeting (Internal Workshop), Wuhan, China, 25 September.
Nakayama T., Watanabe M. (2006) Simulation of irrigation effect on water cycle in Yellow River catchment, China, paper number GC21B-3, AGU Fall Meeting 2006, San Francisco, USA, 11 – 15 December (CD-ROM).
Nakayama T., Watanabe M. (2007) Effect of vegetation change on hydrologic cycle in Changjiang and Yellow River catchments, paper number H52B-07, AGU Joint Assembly 2007, Acapulco, Mexico, 22 – 25 May (CD-ROM).
Nakayama T. (2007) Relationship between hydrogeological process and vegetation change in Kushiro Mire, session number #COS43-5, ESA-SER Joint Meeting, San Jose, USA, 5 – 10 August (CD-ROM).
Nakayama T. (2007) Innovative analysis model of integrative environmental fluxes, NICE model, its application in Asian regions and findings for policy proposal, Int. Workshop of Innovative Theory, Technologies and Practice for Industrial Symbiosis in Dalian (Internal Workshop), Dalian, China, 30 May – 2 June.
Nakayama T., Watanabe M. (2007) Estimation of hydrologic cycle in shallow eutrophic lake by integrated approach, session number #SS13, SIL2007, Montreal, Canada, 12 – 18 August (CD-ROM).
Nakayama T., Watanabe M. (2007) Shrinking of Dongting and Poyang Lakes and its relation to large-scale flood in Changjiang River catchment, ICGRHWE'07/FM2S'07, Guangzhou, China, 9 – 13 September (CD-ROM).
Nakayama T. (2007) General structure of process-based NICE (NIES Integrated Catchment-based Eco-hydrology) model and simulation of ecosystem dynamics in the catchment of East Asia, CEH-NIES research meeting (Internal Workshop), Wallingford, UK, 21 September.
Nakayama T. (2007) Integrative disaggregated environmental assessment model, theory and application in basin

region and urban district, Int. Workshop for Sustainable Urban and Industrial Management (Internal Workshop), Wuhan, China, 3 – 6 December.

Nakayama T., Fujita T. (2007) Simulation of cooling effect of newly-innovated urban pavements on water and heat budgets, paper number H43D-1608, AGU Fall Meeting 2007, San Francisco, USA, 10 – 14 December (CD-ROM).

Nakayama T. (2008) Simulation of intertwined relations between water stress, crop productivity, and ecosystem degradation in Northern China, ENVR176OR, Food Security and Environmental Change, Univ. of Oxford, UK, 2 – 4 April.

Nakayama T. (2008) Development of NICE-URBAN model applicable to urban district, Int. Workshop on Sustainable Regional Development through Circular Economy (Internal Workshop), Shenyang, China, 19 May.

Nakayama T., Fujita T., Hashimoto S., Hamano H. (2008) Simulation of hydrothermal recoveries by adopting symbiotic urban scenario in the Japanese megalopolis, paper number GC43A-11, AGU Joint Assembly 2007, Florida, USA, 27 – 30 May (CD-ROM).

Nakayama T. (2008) Effect of freshwater over-exploitation on seawater intrusion in grain-cropping plain area, session number GS21, ASLO 2008 Summer Meeting, Newfoundland, Canada, 8 – 13 June (CD-ROM).

Nakayama T. (2008) Simulation of hydrologic change related to ecological condition in the Japanese mire, session number 15, 2008 AWRA Summer Specialty Conference, Virginia, USA, 30 June – 2 July (CD-ROM).

Nakayama T. (2008) Estimation of relationship between hydrologic change, seawater intrusion, and crop production by using integrated approach, 93rd ESA Annual Meeting, Milwaukee, USA, 3 – 8 August (CD-ROM).

Nakayama T., Fujita T., Geng Y., Hashimoto S. (2008) Simulation of water resource and its relation to urban activity in Dalian City, Northern China, session number Y2, HydroPredict2008, Prague, Czech Rep., 15 – 18 September (CD-ROM).

Nakayama T. (2008) Integrative model approach for sustainable watershed management in Liaohe River Basin, Expert Workshop on Sustainable Watershed Management (Internal Workshop), NIES, Japan, 26 September.

Nakayama T. (2008) Simulation of anthropogenic effects on hydrologic cycle in Changjiang and Yellow River Catchments, China, session number 54, AWRA 2008 Annual Water Resources Conference, New Orleans, USA, 17 – 20 November (CD-ROM).

Nakayama T. (2008) Impact of anthropogenic activities on floods and droughts in Changjiang and Yellow River Catchments, WATCH Project Workshop (Internal Workshop), Beijing, China, 24 – 26 November.

Nakayama T., Fujita T., Hashimoto S., Hamano H. (2008) Multi-scale analysis of hydrologic change in the Japanese megalopolis by using integrated approach, paper number GC34A-08, AGU Fall Meeting 2008, San Francisco, USA, 15 – 19 December (CD-ROM).

Nakayama T., Fujita T., Hashimoto S., Hamano H. (2009) Impact assessment of hydrothermal dynamics in urban area by using multi-scaled integrated approach, session number 26, AWRA 2009 Annual Water Resources Conference, Seattle, USA, 9 – 12 November (CD-ROM).

Nakayama T., Fujita T., Hashimoto S. (2010) Multi-scaled analysis of water resource ability to tackle heat island in Japanese megalopolis, paper number O34, Urban Environmental Pollution 2010, Boston, USA, 20 – 23 June (CD-ROM).

Nakayama T., Sun Y., Don N.C. , Fujita T., Geng Y. (2010) Assessment of simulated water resource and its relation to economic growth in urban city of northern China, paper number P2.37, Urban Environmental Pollution 2010, Boston, USA, 20 – 23 June (CD-ROM).

Nakayama T. (2010) Nonlinear interaction and feedback of mire ecosystem in northern Japan, paper number COS28-2, 95rd ESA Annual Meeting, Pittsburgh, Pennsylvania, USA, 1 – 6 August (Proceeding).

Nakayama T. (2010) Irrigation effect and feedback process of hydrologic cycle in highly cultivated region of northern China, paper number O8.3, Hydrology Conference 2010, San Diego, USA, 11 – 13 October (CD-ROM).

Nakayama T. (2010) Impact of anthropogenic activities on droughts in Northern China and floods in Southern China, session number 72, AWRA 2010 Annual Water Resources Conference, Philadelphia, Pennsylvania, USA, 1 – 4 November (Proceeding).

Nakayama T. (2011) Impact of anthropogenic activity on eco-hydrological process in continental scales, paper number 00027, ISEM2011, Beijing, China, 20 – 13 September (CD-ROM).

Nakayama T., Shankman D. (2011) Prediction of effect of huge structures on eco-hydrological changes in Changjiang basin, session number J-1-265, ICFM5, Tokyo, Japan, 27 – 29 September (CD-ROM).

Nakayama T. (2011) Visualization of missing role of hydrothermal interactions in Japanese megalopolis for win-win solution, session number 19-2-3, 4th IWA-ASPIRE Conference, Tokyo, Japan, 2 – 6 October (CD-ROM).
Nakayama T., Shankman D. (2011) Seesaw between droughts and floods affected by anthropogenic activities in China, session 4-3, EXTREME2011, Kyoto, Japan, 24 – 28 October (Proceeding).
Nakayama T. (2011) Understanding linkages in boundary spheres through multi-level evaluation of hydrologic cycle, 14th World Lake Conference, Austin, Texas, USA, 31 October – 4 November (Proceeding).
Nakayama T. (2011) Nonlinear interaction between hydrology, geomorphology, and ecology in mire, session number 32, AWRA 2011 Annual Water Resources Conference, Albuquerque, New Mexico, USA, 1 – 4 November (Website).
Nakayama T. (2011) Impact of water degradation on ecosystem change and adaptation strategy for sustainable development, session4-3, Water and Society 2011, Las Vegas, USA, 5 – 7 December (CD-ROM).
Nakayama T. (2011) Impact of hydrologic cycle on ecosystem function and evaluation of complexity, Watershed Symposium endorsed by Japan Society of Civil Engineers, Tokyo, Japan, 15 December.
Nakayama T. (2012) Future prospects of water crisis in the globe (Keynote speech), 2012 International Water Market Symposium: Experiences and Challenges, Shiga, Japan, 13 – 14 February (accepted).
Nakayama T. (2012) Coupling with satellite data and eco-hydrology model for evaluation of two extremes in continental scale, AGU Chapman Conference on Remote Sensing of the Terrestrial Water Cycle, Hawaii, USA, 19 – 22 February (accepted).
Nakayama T. (2012) Toward construction of process-based tipping-point early warning system, Planet Under Pressure 2012, London, UK, 26 – 29 March (accepted).
Nakayama T. (2012) Achievement of win-win solution to intertwined environmental pollutions for eco-conscious society, Planet Under Pressure 2012, London, UK, 26 – 29 March (accepted).
Nakayama T., Shankman D. (2012) Integrated assessment toward trans-boundary solution and sustainable development, Planet Under Pressure 2012, London, UK, 26 – 29 March (accepted).

Contact Person

Tadanobu Nakayama
Center for Global Environmental Research (CGER),
National Institute for Environmental Studies (NIES)
16-2 Onogawa, Tsukuba, Ibaraki 305-8506, Japan
Phone: (+81)29-850-2564, Facsimile: (+81)29-850-2219, E-mail: nakat@nies.go.jp
http://www.nies.go.jp/rsdb/vdetail-e.php?id=100190

CGER'S SUPERCOMPUTER MONOGRAPH REPORT
Back Issues

Vol. 1 CGER-I021-'96 (Out of stock)
KOMORI S.: Turbulence Structure and CO_2 Transfer at the Air-Sea Interface and Turbulent Diffusion in Thermally-Stratified Flows

Vol. 2 CGER-I022-'96
TOKIOKA T., NODA A., KITOH A., NIKAIDOU Y., NAKAGAWA S., MOTOI T., YUKIMOTO S., TAKATA K.: A Transient CO_2 Experiment with the MRI CGCM -Annual Mean Response-

Vol. 3 CGER-I025-'97
NUMAGUTI A., SUGATA S., TAKAHASHI M., NAKAJIMA T., SUMI A.: Study on the Climate System and Mass Transport by a Climate Model

Vol. 4 CGER-I028-'97 (Out of stock)
AKIYOSHI H.: Development of a Global 1-D Chemically Radiatively Coupled Model and an Introduction to the Development of a Chemically Coupled General Circulation Model

Vol. 5 CGER-I035-'99
WATANABE M., AMANO K., KOHATA K.: Three-Dimensional Circulation Model Driven by Wind, Density, and Tidal Force for Ecosystem Analysis of Coastal Seas

Vol. 6 CGER-I040-2000
HAYASHI Y.Y., TOYODA E., HOSAKA M., TAKEHIRO S., NAKAJIMA K., ISHIWATARI M.: Tropical Precipitation Patterns in Response to a Local Warm SST Area Placed at the Equator of an Aqua Planet

Vol. 7 CGER-I045-2001
NODA A., YUKIMOTO S., MAEDA S., UCHIYAMA T., SHIBATA K., YAMAKI S.: A New Meteorological Research Institute Coupled GCM (MRI-CGCM2) -Transient Response to Greenhouse Gas and Aerosol Scenarios-

Vol. 8 CGER-I055-2003 (Out of stock)
NOZAWA T., EMORI S., NUMAGUTI A., TSUSHIMA Y., TAKEMURA T., NAKAJIMA T., ABE-OUCHI A., KIMOTO M.: Transient Climate Change Simulations in the 21st Century with the CCSR/NIES CGCM under a New Set of IPCC Scenarios

Vol. 9 CGER-I057-2004
MIYAZAKI T., FUJISHIMA S., YAMAMOTO M., WEI Q., HANAZAKI H.: Vortices, Waves and Turbulence in a Rotating Stratified Fluid

Vol. 10 CGER-I060-2005
HAYASHI S., MURAKAMI S., XU K., WATANABE M.: Modeling of Daily Runoff in the Changjiang (Yangtze) River Basin and Its Application to Evaluating the Flood Control Effect of the Three Gorges Project

Vol. 11 CGER-I063-2006
NAKAYAMA T., WATANABE M.: Development of Process-based NICE Model and Simulation of Ecosystem Dynamics in the Catchment of East Asia (Part I)

Vol. 12 CGER-I073-2007
NOZAWA T., NAGASHIMA T., OGURA T., YOKOHATA T., OKADA N., SHIOGAMA H.: Climate Change Simulations with a Coupled Ocean-Atmosphere GCM Called the Model for Interdisciplinary Research on Climate: MIROC

Vol. 13 CGER-I080-2008
SHIBATA K., DEUSHI M.: Simulations of the Stratospheric Circulation and Ozone during the Recent Past (1980-2004) with the MRI Chemistry-Climate Model

Vol. 14 CGER-I083-2008
NAKAYAMA T.: Development of Process-based NICE Model and Simulation of Ecosystem Dynamics in the Catchment of East Asia (Part II)

Vol. 15 CGER-I092-2010 (Out of stock)
MAKSYUTOV, S., NAKATSUKA Y., VALSALA V., SAITO M., KADYGROV N., AOKI T., EGUCHI N., HIRATA R., IKEDA M., INOUE G., NAKAZAWA T., ONISHI R., PATRA P.K., RICHARDSON A.D., SAEKI T., YOKOTA T.: Algorithms for Carbon Flux Estimation Using GOSAT Observational Data

Vol. 16 CGER-I097-2011
NAKAJIMA K.: Idealized Numerical Experiments on the Space-time Structure of Cumulus Convection Using a Large-domain Two-dimensional Cumulus-Resolving Model

Vol. 17 CGER-I098-2011
UEDA H.: Atmospheric Motion and Air Quality in East Asia

Copies of these reports can be obtained by contacting:
Center for Global Environmental Research
National Institute for Environmental Studies
16-2 Onogawa, Tsukuba, Ibaraki, 305-8506, Japan

These reports are also available as PDF files.
See: http://www.cger.nies.go.jp/ja/activities/supporting/publications/report/index.html